Republic of Iraq
Ministry of Higher Education
and Scientific Research
University of Babylon/College of Science
Department of Physics

Measuring Radon Gas Concentration in Soil and Water and Transforming Natural Radionuclides to Plants in Agricultural Areas of Al-Haydaria

A Thesis
Submitted to the Council of College of Science/ University of Babylon in Partial Fulfillment of the Requirements for the Degree of Doctor of Philosophy in Science/Physics.

By

Layth Yousif Jebur Taher

B.Sc in Physics/2001

M.Sc in Physics/2017

Supervised by

Prof. Dr. Mohsin Kadhim Muttaleb Al-Jnaby

1445 A.H. 2023 A.D.

بسم الله الرحمن الرحيم

﴿يَرْفَعِ اللَّهُ الَّذِينَ آمَنُوا مِنْكُمْ وَالَّذِينَ أُوتُوا الْعِلْمَ

دَرَجَاتٍ وَاللَّهُ بِمَا تَعْمَلُونَ خَبِيرٌ ﴾

صَدَقَ اللهُ العَلِيُّ العَظِيم

(سورة المجادلة: الآية ١١)

Certification of the Supervisor

I Certify that this thesis entitled **“Measuring Radon Gas Concentration in Soil and Water and Transforming Natural Radionuclides to Plants in Agricultural Areas of Al-Haydaria”** was prepared by **(Layth Yousif Jebur Taher)** under my supervision at Department of Physics, Faculty of Science, University of Babylon, as a partial fulfillment of the requirements for the degree of doctor of philosophy science in physics.

Signature:

Supervisor: Dr. Mohsin Kadhim Muttaleb Al-Jnaby

Title: Professor

Address: Department of Physics - College of Science - University of Babylon.

Date: / /2023

Certification of the Head of the Department

In view of the available recommendation, I forward this thesis for debate by the Examination Committee

Signature:

Name: Dr. Samira Adnan Mahdi

Title: Assistant Professor

Address: Head of Physics Department- College of Science - University of Babylon

Date: / /2023

DEDICATION

To who taught me the success and patience to face difficulties and did not lower stayed he fed with affection for my father

To the kindest woman with most pure endless love in the universe, my mother

To my lovely sisters and brothers

To my wife who shared with me through thick and thin The completion of my work would not have been possible without her support, and I hope that it will satisfy her

To my beloved country, Iraq

The fighters and martyrs of Iraq with all the love and appreciation.

Layth

ACKNOWLEDGMENTS

Thanks be to Allah His majesty for all things which led me during the critical time.

I wish to express my deep thanks and gratitude to my supervisor **Prof. Dr. Mohsin K. Al-Janaby** for his supervision, encouragement and efforts during preparation of this thesis.

My great thanks are expressed to the head of the department of physics, of the college of science Assistant Professor Dr. Samira A. Mahdi and staff of the Physics department at University of Babylon for offering me the opportunity to complete my research.

Special thanks are due to Prof. Dr. Hayder Hamza Hussain for providing the necessary facilities and help and the Physics department laboratories at University of Kufa.

Many thanks and appreciations are expressed to my family for their patience and help during this work. Finally, I would like to express my thanks to all my friends for spicial Faris Mandell Abed and to all the people who helped me, in one way or another to complete this study and I ask Allah to help them all.

***Layth*.**

Summary

This study examines the agricultural area of Al-Haydaria in Al-Najaf Al-Ashraf Governorate, where the study area was divided into two areas, the first of which depends for irrigation on groundwater and the other on surface water, These areas are important sources of seasonal agricultural products for local markets.

The study aims to calculate the concentrations of radon gas, the specific activity, and the transfer factor of natural radionuclides in the two areas mentioned above and for different samples of ground and surface water, agricultural soil, plants, and fruit (tomato crop) in those areas. Samples of groundwater, surface water, agricultural soil, and tomato crop samples (plants and fruits) were collected, and three measurement techniques were used: the Rad-Seven detector scale for groundwater and surface water samples, the gamma ray spectrum (NaI (Tl) for soil, plants, and fruits, and the CR-39 solid-state nuclear trace detector for soil and fruits.

The results indicated that the average concentration of the gas ^{222}Rn in groundwater was higher than in surface water, and its value was 0.23 Bq/l, but it was lower than the global average, such as that of the US Environmental Protection Agency Water Office. The average specific activity value ^{238}U and ^{232}Th in all soil, plant and fruit (tomato) samples for the two regions was less than the global average values, with the exception of ^{40}K and for all samples it was Higher than the global average values. However, the values of the risk indicators for all samples were lower than the global average values. The study also found that the rate of the transfer factor for radionuclides ^{238}U , ^{232}Th and ^{40}K from the soil to the plant and fruit is less than one n in the first

region, while the rate of the transfer factor For the radionuclides ^{238}U and ^{232}Th from the soil to the plant the second region was greater than one, and from the soil to the fruit, , it was less than one, while the values of the transfer coefficients for the nucleus ^{40}K were less than one in the soil for plants and fruits. ^{222}Rn gas concentrations were measured in the air and inside samples, as well as ^{226}Ra in selected samples of agricultural soil and tomato fruits from both regions. All values of ^{222}Rn gas concentrations in the air and ^{226}Ra for the two regions are lower than the global averages, and the gas concentrations ^{222}Rn within the samples were all higher than the global average.

CONTENTS

CHAPTER FOUR: RESULTS AND DISCUSSIONS	

LIST OF TABLES

LIST OF FIGURES

LIST OF SYMBOLS

Symbol	*Description*
α	Alpha Particle
Ci	Cure
Sv	Sievert
Gy	Gray
^{o}C	Degree centigrade
RAD 7	Radon Activity Detector 7
A	Activity
H_{ex}	External hazard index
H_{in}	Internal hazard index
AED	Annual Effective Dose
AEDE	Annual effective dose equivalent
AGDE	Annual Gonadal Dose Equivalent
ELCR	Excess Lifetime Cancer Risk
Bq	Becquerel
Bq/m^3	Becquerel per cubic meter
Bq/L	Becquerel per Liter
eV	Electron Volt
ICRP	International Commission on Radiological Protection
UNSCEAR	United national scientific committee on the effects of atomic radiation

MCA	Multi-channel analyzer
kBq/m^3	kilo Becquerel per cubic meter
µg/L	Micro gram per Liter
µS/cm	Micro Siemens per centimeter
mSv	Mille Sievert
mSv/y	Mille Sievert per year
ppm	Part Per million
^{210}Po	Polonium-210
^{214}Po	Polonium-214
^{218}Po	Polonium-218
CR-39	Colomb Reside Detector
$C_{Rn}^{s,a}$	Radon activity concentration inside the sample
C_{Rn}^{a}	Radon concentration in the air of the tube
C_{Rn}^{s}	Radon concentration in the sample
NaOH	Sodium Hydroxide
SSNTD	Solid State Nuclear Track Detectors
mSv/y	Mille Sievert per year
$nGyh^{-1}$	Nano gray/hour
MeV	Million electron Volts
λ	Constant Decay
OECD	Organization for economic cooperation and development
WHO	World Health Organization
EPA	Environmental protection agency

μ	Linear Absorption Cofficient
m_e	Electron Mass
I_O	Gamma-rays Intensity befor it Penetrates a Matrerrials
I	Intensity of Gamma-rays Incident on Matrerrials

Chapter One

General Introduction

1.1 Introduction

Rutherford and Soddy were pioneers in proposing that radioactive atoms undergo a process of decay, emitting radiation and transforming into lighter forms. This idea gained significant validation when it was revealed that α-particles were essentially ionized helium atoms. Many of the newly discovered elements were found within different portions of uranium ores, leading to suspicions that uranium, the heaviest naturally occurring element, served as the parent substance [1]. Presently, we understand that uranium exists naturally as a blend of ^{238}U (99.27%), ^{235}U (0.72%), and ^{234}U (0.006%). Additionally, ^{232}Th and ^{40}K have been identified as radioactive progenitors, along with their respective decay products. Naturally occurring radioactivity in soils is primarily attributed to their mineral composition. The principal radionuclides involved are ^{238}U, ^{232}Th, and ^{40}K. The levels of radioactivity vary among different soil types based on their mineral content and composition [2]. The primary goal of measuring soil radioactivity is to evaluate radionuclide concentrations, and these concentrations can be used to characterize substances and establish connections between radiometric properties and material physical properties.

Currently, radiation pollution stands out as a critical environmental concern, posing a threat to all living beings on our planet. Despite notable technological and scientific advancements made by humanity, they remain inadequate in effectively tackling radiation contamination. As a result. The radiation and radioactive materials present a grave danger to life as we know it on Earth [3]. The process of unstable nuclei emitting diverse forms of radiation includis (alpha-particlaes, beta-particlaes and gamma-rays), either naturally occurring or induced for industrial use, is referred to as radioactivity [4].

In our everyday lives, the consistently exposed to natural radioactivity, an enduring and widespread phenomenon that has always been present in our environment. It can be found in various geological and natural elements such as air, soil, water, rocks, and plants [5]. A notable example of natural radiation arises from the decay and decomposition of organic matter in the soil, emitting radiation and thereby exposing humans to continuous radiation doses. Moreover, this process contributes to radioactive contamination in the surrounding environment. Several factors, including soil composition, geological formations, and human activities among others, influence the levels of natural radiation. These factors have the potential to modify and potentially intensify the natural radiation levels [6,7].

Natural radionuclides permeate ecosystems and the human food chain, undergoing transportation and circulation through natural processes that span across different environmental components [8]. These radioactive nuclides accumulate in soil, become incorporated into plants through metabolic processes, and eventually enter the bodies of animals when they consume contaminated food. In addition to being absorbed by plant roots, direct deposition can also occur where the pollutants are either metabolically assimilated by plants or directly ingested by animals feeding on the contaminated vegetation [9]. It is well-established that exposure to radionuclides through ingestion or inhalation can increase the risk to human populations through the food chain, as these substances disperse throughout various organs in the body [10].

Natural radionuclides that are present in water can originate from both the water source itself and human, particularly in areas where fertilizers have been used for agricultural purposes [11]. In regions where groundwater is present, radionuclides can be identified in solid aquifers or adjacent rocks of lithological nature. These geological materials, such as solid aquifers and rocks, often contain trace amounts of radioactive elements like radon gas, which can dissolve into groundwater during the interaction between water, rocks, and soil [12-14]. Certain substances, like radon gas, contain trace constituents that can elevate the concentration of natural radionuclides in the soil.

The escape of soil radon gas into water is a straightforward process, facilitated by its origin deep within the Earth's strata. As water interacts with the gas, it becomes dissolved in the water. Moreover, suspended particles in the water, including dust, are associated with short-lived byproducts of radon decay known as alpha particles [15].

The naturally occurring noble gas is ^{222}Rn, it is a half-life (3.82 d), and is produced through the indirect decay of ^{232}Th and ^{238}U. Given the widespread presence of uranium in the Earth's crust, both ^{226}Ra and ^{222}Rn can be found in almost any rock, soil, and even water [16,17].

Radon and its decay products contribute to approximately 50% of the population's exposure to ionizing radiation from natural sources [18–20]. Although inhaling radon does not cause immediate harm to humans, its decay products can adhere to the lining of the lungs. Being an alpha emitter, radon poses a risk to the internal soft tissues and can be detrimental to one's health [21]. While there are additional sources such as ground and surface water, natural and volcanic gases, the soil surface is the primary contributor of radon gas to the atmosphere [22]. Therefore, it is crucial to monitor radon levels in the surrounding environment.

1.2 Motivation and Problem Statement

The motives for choosing to study radon gas in the water and soil of of Al-Haydaria district in Al-Najaf governorate can be clarified with the following:

1. During the recent battles that Iraq was subjected to during the previous period, many areas in the Al-Najaf governorate were bombarded.
2. The incidence of cancerous diseases has increased recently, especially in the center and southern regions of Iraq, with high numbers recorded compared to the previous times.
3. The evaluation of water and agricultural soil, as well as how they directly affect people, animals, and agricultural products.
4. Finding a comprehensive study of water and agricultural soil and its effect on plants and fruits of Al-Haydaria district in Al-Najaf governorate.

1.3 Literature Review

In (2007), Vaupotic J. et al., studied radioactivity in soil samples in the Slovenian and Croatian karstic region (Rossi) using the gamma spectrometer. The results of their study were $(320\ to\ 510)\ Bq/kg$ to ^{40}K (50 to 85)Bq/kg to ^{226}Ra, (52 to 75) Bq/kg for ^{226}Ra and (52 and70)Bq/kg for ^{238}U. Determination groups were discovered to be located outside of the vaicinity ofthe effect zone ofthe coalfired power station [23].

In (2008), Lu X. and Zhang X., measured activities unique to ^{226}Ra, ^{232}Th and ^{40}K insoil for cuihiuoa Nation Geographic Park of the Mountains (China).By using detector of NaI(Tl). The main concentration of ^{226}Ra, ^{232}Th and ^{40}K was 27.2 ± 6.5, 43.9 $Bq.kg^{-1}$, 6.2 Bq.kg and respectively 653.10 and 127.60 Bq.kg. Activity concentrations to the radioactivity nuclides are when compared to global norms of values and the means of activities in soil at China. Results were less than the permissible global limits [24].

In (2008), AlaamerA. S., determined cons. activity for thorium, potassium and radium at soil taken from Riyadh, By using a NaI (Tl) detector in soil Saudi Arabia. The calculated specific activity of those radioactivity nuclides was compared to the forms reported around world. Average calculated specific activity for ^{226}Ra, ^{232}Th and ^{40}K were (14.50 ± 3.90, 11.20 ± 3.90 and 225.0 ±6.3) Bq.kg^{-1} respectively [25].

In (2009), Al-Hamarneh I. F. and Awedallah M. I., used a NaI(Tl) detector, researchers investigated nature radioactivity concentration in surface samples of soil and assessed radioactivity hazard in the northern Jordanian highlands. Inclined ^{226}Ra, ^{232}Th, and^{40}K , were 42.5 Bq/kg, 49.91 Bq/kg and 291.11 Bq/kg respecitively .The total avaerage D_r in the research areas is 50.5 nGy.h^{-1}, while AEDE is 51.5 nGy.h^{-1} [26].

In (2010), Senthilkumar B. et. al., measured levels of gamma rays of radiation in soil samples from Thanjavur (India) by using detector of NaI(Tl). Concentration of activity for ^{238}U, ^{232}Th and ^{40}K were (43.0 ± 9.04, 14.70 ±1.70 and 149.50 ± 3.10) Bq/kg respectively. D_r outdoors were determined was between (31.9 – 59) nGy.h^{-1} and average 43.30 ± 9 nGy/h. The world-averaged population measured value of 60 nGy.h^{-1} was max. from these figures. An effective dose ranged from 39.2 to 72.6 Sv/y, and with rate of 53.111 Sv/y [27].

In (2011), Hasan, A. K., Subber, A. R., & Shaltakh, A. R., using the RAD7 radon monitoring device from the USA-based Durridge firm, (15) locations in the Najaf Al-Ashraf city had their ^{222}Rn soil gas concentration analyzed. Four distinct depths were measured for soil gas in each location, starting from the ground's surface. According to the findings, the maximum concentration was $(9290 \pm 400)\ Bq/m^3$ for a depth of (60) cm in Al – Amir district, point sample (P14), while the least concentration was (9 17) Bq/m^3 for a depth of (5) cm at AlShoara district, point sample (P5). The region's background radiation levels are within the range of natural limitations, according to the study's findings [28].

In (2011) , Hussain, R. O., & Hussain, H. H., a gamma ray spectrometer built around a measurementsof the spaecific activity of ^{238}U, ^{232}Th *and* ^{40}K, were made usinga NaI(Tl) detector. inorder to determine thelevel of radioactivity inthe environment. According to the findings, the specific activities of ^{235}U, ^{232}Th and ^{40}K, were $11.598 - 2275.896$ Bq/kg, $12.846 - 88.585$ Bq/kg, and $1.304 - 26.656$ Bq/kg, respectively. The computed radium equivalent activity ranged from 0.893 to 175.244 Bq/kg [29].

In (2012), Al-Hamidawi A. A. et al., measured radon and thoron concentration in Al-Kufa city soil in twenty regions for 3 - depths about (0.5-1.5) meters The findings revealed as well as that rates for radon and thoron gas emission differed from one area to the next, depending on the rock structures.. Activity concentration of radon in soil was changed from (12775±400 Bq.m^{-3}) in 1.5 m under surface of earth in area 2 to (41.45±17 Bq.m^{-3}), for 1.5 m under surface of earth for (20s). Concentration of thoron for soil was varied between (198±8.5 B.qm^{-3}) at 1.5 m under surface of earth in areas 1 and 2. These concentration values were well below the allowed levels whose range was (0.440 kBq.m^{-3}) [30].

In (2013), Yousuf R. M. and Abdullah K. O., studied natural radioactivity in samples of samples were taken from several depths above the earth's surface, which is (0.1- 0.5) meters in some city on the east governorate of the Suleiman in Kurdistan of Iraq. NaI (Tl) detector is used. The typical value for natural radionuclides concentrations ^{238}U 83.337 Bq.kg^{-1} , for ^{232}Th 19.147 Bq.kg^{-1} and for ^{40}K 284. 86 Bq.kg^{-1}. The findings revealed that the average concentration were larger than the actual global values [31].

In (2014), Ademola A. K. et al., measured the specificactivity for nature radioactivity nuclides of ^{238}U, ^{232}Th , and ^{40}K at samples of soilat gold extracting area in Itagunmodi (Nigeria) by using NaI(Tl) detector. These natural radionuclides were subjected to radiological hazard assessments. Values of activity concentration are rated at different rates. The values for ^{238}U, ^{232}Th, and ^{40}K calculated inmining operations weres (55.30 ± 1.20), (26.40 ± 2.70) and (505.10 ± 7.10) Bq.kg^{-1}, respectiviely [32].

In (2014), Al-Gazaly H. H. et al., studied of the nature radiation at samples of soil in Iraq, Al-Najaf Province by the detector of NaI(Tl). The findings revealed that the particular activity for ^{238}U 77.33±5.8535 Bq.kg^{-1}, ^{232}Th 9.36 ± 0.9735 Bq.kg^{-1} and ^{40}K 426.31 ± 21.35 Bq.kg^{-1}. When the measured values were comparetion to the corresponding worldwide average, it was discovered the most specificactivity of ^{238}U and ^{40}K radionuclides in thestudied sampleswas greater than theglobal mean activity [33].

In (2015), Alsaffar M. S. et al., determined the distribution of radioactivity and factors transfer for plants are important parameters used for evaluating radionuclides contamination in environment and its dangerous to people. From that study activities of ^{226}Ra, ^{232}Th and ^{40}K were determined via gamma ray spectrometer for samples of components of rice (root, straw, husk, and grain) as well as soil took extracted from crops fields in Penang from Malaysia. They were also studied for their predictions the transfer factor from soil to grain [34].

In (2015), Isinkaye M. O. and Emelue H. U., evaluated the specific activity concentration of the natural radioactivity nuclides and their risk indexes in the samples collected from the soil of Oguta Lake/ Nigeria uses NaI (Tl) detector, mean value of the specific activity 47.89 $Bq.kg^{-1}$, 55.37 $Bq.kg^{-1}$ and 1023 $Bq.kg^{-1}$ for all ^{226}Ra ,^{232}Th and ^{40}K respectively. They found that the absorbed does is higher than the global allowable does due owing to environmental harm caused by oil exploration [35].

In (2015), Almayahi B., used a NaI (Tl) detector to evaluate nature radiation isotopes. that machine was used for determining the quantity and quality levels the ^{238}U and ^{232}Thin samples ofsoil taken from Al-Najaf. Mean concentration are about (102 to 448) Bq/kg and (79 to 1887) Bq/kg of ^{238}U and ^{232}Th respectivily [36].

In (2015), Hatif K. H. and Muttaleb M. K., studied the measured level of radioactivity in ten soil sites in the city of Hilla (Iraq) NaI(Tl) detector is used., the average specific of radioacativity of ^{328}U, ^{232}Th and ^{40}K were (14.079 ± 0.46, 12.326 ± 0.43 and 416.655±2.86 Bq. Kg^{-1} respectively [37].

In (2016), Hatif K. H. and Muttaleb M. K., studied the concentration of radon and for ten sites of the soil of the city of Hilla (Iraq). Solid state nuclear detectors were utilized in this experiment, and samples were gathered at 30 cm of depth below the surface at each location. The maximum radon activity measured was 12700 Bq.m-3, while the lowest was 25 Bqm^{-3} [38].

In (2016), Ajiboye Y. et al., determined the concentration of radon in the soil of Aramoko, Ekiti State, Nigeria, using CR-39. Gas concentration was found in the study area between (630 and 35040) $Bq.m^{-3}$ and mean value was 9820±0.56 $Bq.m^{-3}$. this results were higher than the allowable limit [39].

In (2016), Karim M. S. et al., used NaI(Tl) scintillation detector of crystal dimensions (3"×3"), an active site of radioactive elements was calculated for 10 samples of soil taken from the antiquity's region of archaeology Al-Hilla city. Values of concentrations to ^{238}Uabout (9.050 $Bq.kg^{-1}$) and (21.221 $Bq.kg^{-1}$), its mean is(15.485 $Bq.kg^{-1}$), concentrations to ^{232}Th about (11.159 $Bq.kg^{-1}$) and (19.400 $Bq.kg^{-1}$) and mean is (15.5005 $Bq.kg^{-1}$), while a concentration activity for ^{40}K about (122.255 $Bq.kg^{-1}$) to (232.550 $Bq.kg^{-1}$), and average was (170.200 Bq/kg) [40].

In (2016), Kadhim I. H. and Muttaleb M. K., measured the amount of natural radiation of the Tuirij region in the province of Karbala (Iraq).Using a NaI(Tl) gamma ray detector,the gamma-ray spectrometry technique wasused, and activitycons. ^{40}K, ^{232}Th and ^{238}U values were detected. The following were the negative effects of the radioactive nuclides of concern for the soils: With a meanof (245.1 Bq/kg) and ^{40}K being (271.2170 Bq/kg) ^{232}Th was (67.092.9 Bq/kg) with an a mean (24.47 Bq/kg), whereas ^{238}U was (30.965.86 Bq/kg) with a mean (19.45 Bq/kg) [41].

In (2017), Rejah B.K. and Ashoor G. T., studied the concentration of the radon gas was calculated in Al-Haswa city in Baghdad governorate using a technique Nuclear Impact Tracking Detector (CR-39). Eight samples were selected in eight districts of the city Al-Hasswa in Baghdad governorate and VIA set the dose measures for 30 days. The rate of concentration of the radon gas was (424.24 $Bq.m^{-3}$), which was less than the global permissible range

(1100 Bq.m^{-3}). Calculate the concentration the annual effective dose and possible alpha energy. The relative relationship between the dose determined the annual equivalent and the concentration of the radon gas for a region under the study [42].

In (2017), Alausa S. K. et al from Nigeria., studied the (TF) of radionuclides, from soil-to-palm oil using NaI(Tl) gamma ray detector. They found For ^{40}K, ^{232}Th and ^{238}U, the mean (TF) were 0.17, 0.06, 0.27, and 0.28, respectiviely [43].

In (2018), Rajesh S. et al., studied the ionizing radiation emitted from the nuclei of ^{40}K, ^{232}Th and ^{238}U for soil samples from Devadurga and Lingasugur of Raichur area of Karnataka, India. Which were found in environmental materials and which it contributed significantly to the radiation dose received by humans, using NaI(Tl) detector(4” × 4”) the sample spectrum was measured for 60,000 s. They found in range (10 – 119) Bq/kg, (8 – 285) Bq/kg and (46 – 1646) Bq/kg of ^{238}U, ^{232}Th and ^{40}K respectivily [44].

In (2019), O. Ntim et al., determined concentrations of radon and annual effective dose to 50 Ghanaian bottled water samples of Greater Accra, Ghana. In all analyzed water, the range and mean radon concentrations were 0.03 to 0.09 Bq/L and 0.06±0.01 Bq/L correspondingly. Measurements of radon concentrations were done by using RAD7-H_2O. The "United States Environmental Protection Agency (US-EPA)" contained the annual effective dose and measured radon concentrations [45].

In (2019), E. El-Araby et al., the level of radon in samples of drinking and ground water gathered from several positions in the Saudi Arabian city of Jazan was measured. Radon levels in groundwater and drinking water, respectively, were found to be 2.470.14 and 2.950.22 Bq/L. The average annual effective dose from drinking and breathing ground water was measured at 24.25 1.33 and 28.99 2.12 μSv/y, respectively. correspondingly, using the sealed cup approach [46].

In (2019), Rejah B. K. et al., calculated the (TF) of ^{238}U from soil to plants using CR-39 (nuclear track detector). For the transfer factor, It is concluded that highest value 0.416 were found in Spinacia plant and the lowest value 0.323 were found in BEASSICA Oleracea Var Capitata plant [47].

In (2019), I. Al-Alawy and A. Hasan., studied the concentrations of radon in underground watersamples in Karbala, Iraq by using CR-39 detector. The results were that highest were 4.152±2.2 Bq/L, where lowest were 2.165±1.6 Bq/L. The maximum Annual Effective Dose (AED) were 14.34±3.5 μSv/y, whereas the minimal value were 8.66±3.1μSv/y. Radon level concentrations, in the investigated groundwater samples was less compare with allowed permissible value [48].

In (2020), Ridha A. A. et al from Iraq., studied the (TF) of employing soil-derived natural radionuclides to create silhouettes of plants by useing NaI(Tl) γ-spectrometry. They discovered that before and after irradiation, the mean transfer factor was 1.06, 0.72, and 1.4, respectively. Before irradiation, it was 1.0.2, 0.7, and 0.8, respectively. The Yucca elephant plant had the highest level of radon adsorption, whereas the Syngonium plant had the lowest level [49].

In (2020), Elsaman R. et al., studied the gamma-ray spectrometer's (TF) of naturally existing radionuclides to sesame and cowpea from Egyptian clay loam soil. They discovered that the average transfer factor values for ^{226}Ra, ^{232}Th, and ^{40}K were respectively 0.51, 0.53, and 1.36 for cowpea and 0.42, 0.43, and 1.33 for sesame. According to the findings, sesame and cowpea have quite different transfer factors [50].

In (2020), Ilemona C. et al., A study focused on monazite and zircon minerals containing radionuclides ^{238}U and ^{232}Th, with monazite being more common. These radionuclides, ranging in size from 10 to 80 micrometers, exhibit surface features suggesting potential dissolution into hazardous PM2.5 aerosol particles, posing a risk of concentrated exposure and long-term respiratory problems. To mitigate these risks, proper storage in wet ponds is crucial for preventing the release of radionuclides, radon gas, and high indoor gamma radiation levels. Coal ash samples from both mines showed three to five times higher activity rates and radioactivity damage indices compared to average soil levels[51].

In (2020), El-Taher, A., Abojassim, A., Najam, L., & Mraity, H., determining the level of contamination in groundwater with radon. The RAD7 detector was used to carry out the measurement. With a mean of 5.18 0.39 Bq/L, the observed radon concentration values varied from 1.20 to 15.43 Bq/L. Based on radon levels in drinking water, the predicted total annual effective doses for babies, children, and adults ranged from 6.34 to 81.62 Sv/y, 2.34 to 30.04 Sv/y, and 3.07 to 39.42 Sv/y, respectively. Additionally, it was determined that the corresponding mean values were 27.412.06, 10.080.76, and 13.230.99 Sv/y, respectively [52].

In (2021), Abojassim, A. A., stuied the natural radioactivity used in this investigation in 12 groundwater samples taken from various locations in several Mashhad, Iran cities was examined. Using a NaI(Tl) detector, thespaecific activity of ^{238}U, ^{232}Th, and ^{40}K was datermined. For allsamples inthe current study, radiological and chemical hazards based on uranium-238 were also calculated. The particular activity results in units of Bq/L for ^{238}U varied from 1.750.15 to 15.880.46 with an average of 7.791.3, ^{232}Th from BLD to 1.550.07 with an average of 0.830.3, and ^{40}K from BLD to 79.701.10 with an average of 53.547.49. The AED (annual effective dose) and LCR (lifetime cancer risk) of uranium-238, on average, were 0.25 mSv/y and 0.98 mSv/y, respectively [53].

In (2021), Leandro B. et al., calculating committed effective dose and the risk of cancer as a result of ^{40}K, ^{226}Ra, and ^{232}Th intake from crops grow in H.B.R.A. For ^{40}K, ^{226}Ra, and ^{232}Th, larger activity cons. are (606.20 - 25.130), (8.07 6.37), (10.010 - 1.450) Bq.kg^{-1}respectively. The willing to commit effective dose was assumed to be 0.5 mSv.y^{-1}, and the risk of developing cancer suggests that unrestricted usage of beans grown in this H.B.R.A. is not beneficial [54].

In (2022), Ahmed, R. S., the results demonstrate that, with the exception of Sulaimany, Baserah, where eleviated quantities of radioactivity material has been found, andthe Al-Dura thermal power plant, radonand radioactive elementsin soil samplesare within the international standard limits. Here, we analyze the research done to gauge the radioactive levels in the soil, water, and vegetation of Iraqi cities [55].

In(2023), Hady, H. N., & Baqer, Z. S., the study examined radiation transfer factors (TFs) in plant life in the Al-Hussainiya region of Karbala, Iraq. The Okra plant had the highest specific activity of ^{238}U at 17.89 Bq/kg, while soil had 24.52 Bq/kg. For ^{232}Th, the common pea plant had 10.96 Bq/kg, and the soil had 12.86 Bq/kg. In the case of ^{40}K, soil had 324.40 Bq/kg, and the eggplant plant had 274.58 Bq/kg. Eggplant samples had the highest TF at 0.885, common pea samples had the highest ^{232}Th TF at 0.847, and eggplant samples also had the highest ^{40}K TF [56].

In (2023) Amoatey, E. A., Glover, E. T., Kpeglo, D. O., Otoo, F., & Adotey, D. K., found in their study that prior to disposal, knowledge of the precise radio-isotopic signatures of the NORM waste disposal location is crucial to determining the baseline radiation levels. The soil and water from a NORM waste site at Sofokrom in Ghana's Sekondi-Takoradi Metropolis are identified and described in this article. In soil samples, the average activity concentrations of of^{226}Ra, ^{232}Th, and ^{40}K were determined for these elements were 40.31 ± 13.8 Bq/kg, 63.29 ± 23.18 Bq/kg and 198.71 ± 49.10 Bq/kg, respectively. The avereage values for ^{226}Ra and ^{232}Th were greater than the UNSCEAR's average global values. Additionally, the ^{226}Ra and ^{232}Th average activity levels of water samples taken from monitoring boreholes are within the 1 Bq/L WHO recommended range [57].

1.4 The Aim of the Present Syudy

This study aims to measure natural radioactivity and radon gas (^{238}U, ^{232}Th, ^{40}K and ^{222}Rn) in soil, water and crops from the Haidariyah region using nuclear techniques such as (RAD7, NaI(Tl), CR-39), there are also other goals, including:

1. Determinaing radon gas concentrations in water
2. To determine gamma emitters in soil and crops.
3. To determine risk factors due to alpha in water.
4. dentifying risk factors due to soil moisture
5. dentifying risk factors due to kamma in crops

6. Establishing is to establish an alpha emitters map that will serve as a reference for future studies using GIS technology.

Chapter Two

Theoretcal Part

2.1 Introduction

The word "radiation" can mean various forms of radioactive energy like radio waves, microwaves, and visible light. Ionizing radiation, the most common type, causes atoms to lose electrons. We use radiation detectors to find it. Things like aviation gear, medical devices, power plants, nuclear weapons, and cosmic rays release ionizing radiation. People often encounter this type of radiation, and about 80% of it comes from natural sources [2].

2.2 Types of Radiation

There are two kinds of radiation can be classified according to charge, mass and other parameters. Bat the most important classification is the amount of energy. The radiation with a low energy level is called as non-ionizing radiation and the one with a high energy level as ionizing radiation [58].

2.2.1 Alpha Particles

An alpha particle is a form of radiation that carries a positive electric charge. It consists of two neutrons and two protons, similar to a helium atom (^{4}He). Alpha particles are emitted when unstable isotopes undergo fission. Alpha particles have mass and a positive charge but lack the ability to penetrate materials. They can be stoppted by a sheete of paiper. This characteristic makes it relatively easy to protect oneself from external exposure to alpha particles. However, internal exposure through inhalation, swallowing, or wounds can cause significant damage to human cells if subjected to a high degree of ionization [59].

2.2.2 Beta Particles

Beta particales are electerons emiatted from the nucleuis, and they have continuous distribution of energy. They can carry either a negative or positive charge. The main difference between beta particles and alpha particles is that beta particles have a smaller mass, allowing them to penetrate materials more easily. To stop beta particles, thin foils made of materials like aluminum or plastic are required. Therefore, it is crucial for human beings to be protected from external and internal exposure to beta particles due to their ability to penetrate human tissue. Internal exposure to beta particles can be harmful, similar to exposure to alpha particles [59].

2.2.3 Gamma Rays

Gamma rays belong to the electromagnetic spectrum and have a short wavelength and high frequency. They are emitted from certain nuclei following processes such as nuclear fission or the decay of radioactive isotopes after the emission of alpha particles. The emission of alpha particles from unstable nuclei, in their journey towards stability, ressults in the emeission of gamma-ray with specific energies corresponding to the transitions between nuclear energy levels. The gamma-ray spectrum provides a precise and advanced means of studying radioactive nuclei. Gamma rays possess high energy and great penetration capabilities through materials and the human body. To shield the body from these rays, it is necessary to use materials with high atomic numbers like lead [59].

2.3 Sources of Natural Radiation

There are three sources of natural radiation that can be arranged into cosmic radiation, terrestrial radiation, and internal radiation [60]. All are explaind below:

2.3.1 Cosmic Rays

This type of natural radiation refers to primary energetic particles originated from outer spaec that penetraten the Earth's atmosphere, as well as the secondary particles produced as a result of their interactions within the atmosphere. Cosmic radiation consists primarily of highly energized and positively charged particles, with protons being the most common, along with high-energy photons [61]. Due to the high atmosphere, most cosmic rays do not reach the Earth's surface, but interactions between cosmic rays and the Earth's atmosphere can lead to the creation of certain radionuclides [2]. These interactions give rise to various radionuclides known as cosmogenic radionuclides, including $^{3}H,\ ^{7}Be, ^{22}Na$ and others [62].

The interaction between atmospheric atoms and cosmic rays leads to the generation of considerable cosmogenic radioactivity [63].

2.3.2 Terrestrial Radionuclides

Terrestrial radionuclides are commonly present in rocks, soil, water bodies, rivers, and construction materials. These radionuclides were originated during the early stages of Earth's formation and are characterized by extremely long half-lives relative to the age of the Earth [63,64].They include for a half-life of (1.39$\times 10^{10}$ years), (4.51$\times 10^{9}$years), and (7.4$\times 10^{8}$years), respectively, are a few of them. Other radionuclides, such as ^{235}U with a half-life of 4.7 years, are only of little significance.

The radionuclides ^{232}Th and ^{238}U are part of a series of other radioactive elements that contribute to human exposure through external sources, such as radioactive materials deposited on the ground, as well as internal sources, including inhalation or ingestion of radioactive materials in the air, food, or water [1].

2.3.3 Internal Radiation

The human body naturally contains radioactive elements that contribute to internal radiation. Carbon and potassium are among the primary sources of internal radiation [65]. Additionally, the alpha decay products of the thorium radioactive series, along with uranium, make significant contributions to the radioactivity within the human body, particularly radon and thoron [66].

2.4 Decay Series of Natural Radionaclide

Regarding the isotopes related to terrestrial radiation, notable ones include the ^{238}U and ^{232}Th series, as well as ^{40}K. The decay products of ^{238}U, such as ^{226}Ra and ^{222}Rn, are primarily formed through terrestrial radiation. The presence of these radionuclides in soil and air leads to external irradiation. On the other hand, internal radiation occurs when radionuclides are ingested or inhaled [86]. Figures (2.1), (2.2), (2.3), and (2.4) show the three natural series (^{238}U, ^{235}U, and ^{232}Th), and the single series (^{40}K) [67-69]. Among these series, the longest-lived member is ^{238}U, which belongs to the $(4n + 2)$ series (with n ranging from $59\ to\ 51$). The longer half-life member of the $(4n + 3)$ series is ^{235}U (with n ranging from $58\ to\ 51$). The paraent of the $(4n)$ radioactivity decay seiries is ^{232}Th, , with n varying from $58\ to\ 52$ [70,71].

Natural potassium, specifically ^{40}K, has a half-life of approximately 1.277 billion years. It exists with an isotopic abundance of 0.0118%. The decay of ^{40}K predominantly occurs through beta decay, where 89% of the time it decays into ^{40}Ca. The remaining 10.72% of ^{40}K undergoes electron capture to transform into the stable isotope ^{40}Ar. This decay process releases gamma rays at a characteristic energy of 1.461 MeV [72].

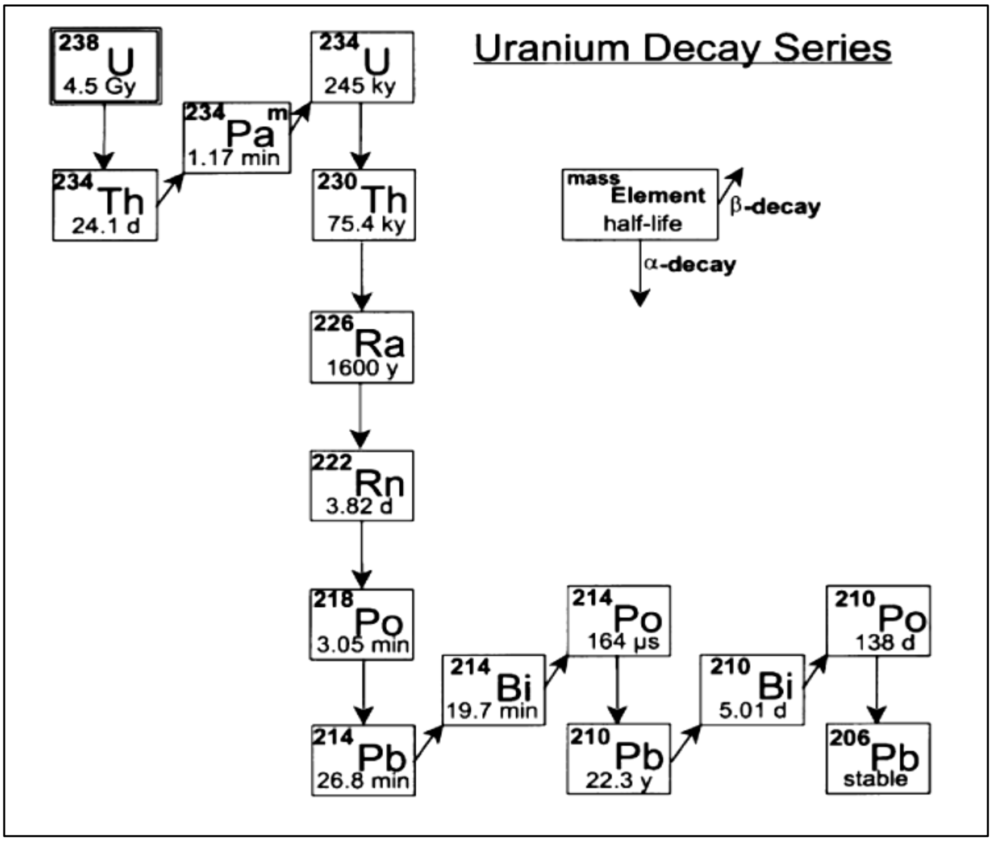

Figure 2.1: Decay Series of ^{238}U [67].

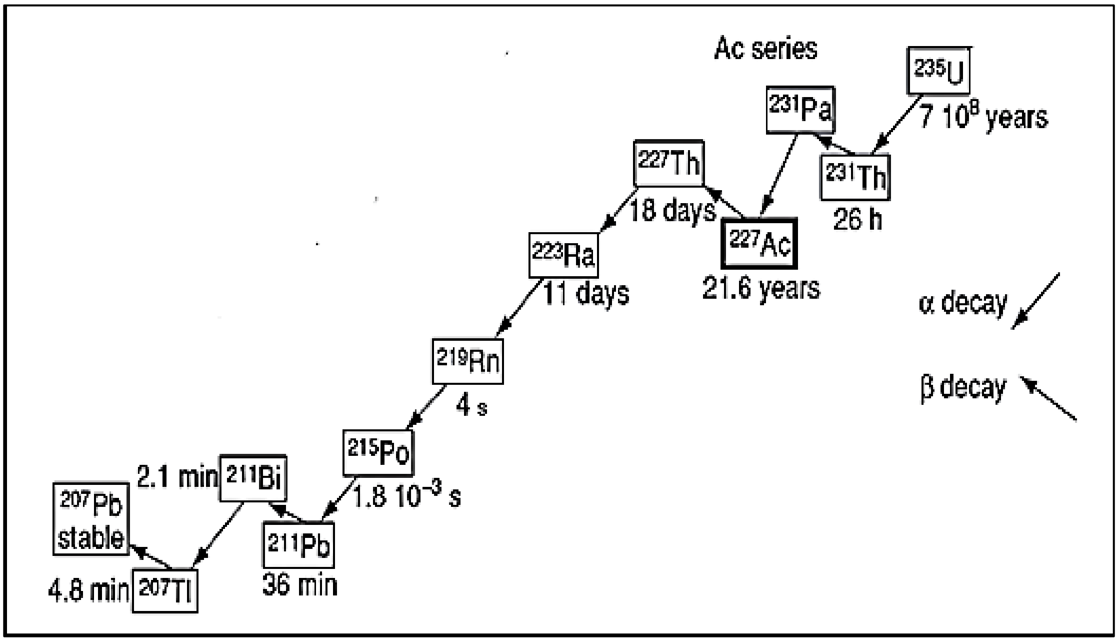

Figure 2.2: Decays Series of ^{235}U [68,69].

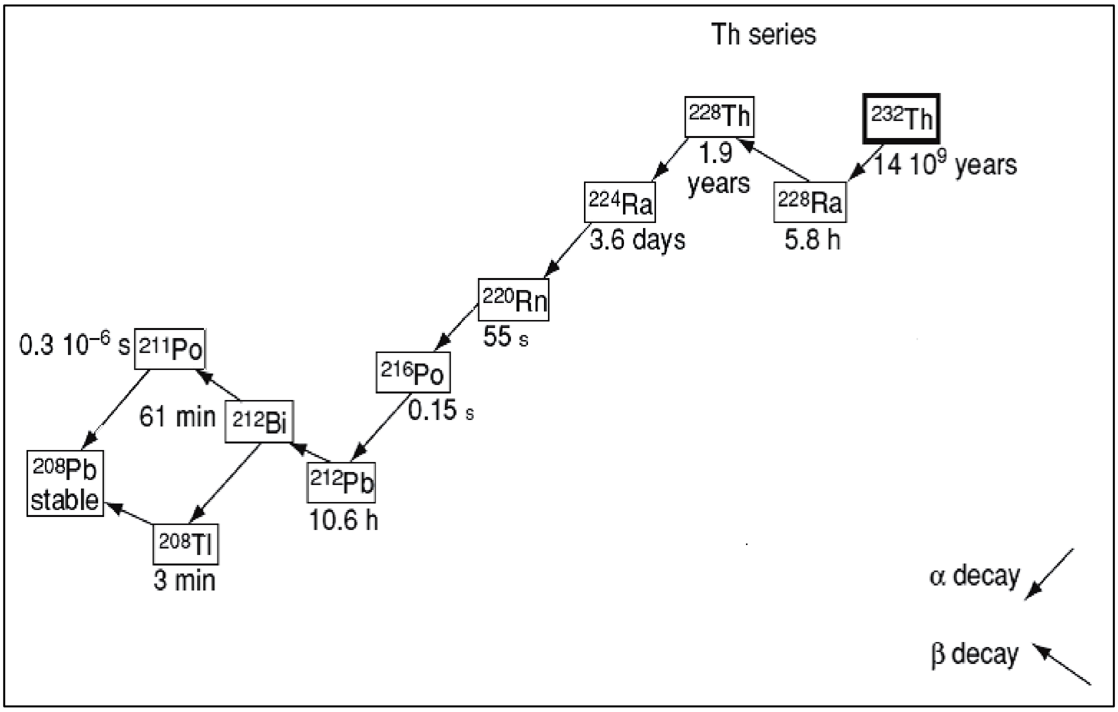

Figure 2.3: Decays Series ^{232}Th [69].

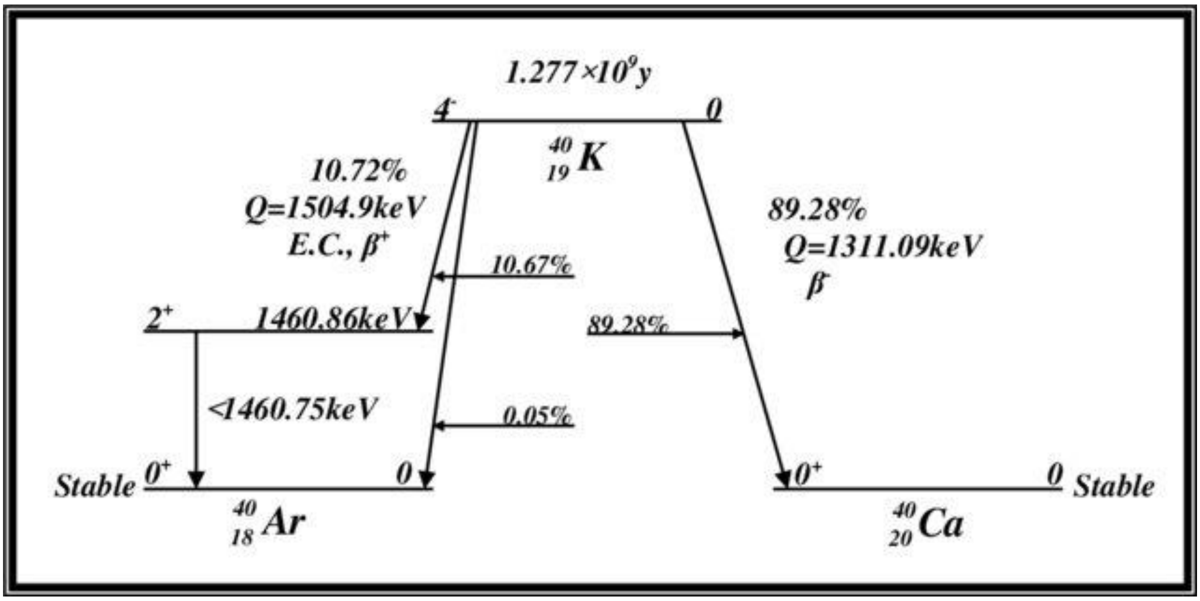

Figure 2.4: Decay-scheme of ^{40}K [69].

2.5 Gamma-Rays Interaction with Matter

The interaction of gamma-rays with matter differs from that of heavy charged particles and electrons. When gamma-rays (photons) interact with matter, they lose energy in a single collision. This energy loss can occur through absorption or scattering, causing a decrease in the photon's energy. As gamma-rays penetrate through materials, their intensity decreases, following the relation [73]:

$$I = I_o e^{-\mu x} \qquad (2.1)$$

I_o: Gamma-rays intensity before it penetrates a materials.

I: The intensity of gamma-rays incident on materials..

X : Thick-ness of materials.

μ : Linear absorption coefficient.

The factor (μ) depends on the kind of materials and on the energy of the incident gamma rays on it. Therefore, the equation (2.1) represents the proportion radiation between the incident gamma-rays and the interaction with the material of detector as photoelectric absorption, Compton effect,and pair production as follows [74]:

2.5.1 Photoelectric Effect

When incident photons interact with bound electrons in an atom, the result is the photoelectric effect. The electrons absorb all of the photon's energy, providing enough energy for them to be released from the atom [74].

$$E_e = hv - B.E \qquad (2.2)$$

Where:

E_e : The kinetic energies of the released electeron.

hv : The nergy of incident photons.

$B.E$: The binding energies of the shell electeron.

This idea is based on the fact that the energy related to an atom is much smaller than the energy of an electron, mainly because atoms are much heavier (have a larger mass) than electrons. In the photoelectric effect, the outer electron in an atom absorbs all the energy from the incoming photon. This leaves an empty space in the outer orbit, but the atom quickly adapts by rearranging its electrons. To fill the gap, an inner-orbit electron is shifted, which causes the emission of X-rays. Sometimes, instead of X-rays, an Auger electron can be emitted.

When dealing with a thick material, there's a high chance that any secondary rays will be absorbed by the material itself. Because of this, most detectors are designed to specifically detect and study gamma rays. The likelihood of a photoelectric reaction happening increases as the atomic number (Z) of the absorbing material gets higher. You can see this phenomenon illustrated in Figures 2.5(a,b) [74, 75].

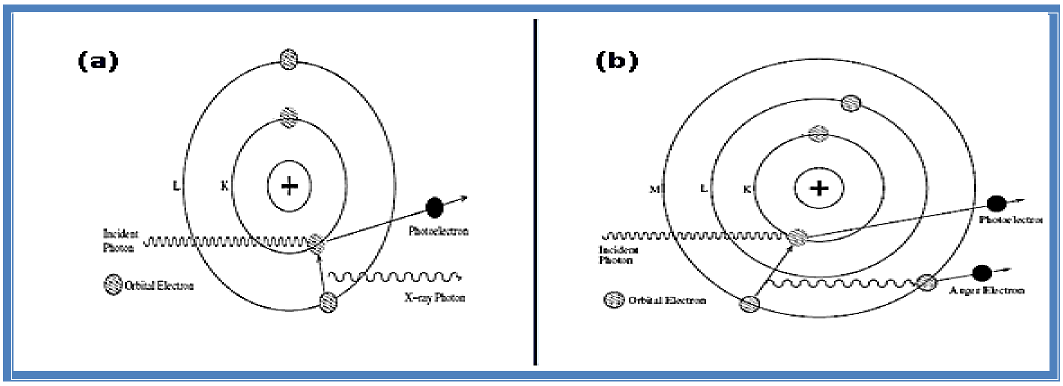

Figure 2.5: Photoelectric effect [74].

2.5.2 Compton Scattering

Compton scattering occurs when photons with energies in the range of 0.1 to 10 MeV interact with free electrons. During this process, a free electron absorbs energy from the incoming photon by interacting with the free electrons in an atom. Consequently, the photon loses some of its energy to these electrons, leading to the release of the free electron from the atom. The remaining energy is carried by the scattered photon, which now has less energy compared to the incident photon and changes direction by an angle Φ due to its interaction with the atomic nucleus (Z) as shown in Figure 2.6 [73-75].

The kinetic energies of the liberated electrons can be calculated using the equation:

$$E_e = hv - hv' \qquad (2.3)$$

Change in wavelength can be determined using the following calculation:

$$\Delta\lambda = \frac{h}{m_o c}(1 - \cos\theta) \qquad (2.4)$$

From equation (2.3) defines the relationship of Compton:

$\frac{h}{m_e c}$ This amount equals (0.024 $\mathring{A}$) which is the wave length of the compton wave ($\lambda_{cp.}$).

Δλ : the Compton shift is the change in wave length of radiation before and after the collision ('λ-λ) [74].

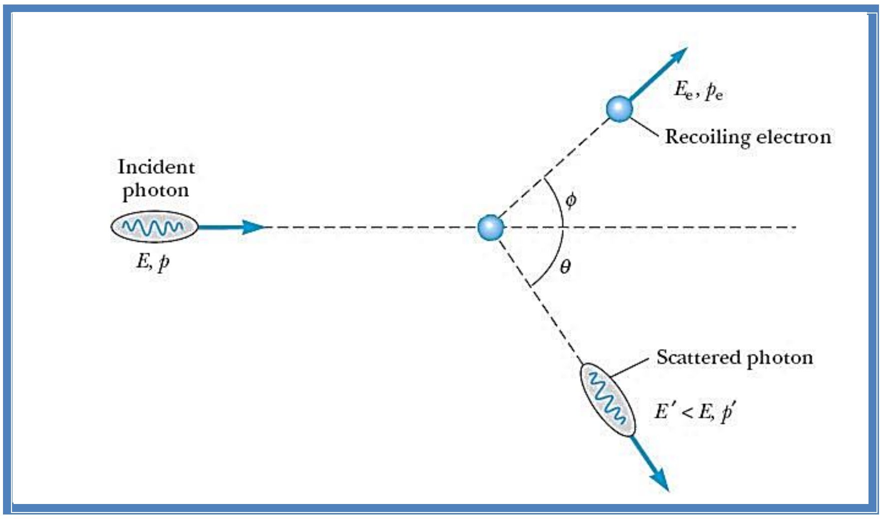

Figure 2.6: The compton scattering [74].

2.5.3 Pair Production

The pair production process takes place when the energies of the incoming photons surpass twice the rest energies of an electron, which is equivalent to 1.022 MeV. When a gamma-ray with energy (Eγ) encounters the intense Coulomb barrier of a nucleus within a material, it results in the creation of a pair of electrons and positrons. This process is guided by the conservation of energy law, as depicted in Figure 2.7. The energy of the photon can be calculated using the following equation [76]:

$$E_{e^-} + E_{e^+} = hv - 2m_o c^2 \qquad (2.5)$$

Where:

$E_{e^-} + E_{e^+}$: The kinetic energies of the positron and the electeron respectively.

hv : The kinetic energies of the photon.

$2m_o c^2$: The sumation of the resters energy of the electeron and positeron.

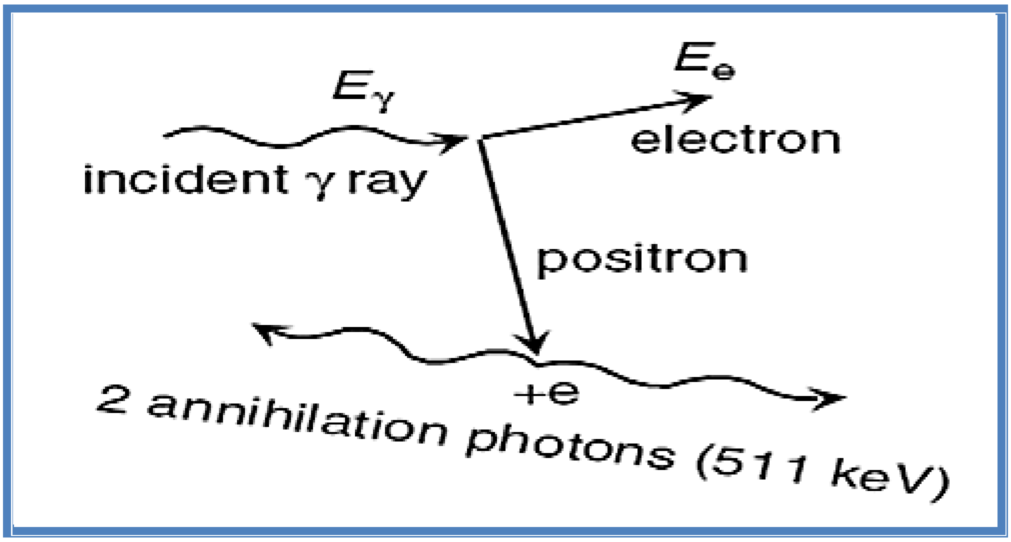

Figure 2.7: Pair Production [73].

The excess energy of gamma rays is transferred to the kineatic energies of the electeron (e^{-}) and positron (e^{+}). As the positron loses energies, it tends to combine with a nearby electron, causing both particles to annihilate. This annihilation process results in the production of gamma-ray photons with an energy of 0.511 MeV, emitted in opposite directions [77].

The probability of this reaction occurring increases with the square of the atomices numbuer (Z) of the matereial and the energies of the incidental gamma-ray E_γ [78].

2.6 Interactions of Alpha Particles with Matter

The alpha particle, denoted as (^4_2He), can be emitted from the parent atom and the resulting nucleus. It has two fewer protons and two fewer neutrons compared to its parent atom. Alpha particles, which are a type of ionizing radiation, are the least harmful among the various forms of radiation emitted by unstable heavy metals [79]. These particles are larger and carry a greater charge than other sources of ionizing radiation, making them more dangerous to biological tissues. As the positively charged alpha particle travels through a substance, it attracts many orbital electrons from nearby ionic pairs.

Uranium, represented by the symbol U, serves as a significant source of alpha particles. It is a naturally occurring radioactive element characterized by its heavy metal properties and toxicity. Uranium comprises several radioactive isotopes, such as ^{238}U, ^{236}U, and ^{235}U, which undergo particle emission and nuclear radiation. Some noteworthy attributes of uranium include its substantial weight, silvery-white appearance, toxic nature, high melting point (1132 °C), and density at 25 °C (18.9 g/cm^3) [80].

Uranium (^{238}U), radon (^{222}Rn), and radium (^{226}Ra) belong to the same group because they are radionuclides. These elements are very unstable and release ionizing radiation [81]. Radium (^{226}Ra), radon (^{222}Rn), and uranium (^{238}U) are found naturally in the environment. The presence of uranium (238U) in the Earth's crust, at approximately 3 parts per million as estimated by geologists, is essential for the occurrence of radium (^{226}Ra) in its natural surroundings. Radium (^{226}Ra) is the main source of radon (^{222}Rn),which goes through a series of radioactive decay steps until it eventually changes into lead, a stable non-radioactive element (206). This process leads to the creation of radon (^{222}Rn). Although radon is primarily in a gaseous state, various types of rocks contain solid forms of uranium (^{238}U) and radium (^{226}Ra). Radon can also be dissolved in both water and air [82].

2.7 Radioactive Equilibrium

Decay series occur when all radionuclides undergo decay at the same rate, resulting in three different forms of equilibrium: no equilibrium, temporary equilibrium, and secular equilibrium. The specific type of equilibrium that is achieved depends on whether the half-live of the parentes nuclide is longer or shorter than of the doaughter nuclide [83].

2.7.1 Secular Equilibrium

Secular equilibrium occurs in a decay series when one radionuclide has a considerably longer half-life compared to the others, resulting in the daughter activity being equal to the parent activity, (A_P=A_D). This equilibrium state can be observed in Figures (2.8) [84].

$$\lambda_D \gg \lambda_P \quad or \quad (t_{D\,1/2} \ll t_{P\,1/2}) \qquad (2.6)$$

$$\frac{A_D}{A_P} = 1 \qquad (2.7)$$

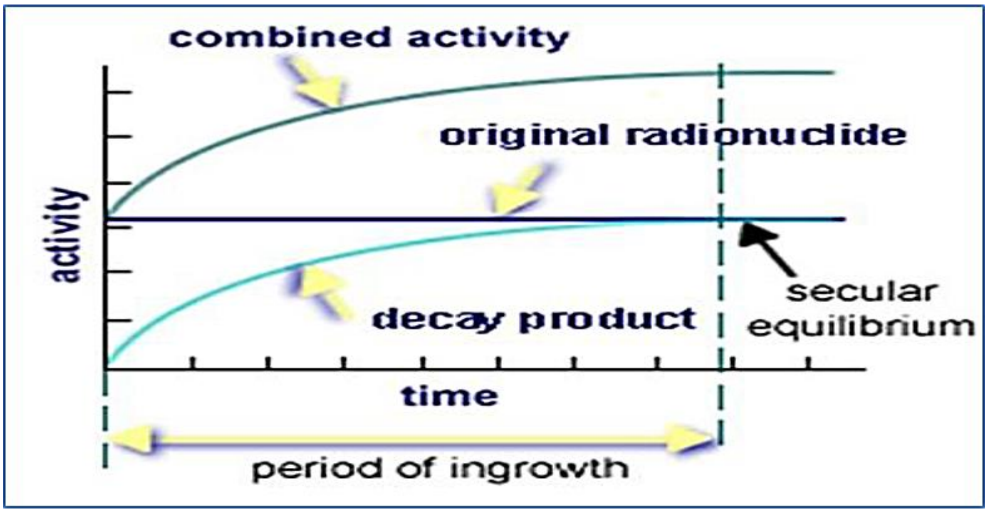

Figure 2.8: The secular equilibrium [84].

2.7.2 Transient Equilibrium

Transient equilibrium takes place in a decay series when the parent radionuclide has a longer half-life than the daughter radionuclide. You can see this in Figure 2.9. When the parent and daughter have the same half-life, the daughter will start to decay once its activity surpasses that of the parent. The activity of the daughter, indicated as A_2, gradually increases with time following the equation ($A_2 = \lambda_2 N_2$). As time goes on, the term ($e^{-\lambda_2 t}$) becomes much smaller compared to ($e^{-\lambda_1 t}$), resulting in the following relationship[85]:

$$A_2 = \frac{\lambda_2 \lambda_1 N_1 e^{(-\lambda t)}}{(\lambda_2 - \lambda_1)} \qquad (2.8)$$

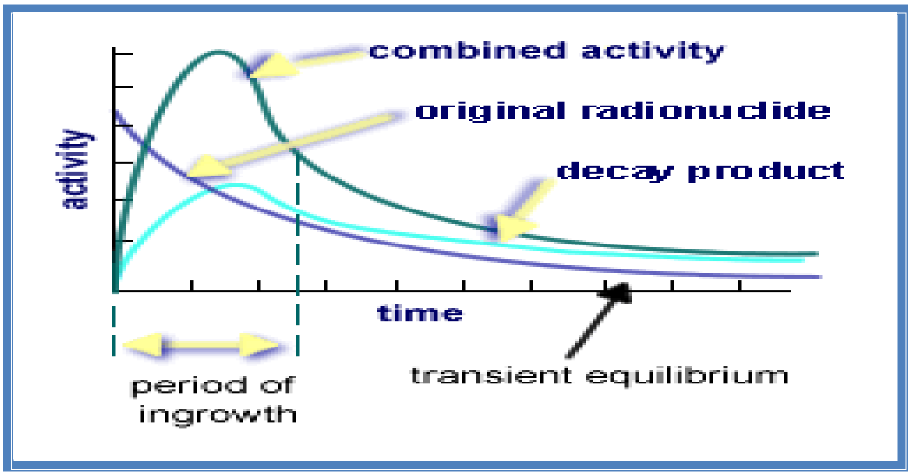

Figure 2.9: The transitional equilibrium[85].

2.7.3 No Equilibrium

When the half-life of a parent radionuclide is shorter than that of the daughter, equilibrium is not attained. This can be seen in Figure 2.10. In this scenario, the activities of the parents decrease over time, while the activities of the daughter undergo changes [106].

$$(t_{1/2})_1 < (t_{1/2})_2 \quad , \qquad or \quad \lambda_1 > \lambda_2 \qquad (2.9)$$

$$\lambda_P > \lambda_D \qquad (2.10)$$

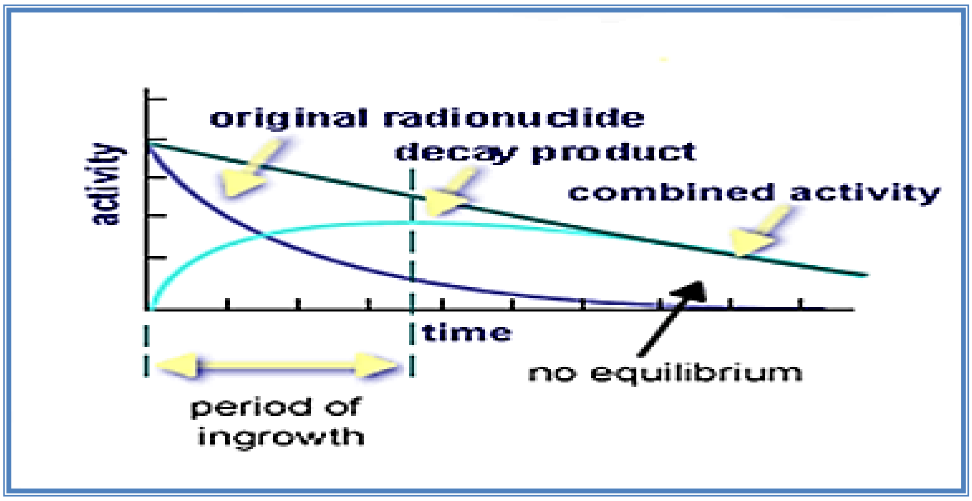

Figure 2.10: No Equilibrium[86].

2.8 Radon Gas

A noble gas known as radon is tasteless, colourless, radioactive, and odourless. Radon is considered to be a substantial source of radioactivity in the atmosphere since it is really the heaviest noble gas in nature. When thorium and uranium are present in sufficient quantities in rocks, soil, and building materials, radon can be created. Because of the disintegration of uranium, radon naturally exists. Radon accounts for almost 50% of the natural radiation that people are exposed to. Three separate radioactive decay paths, each starting with ^{235}U, ^{232}Th, or ^{238}U, produce the three naturally occurring isotopes of radon: ^{219}Rn, ^{220}Rn, and ^{222}Rn. Radon-222 (half life 3.83 day) is a radionuclide that normally emanates from the soil in the form of gas. It is derived from the decaying uranium-238 series existing in the earth's rocks and soils. Once inhaled, some of the short-lived Radon decay products, primarily ^{218}Po and ^{214}Po, are stored in the lungs and irradiate cells with alpha particles in the respiratory tract [89].

The primary source of Radon found in buildings and homes is the soil and air. It enters the atmosphere through diffusion. Radon in the soil and air can also dissolve in groundwater, which becomes a complicating factor as it carries the radon to locations far from its original formation site [90].

Actineon (^{219}Rn) with a half-life of 3.96 seconds and Thoruon (^{220}Rn) with a half-life of 55.6 seconds have shorter half-lives and lower abundances compared to ^{222}Rn (Radon) with a half-life of 3.82 days. Alpha particles delivered to the tracheobronchial tree by 220Rn are only 1 to 3 times that of 222Rn per unit of exposure. This is an important factor to consider in dosimeter measurements. While the measurement of actinon (^{219}Rn) or thoron (^{220}Rn) may be a primary concern in certain exceptional occupational or environmental settings, such situations are rare up to this point [91, 92].

The radioactive decay characteristics of the three naturally occurring radon isotopes are summarized in Table 2.1 and Figure 2.11.

Table 2.1: The radioactivity decay property of radon isotopaes [93].

Series	Isotope	Historical name	Half-life	Principal radiation energies of alpha and intensities	
				MeV	%
Actinium	^{119}Rn	Actinon(An)	3.96 s	6.81 6.54	81 12
Thorium	^{220}Rn	Thoron(Tn)	55.60 s	6.288	100
Uranium	^{222}Rn	Radon (Rn)	3.82 d	5.490	100

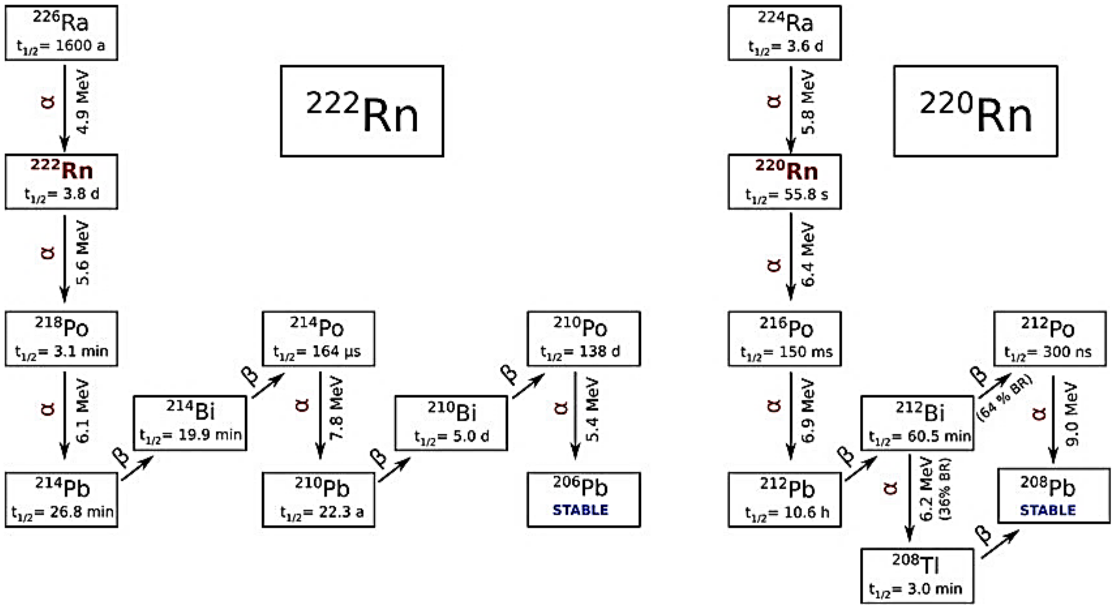

Figure 2.11: The radon and thoron-decay chart [94].

2.9 Sources of Radon

2.9.1 Sources of Radon in Groundwater

It is possible to hypothesize that there are two sources of radon that can enter groundwater [95].

- Direct emission of radon from the uranium and thorium decay series
- Radioactive decay of dissolved radium

In materials containing ^{226}Ra, ^{222}Rn is produced; some of it escapes from these materials and enters the pore space. This portion can move through the pores relatively easily. As a result, radon can enter human-accessible air or water if the transport process is rapid enough to occur before the radon decays [96].

2.9.2 Source of Radon in Soil

At least 80% of the radon present in the atmosphere originates from soil that was formed from rocks rich in ^{238}U. These rocks contain uranium, and as

^{238}U undergoes radioactive decay to ^{226}Ra, ^{222}Rn is produced. Certain types of rocks, such as granites, black shale, light-colored volcanic rocks, phosphate-rich sedimentary rocks, and metamorphic rocks derived from these sources, tend to have higher average levels of uranium [97]. In comparison to ^{238}U and ^{226}Ra, which are fixed within the Earth's rocks and soil, radon is highly mobile as it is a gas. The ^{222}Rn gas can seep out from the soil and rocks, entering the spaces between soil particles and through cracks and fissures in the rocks [98].

2.9.3 Health Effect of Radon

The primary cause of damage from radon gas is the harm inflicted by alpha particles. The potential outcomes depend on the level of exposure. The most significant risk associated with high radon levels is an increased likelihood of developing lung cancer. Although 222Rn, being a noble gas, is rapidly expelled from the body, the radon progeny mixes with other airborne particles like dust, aerosols, and smoke particles, and can easily settle in the airways of the lungs. Once trapped there, the progeny release ionizing radiation in the form of alpha particles, which can harm the cells lining the airways [99].

Human studies have provided direct evidence linking radon exposure to lung cancer. As a result, radon has been classified as a Group 1 carcinogen by the International Agency for Research on Cancer (IARC) [100]. The estimated percentage of lung cancers attributed to radon varies between 3% and 14%, depending on the radon concentration levels in the country and the measurement method employed. It's important to note that not everyone who breathes in radon decay products will develop lung cancer. The quantity of radon, the duration of exposure, and individual smoking habits all contribute to an individual's risk of developing radon-induced lung cancer [101].

Exposure to radon is associated with an increased risk of lung cancer. Radiation, especially from alpha particles, in the lungs is linked to the likelihood of developing lung cancer. In general, alpha particle emissions pose little risk to individuals unless they occur within the body. When radon undergoes decay, alpha particles are released. However, most inhaled radon is expelled before it decays. As a result, only about 5% of the alpha radiation in the lungs is attributed to radon [102].

The primary source of alpha radiation exposure is inhalation of radon particles. The progeny of radon atoms, present in the solid phase, can be ingested as free atoms or attached to particles such as dust, which can be subsequently absorbed by other particles or ingested as a whole. There is a significant chance that these progeny particles will accumulate and decay within the lungs before being inhaled. Polonium-218 and Polonium-214 are two radon progenies that emit alpha radiation, and they are responsible for the majority of the radioactive dose that contributes to lung cancer. The bronchial and bronchiolar regions of the lungs absorb a significant portion of the radiation exposure [103].

2.9.4 Health Eeffect of Radiation

The cell is the fundeamentail unites of a liveing orgeanism, consistinger of complex structures enclosed by a surface membrane. Damage resulting from the interaction of the human body with radiation can lead to cell modification or death, impacting tissues or organ function and resulting in either stochastic or deterministic effects. Radiation can have both direct and indirect biological impacts on living cells. Direct effects occur when ionizing radiation is directly deposited and absorbed, particularly affecting DNA molecules. Compton reactions directly ionize atoms in DNA molecules within the target tissues, and the absorption of energy leads to the photoelectric effect. This energy is sufficient to disrupt bonds, potentially damaging one or both DNA strands and causing electron removal from the molecule. Gamma radiation is a type of ionizing radiation, making it physiologically hazardous[102].

2.10 Radioactivity in Soil

Soil plays a vital role in both agricultural and construction processes. One remarkable property of soil is its ability to serve as a migratory medium, allowing for the continuous transmission of radionuclides into biological systems [113]. The radioactivity present in soil is predominantly influenced by the geology of the rocks that make up the soil [110-113]. However, factors beyond geology also contribute to the distribution of radionuclides in soil, including regional geological events, latitude and altitude of the site, industrial waste, pesticide and fertilizer usage, mineral processing, water treatment, burning of fossil fuels, and unforeseen events such as earthquakes and forest fires. As a result, the natural radioactivity levels can vary significantly among different soil types [114].

2.11 Radioactivity in Food

Various types of food, including fruits, vegetables, grains, pulses, and spices, are part of our diet. Unfortunately, these foods can be exposed to radionuclides emitted into the environment, leading to potential contamination. Since humans consume a diverse range of foods in varying quantities, it is crucial to consider the risk of radioactive contamination in our diet.

The primary sources of radioactive contamination in human nutrition and drinking water are naturally occurring radioactive materials (NORMs). These NORMs consist of radionuclides from the natural decay series ^{238}U , ^{232}Th and ^{40}K [115-119]. Particularly, alpha-emitting radionuclides from the Uranium and Thorium families, such as ^{238}U, ^{234}U, ^{230}Th, ^{226}Ra, and ^{210}Po, pose significant risks of internal radiation exposure and potential health effects [120–123]. These radionuclides are present in the soil, which make a concern as plants can absorb them along with essential nutrients. As a result, varying amounts of these radionuclides can accumulate in different parts of the plants, including their fruits [124]. This uptake occurs through two main pathways: the transfer of radionuclides from the air to the plant and the transfer from the soil to the plant. Ultimately, through the food chain, these radionuclides can find their way into the human body [125,126].

2.12 Theoretical Calculations

2.12.1 Theoretical Calculations for Rad 7

A person's effective dose Ed (Sv/y) from 222Rn in groundwater as drinking water was estimated using the following formula[127]:

$$Ed = Ac\ Ai\ Cf \tag{2.12}$$

where Ac is the radioactive activity content in Bq/l of the sachet water, Ai is the annual consumption of sachet drinking water in liters per year, and Cf is the ingested dosage conversion factor for radionuclides in sieverts per becquerel. In 2000, the United Nations Scientific Committee on the Effects of Atomic Radiations (UNSCEAR) estimated these values to be 23, 5,9, and 3.5 nSv/Bq for newborns, children, and adults, respectively [128]. The annual intake of sachet drinking water for the age groups of ≤ 1, 2–17, and ≥ 17 years were 230, 330, and 730 liters, respectively [129].

2.12.2 Theoretical Calculations for Gamma Emitters

2.12.2.1. Specific-Activity

The specific-activity is defined as its activity per unit mass of a sample, measured in (Bq/kg or Ci/kg). This can be calculated using the equation [130]:

$$A = \frac{N_{net}}{\varepsilon . I_{\gamma} . m . t} \pm \frac{\sqrt{N_{net}}}{\varepsilon . I_{\gamma} . m . t} \qquad (2.13)$$

which:

N_{net}: The net number of counts under the photo peak represents the sample's activity.

$$(N_{Sample} - N_{Background})$$

ε : The efficiency at a specific photo peak energy

I_{γ}: The percentage of gamma emission probability

m : The mass of the measured sample is expressed in kilograms (kg).

The specific activity of ^{235}U can be calculated by using the following equation [131], which relates its specific activity to the specific activity of ^{238}U in soil.

$$A_{U-235} = \frac{A_{U-238}}{21.7} \qquad (2.14)$$

The risk factors related to ^{238}U, ^{232}Th and ^{40}K can be calculated by considering their specific activity values.

2.12.2.2 Radium Equivalent Activity (Ra_{eq})

The Radium Equivalent (Ra_{eq}) is employed to assess the risk associated with a specific activity measured in Bq/kg. This value varies depending on the soil type and provides a standardized measure of the radiation dose it produces from the radionuclides [132,133].

$$Ra_{eq}(Bqkg^{-1}) = A_U + 1.43A_{Th} + 0.077A_K \qquad (2.15)$$

The specific activities of (^{238}U), (^{232}Th), and (^{40}K) are represented as A_U, A_{Th} and A_K, respectively. It is crucial to emphasize that the Radium Equivalent (Ra_{eq}) should not exceed the global limit of 370 Bq/kg [134].

2.12.2.3 Hazard Indices

2.12.2.3.1 Activity Concentration Index (I_γ)

The activity concentration index is employed to evaluate the risk posed by gamma radiation originating from naturally occurring radionuclides found in the subject under investigation. The following formula can be utilized to compute this index [135,136]:

$$I_\gamma = \frac{A_U}{150} + \frac{A_{Th}}{100} + \frac{A_K}{1500} \qquad (2.15)$$

2.12.2.3.2 Alpha Index (I_α)

To determine the alpha index, the equation (2.16) was employed [137].

$$I_\alpha = \frac{A_u}{200(\frac{Bq}{Kg})} \qquad (2.16)$$

2.12.2.3.3 External Hazard Index (H_{ex})

The ionizing risk presented by natural gamma radiation is referred to as the external risk. To assess the risk associated with natural gamma radiation, the external risk factor can be employed and determined using the equation below [138,139]:

$$H_{ex} = \frac{A_U}{370} + \frac{A_{Th}}{259} + \frac{A_K}{4810} \qquad (2.17)$$

2.12.2.3.4. Interenal Hazared Index (H_{in})

Alpha-particales that are emaitted rom short-lives isotopes when inhaling like ^{222}Rn and ^{232}Th, along with gamma-rays, there is a risk that can be expressed as the internal risk factor (H_{in}). This factor can be using the following formula [139]:

$$H_{in} = \frac{A_U}{185} + \frac{A_{Th}}{259} + \frac{A_K}{4810} \qquad (2.18)$$

Ideally, the internal risk factor should be less than one to ensure the safety of respiratory organs and living individuals [140].

2.12.2.3.5 Exposure Rate (X)

To calculate the exposure rate, the equation (2.19) was utilized [141,142].

$$X'\left(\frac{\mu R}{h}\right) = 1.90A_u + 2.82A_{Th} + 0.197A_K \qquad (2.19)$$

2.12.2.4 Radiological doses

2.12.2.4.1. Absorabed Dose Rete in Aire (D_r)

Equation provided below can be utilized to calculate theAbsorbed Dose Ratein Air(D_r), which represents the percentageof airintake in relation to the concentrations of terrestrial nuclei [143,144]:

$$D_r\left(\frac{nGy}{h}\right) = 0.462\,A_U + 0.604\,A_{Th} + 0.0417A_K \qquad (2.20)$$

(0. 462) , (0.621), (0.0417), are the radionuclide conversion factors that normally occur.

2.12.2.4.2. Annuael Eeffective Dose Equivealent (AEDE)

To calculate the annual effective Dose equivalent (AEDE), both the effective dose and the relevant factor should be considered. UNSCEAR (The United Nations Scientific Committee on the Effects of Ionizing Radiation) [145], has provided the conversion factor of 0.7 Sv/Gy, which is used to convert the absorbable dose of gamma-radiation factors in the air into the annual effective dose received by adults. Furthermore, the proportion of time spent outdoors (0.20) is taken into account in the calculations. Based on this information, the annuael effective external dose can be determined by using the following equation [138,142]:

$$(\mathrm{AEDE})_{\mathrm{Outdoor}}\left(\frac{\mathrm{mSv}}{\mathrm{y}}\right) = D_r\left(\frac{\mathrm{nGy}}{\mathrm{h}}\right) \times 10^{-6} \times 8760\ \frac{\mathrm{h}}{\mathrm{y}} \times 0.20 \times 0.7\frac{\mathrm{Sv}}{\mathrm{Gy}} \qquad (2.21)$$

As: the number of hours of the year (8760).

Or

$$AEDE\left(\frac{mSv}{y}\right) = D_r\left(\frac{mGv}{hr}\right) \times 8760\ hr \times 0.8 \times\ 0.7\ (\frac{Sv}{Gy}) \times 10^{-6} \qquad (2.22)$$

2.12.2.4.3 Annual Gonadal Equivalent Dose (AGED)

From equation(2.23) canbe employedto calculatethe annual gonadal equivalent dose [146,120,147].

$$AGED\,(\frac{mSv}{y}) = 3.09A_u + 4.18A_{Th} + 0.314A_k \qquad (2.23)$$

2.12.2.4.4. Excess Life-time Cancer Risk (ELCR)

The (ELCR) is a coefficient that quantifies the increased likelihood of developing lung cancer over a person's lifetime [148]. This risk is calculated based on the assumption of a linear dose-effect relationship with no threshold, following the guidelines of the ICRP (International Commission on

Radiological Protection). According to the ICRP, the fateal cancer risk factor for low doses is $(0.05\ Sv^{-1})$ [149], which means that there is a 5% increase in the probability of dying from cancer for a total dose of (1Sv) received over a lifetime. Therefore, to estimate the cancer risk for an adulterer, the following relationship can be used [150]:

$$ELCR = AED \times DL \times RF \qquad (2.24)$$

Where :

ELCR = The excess lifetime cancer risk.

AED = The annuael effectives dose in mSv.

DL = The verage of life-span (year) = 70 years[151] .

RF = The fatal cancer-risk per Sievert .

2.12.3 Theoretical Calculations for Alpha Emitters

Rn-222 concentration in soil, plant, and tomato crop samples were estimated by using the detected $\mathrm{CR}-39$ (solid-state nuclear track detector). Subsequently, radiological parameters resulting from these radon concentrations were determined as follows:

The following equation is often used to measure the track densities. [152,153]:

$$\text{Track density}\,(\rho) = \frac{\text{Average number of total pits (tracks)}}{\text{Area of field view}} \qquad (2.25)$$

ρ: The average of number, of total pits, (tracks).

2.12.3.1 Radon Concentrations

The concentrations of ^{222}Rn, in the air of the space, for the tube (C_{Rn}^{a}), is determined, using the formula [154]:

$$C_{Rn}^{a}\left(\frac{Bq}{m^3}\right)=\frac{\rho}{K\,t} \qquad (2.26)$$

Where:

ρ : the density of track, CR-39 detector, (Tr/cm^2).

t : the period (90 day) of the exposure.

K : factor of calibration.

$$k=\frac{\rho_0(Trak.cm^{-2})}{C_0(Bq.d.cm^{-3})} \qquad (2.27)$$

K: The calibration coefficient, also known as the calibration factor or calibration coefficient, in terems of ((tarack/cm^2) / (Bq. d./ m^3)), was determined through experimental study.

The factor of calibration factor for CR-39 detectors with a ranged of $(0.5-3)$ days, it was determined to be (0.28 ± 0.033) $((track/cm^2)/(Bq.day/m^3))$ for ^{226}Ra (Radon source) with an activities of (3.3 kBq). This value is consistent with the reported values in various studies [155].

The equation for calculating the concentration of the sample **(**C_{Rn}^{s}**),** of ^{222}Rn is provided below [156]:

$$C_{Rn}^{s}\left(\frac{Bq}{m^3}\right)=\frac{C_{Rn}^{a}\lambda_{Rn}\,h\,t}{l} \qquad (2.28)$$

Where:

λ_{Rn}: ^{222}Rn decay constant equale $(0.1814\ d^{-1})$.

h: The measurement of the disteance between, the flat samples and the detectors.

t: Exposuere times.

l: Thickeness, of samples in tube.

The activity concentaration of ^{222}Rn in the samples ($C_{Rn}^{s,ac}$) is determined using the following equation [157].

$$C_{Rn}^{s,ac}\left(\frac{Bq}{L}\right) = \frac{C_{Rn}^{s}\ l\ A^{s}}{M^{s}} \quad (2.29)$$

Where :

A^s : Refers to the sample's surface area.

M^s : The sample's mass.

2.12.3.2 Radium Concenteration

The activities concentaration of radium (^{226}Ra), of samples **($C_{Ra}^{s,ac}$),** is determin by using the relation provided in [158].

$$C_{Ra}^{s,ac}\left(\frac{Bq}{L}\right) = \frac{C_{Rn}^{a}\ h\ A^{s}}{M^{s}} \quad (2.30)$$

2.12.4 Transfer Factor (TF)

The transfer factor (TF), is a mathematical equation used to represent the uptake of radionuclides by plants or fruit from the soil. It serves as a tool to quantify this process. The transfer factor can be calculated by dividing the activity of dry plant or fruit matter by the activity of ground deposition for radionuclides (^{238}U, ^{232}Th and ^{40}K) [159].

$$TF_g = \frac{\text{Activity concentration plant dry matter}}{\text{Activity deposited on ground}}\left[\frac{Bq_{plant}\times Kg_{dw}^{-1}}{Bq_{soil}\times m^{-2}} = \frac{m^2}{Kg_{dw}^{-1}}\right] \quad (2.31)$$

When assessing natural radionuclides, the process of ground deposition is not considered when dividing the activity concentration in plant matter by the activity in dry soil matter [160].

$$TF_g = \frac{\text{Activity concentration plant dry matter}}{\text{Activity in dry soil matter}}\left[\frac{Bq_{plant} \times Kg_{dw}^{-1}}{Bq_{soil} \times Kg_{dw}^{-1}}\right] \qquad (2.32)$$

Chapter Three

Experemental Part

3.1 Introduction

This chapter encompasses an explanation of the study area, the procedures for sample collection and preparation, as well as the techniques employed for the detection and measurement of natural radiation.

3.2 The Study Area

Al-Najaf Governorate, which covers an area of 28824 Km^2 and rises to a height of 70 m, is situated of center in Iraq. According to the 2017 census, the population of the Al-Najaf governorate is 1500522 people. The surface of it gradually declines from the southwest to the northeast at a rate of decline equivalent to 1 meter per 2 kilometers [161].

The layers of the soil in Al-Najaf Governorate are silty sand, clayey sand, gypsum, and sand. The order of these layers varies from location to location within Al-Najaf Governorate due to the depth, where they are randomly dispersed [162,163].

The city of Al-Haydariyah district is located in the northern part of Najaf governorate, 40 km away from the governorate center, and on the road linking the holy cities of Karbala and Najaf, as it is an administrative sub-district of the Najaf district. It is located astronomically between two latitudes (32°18' .28"- 32°20' .25") north and longitudes (44°14' .30" - 44°17' .13") east ,see Figure (3.1).

This chapter comprises an explanation of the study area, the procedures for sample collection and preparation, and the techniques employed to detect and measure natural radiation. Its significance is underscored by the presence of numerous farms, some reliant on underground water for irrigation while others utilize surface water from streams and rivers. Additionally, it plays a crucial role in providing Iraqi local markets with substantial quantities of seasonal agricultural products, highlighting its economic and agricultural importance.

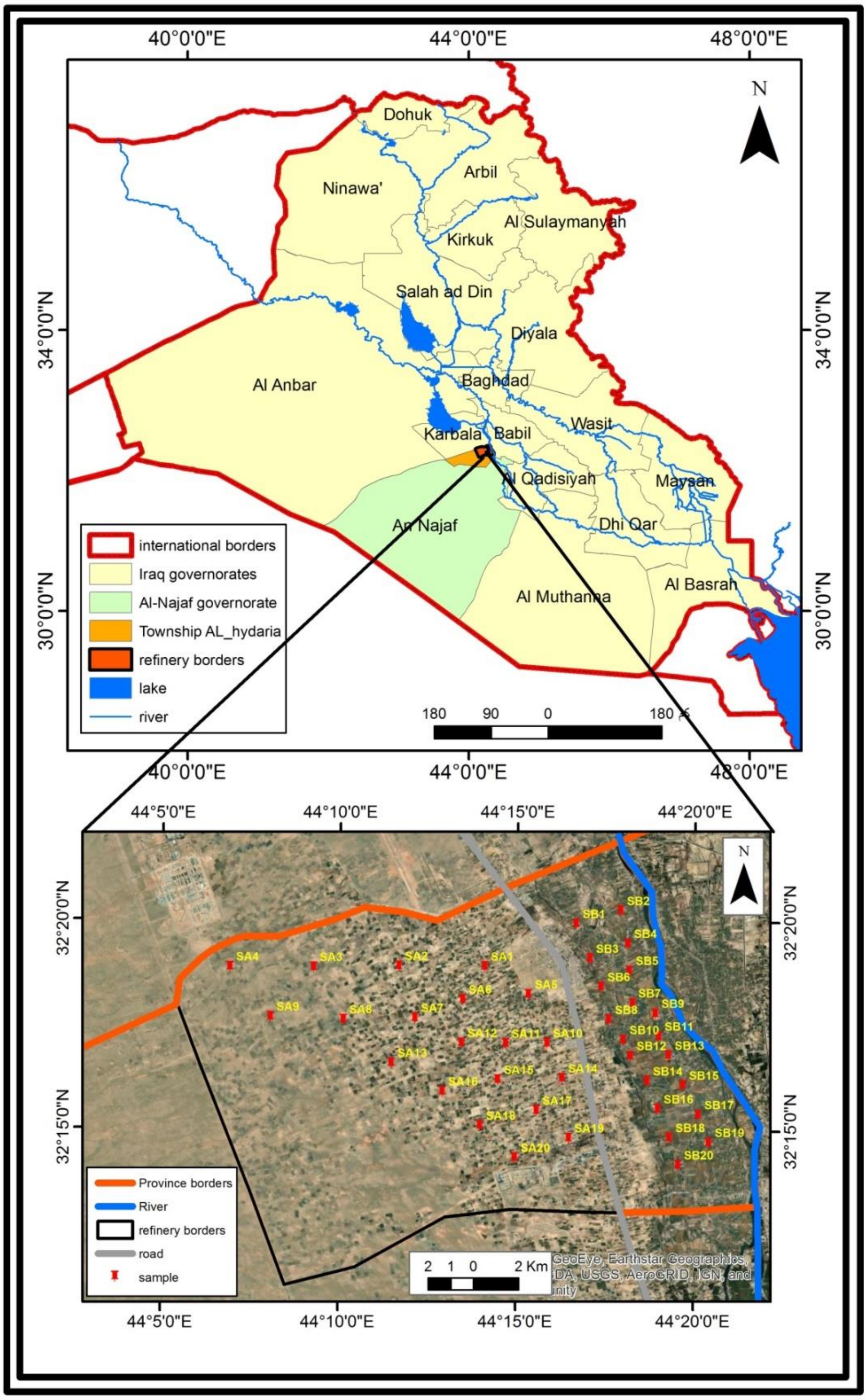

Figure 3.1: Map of the study area.

3.3 Samples Collection

In this study,, focused on studying farms in the Al-Haydariyah district of Al-Najaf, Iraq. These farming areas were divided into two categories: one relied on groundwater for plant irrigation, while the other used surface water. To facilitate our study, we divided each region into 20 sample collection sites, with distances between sites ranging from 2 km to about 2.5 km. At each site, we collected four types of samples: water, soil, plants and fruits for tomato, resulting in a total of 80 samples from each area. We manually used a global positioning system (GPS) to mark the locations, which are illustrated in Figure 3.2 (a,b) and detailed in Tables 3.1 and 3.2.

Table 3.1: Code of the sample location with their latitude and longitude, for agricultural areas that depend on groundwater for irrigation for Al-Haydarea in Al-Najaf.

Site Number of Grauond water	Position	
	Latitude (°N)	Longitude (°E)
SA1	32°18'52.94"	44°14'5.61"
SA2	32°18'52.83"	44°11'40.40"
SA3	32°18'50.62"	44° 9'16.28"
SA4	32°18'50.78"	44° 6'54.78"
SA5	32°18'13.45"	44°15'19.85"
SA6	32°18'5.55"	44°13'28.53"
SA7	32°17'38.32"	44°12'7.96"
SA8	32°17'35.87"	44°10'6.92"
SA9	32°17'39.32"	44° 8'3.79"
SA10	32°17'3.31"	44°15'51.55"
SA11	32°17'2.71"	44°14'41.65"
SA12	32°17'2.83"	44°13'26.76"
SA13	32°16'33.70"	44°11'28.51"
SA14	32°16'13.15"	44°16'17.19"
SA15	32°16'10.68"	44°14'28.49"
SA16	32°15'53.23"	44°12'55.00"
SA17	32°15'26.81"	44°15'34.15"

SA18	32°15'4.33"	44°13'58.77"
SA19	32°14'47.31"	44°16'28.81"
SA20	32°14'18.43"	44°14'57.89"

Table 3.2: Code of the sample location with their latitude and longitude, for agricultural areas that depend on surfce water for irrigation for Al-Haydariyah in Al-Najaf.

Site Number of Grauond water	**Position**	
	Latitude (°N)	Longitude (°E)
SB1	32°19'55.01"	44°16'39.90"
SB2	32°20'14.14"	44°17'54.76"
SB3	32°19'5.07"	44°17'3.17"
SB4	32°19'26.84"	44°18'7.38"
SB5	32°18'48.10"	44°18'10.06"
SB6	32°18'24.64"	44°17'22.47"
SB7	32°18'1.39"	44°18'15.60"
SB8	32°17'37.43"	44°17'35.39"
SB9	32°17'46.53"	44°18'54.23"
SB10	32°17'8.42"	44°18'0.37"
SB11	32°17'14.03"	44°19'0.27"
SB12	32°16'45.59"	44°18'12.59"
SB13	32°16'46.79"	44°19'16.99"
SB14	32°16'9.45"	44°18'40.82"
SB15	32°16'3.78"	44°19'41.62"
SB16	32°15'29.52"	44°18'59.19"
SB17	32°15'21.12"	44°20'7.65"
SB18	32°14'48.51"	44°19'18.98"
SB19	32°14'41.52"	44°20'25.57"
SB20	32°14'9.17"	44°19'33.88"

Figure 3.2: (a) Hand-held GPS (b) Hand-shovel

Collecting and preparing soil, water, plant and fruit samples for the areas shown on the map with fure samples for each area as follows:

3.3.1 Water Samples

Radon concentrations in water wells and streams were collected and examined. 500 mL samples were taken in previously cleaned plastic pet bottles, which were then sealed. Before collection operations, the bottles had also been prewashed with distilled water, diluted with acid (0.1 M HCl), and left to dry. For sources coming from bore holes, samples were taken after the source was turned on and runoff was let for around 10 minutes. This was done to release trapped air and allow the water temperature to settle. No samples that had been preserved in tanks before were gathered. Balers were used to help gather the well sample data. The bottles were carefully dipped to gather the samples for the stream samples. To avoid the development of air pockets, the bottles were completely filled. The time of collection and the location were noted on the labels and meticulously written on the samples. The samples do not need to be preserved for ^{222}Rn analysis[164]. The samples were brought to the laboratory practically immediately in order to lower the decay coefficient because the maximum holding duration is only three days.

3.3.2 Sampling Preparation

Samples were collected from the study area over a three-week period From mid-February to mid-March 2022, and they included the following:

Twenty agricultural soil samples were collected at a depth of (15)cm from each of the agricultural areas that rely on surface water for irrigation and those that rely on groundwater. The samples were exposed to sunlight for (48 to72) hours in an open area to obtain dried samples devoid of moisture. In order to obtain uniform and impurity-free soil, the samples were pulverized and sieved using a (1) mm mesh size.

To ensure complete drying, the samples were dried in an electric oven at a temperature of 100°C. After an hour, the samples were weighed to determine their fixed weight. The dried soil samples were then transferred to a 1-liter Marinelli container as in Figure 3.3 (a,b,c,d), which had been washed with diluted hydrochloric acid and subsequently rinsed with distilled water. To prevent the escape of ^{222}Rn and ^{220}Rn gases, the containers were sealed with tape.

Twenty tomato plant samples and twenty tomato crop were collected from each of the agricultural areas that rely on surface water and those that rely on groundwater for irrigation. The samples were exposed to sunlight for (5 to 7) days in an open area to ensure complete drying and remove any moisture. To obtain uniform and impurity-free plant material, the samples were pulverized and then sieved using a (1) mm mesh size.

The samples were placed in an electric oven at (70°C) for one hour to ensure thorough drying and achieve a consistent weight. Afterward, the dried plant samples were transferred to a 1-liter Marinelli container (as to Figure (3.3)), which had been washed with diluted hydrochloric acid and rinsed with distilled water. To prevent the escape of ^{222}Rn, and ^{220}Rn gases, the containers were sealed with tape.

Three samples of chemical fertilizers were taken, whose use rate is about 95% by farmers in the study area (agricultural lands). These samples are represented in the Table 3.3:

Table 3.3: Samples of fertilizers.

Fertilizer name	code	Enterprise	production date	Expiry date	Content
OVERTOUN	**S1**	**China**	**10/2022**	**5 years**	**N-P-K 12-12-36**
-	**S2**	**-**	**1/6/2022**	**1/6/2025**	**N-P-K 12-12-36**
Rich Nutrient	**S3**	**China**	**30/4/2021**	**29/4/2026**	**N-P-K 12-12-36**

Where: N: Nitrogen, P: Phosphorous, K: Potassium.

All samples were weighed using a sensitive digital scale with (± 0.01%), and the samples were stored for thirty days prior to the measurement in order to achieve the permanent radiation balance among ^{226}Ra, ^{228}Ac, short-term chains (half-life > 7), ^{222}Rn, and ^{220}Rn. In addition, approximately (25) grams of each sample for soil and tomato crop were taken and placed in plastic cups of specific dimensions and stored for three months with a nuclear trace detector.

(a) Mash

(b) Oven for drying.

(c) Marinelli beaker.

(d) Sensitive balance.

Figure 3.3: Tools for sample preparation.

3.4 Measurement Techniques Employed in this Study

There are three systems that are used for measuring gamma and alpha emissions in this study, as follows:

3.4.1 Using RAD 7 Detector

The RAD-H_2O detector, an accessory for RAD7, is specifically designed to monitor gas concentrations in water. After collecting the water sample, it is essential to obtain the results within 60 minutes, while ensuring sterilization. To measure the radon concentration using the Grab technique, a pump is placed in the water. Each time, the pump runs for five minutes to remove radon samples from the main sample, which is then transferred to the RAD 7 detector for measurement. Following this, a five-minute break is taken to restore equilibrium, after which the process is repeated for a total test time of 30 minutes, including four additional sessions involving measurement of standard deviation, temperature, moisture content, and radon concentration [165]. The operational number, ferromagnetic-circuit diagram, cumulative spectrum, and number of turns are all included [166]. The elimination of radon from a 250 ml sample, with 94% of the air volume replaced by water, exhibits a significantly high ratio. The schematic diagram of the RAD-H2O supplement is illustrated in Figures (3.4) and (3.5) [164,167]. Figure (3.4-a) presents a map or bar chart depicting the four-cycle measurements, accompanied by an accumulative spectrum [168]. Moreover, Figure (3.4-b) demonstrates the radon concentration per volume of water, as determined by the RAD7 device [169].

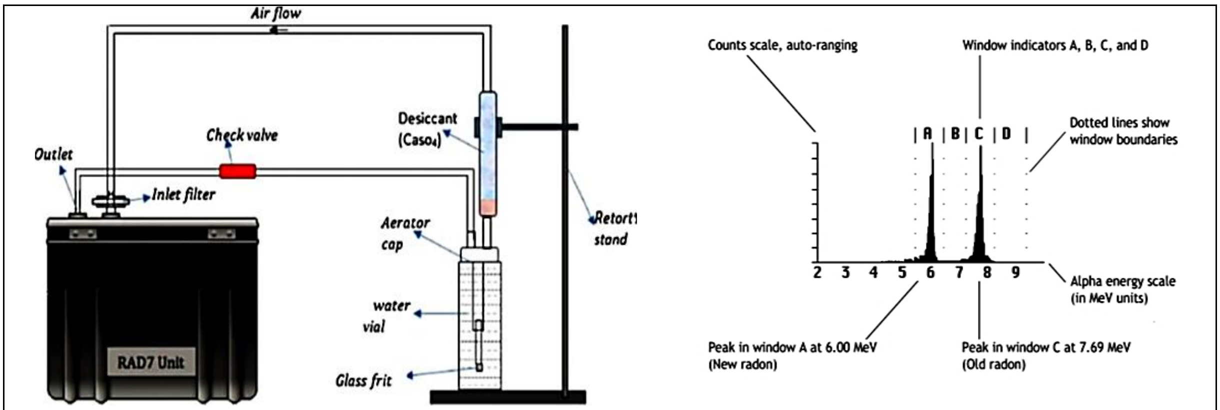

(a) a picture of the alpha spectra in channels A and C, together with the elements Po-218 and Po-214, respectively.

(b) Illustration demonstrating the use of RAD7 and its RADH2O derivatives to test a water sample.

Figure 3.4: Two images demonstrating the cumulative operational spectrum and the analysis of a water sample using RAD7

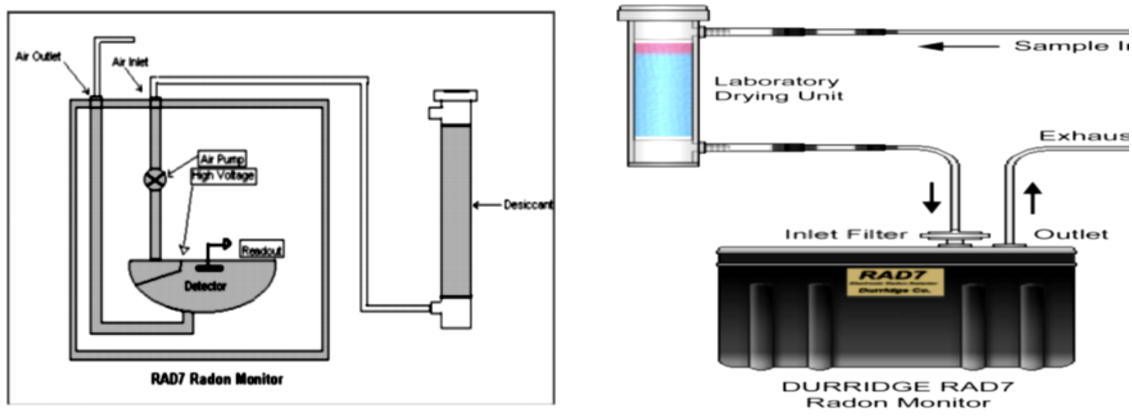

(a) The internal RAD7. **(b) The diagram in Part a.**

Figure 3.5: The diagram and image show how the RAD7 looks on the inside and out.

3.4.2. NaI (Tl) System

The most commonly used scintillator is thallium-activated sodium iodide (NaI(Tl)). It possesses several important characteristics, including the capability to construct large crystals, high light yield, extremely low scintillation light self-absorption, excellent spectroscopic performance, easy availability, and cost-effective manufacturing. Figure (3.6-a) presents a photograph of the NaI(Tl) detector, while Figure (3.6-b) displays a schematic diagram of its internal structure [170].

As depicted in Figure (3.7) a computer-based multichannel analyzer was employed to evaluate the samples for a duration of 18.000 seconds while they were in the detector. This analyzer captures the gamma spectrum from each sample and processes it using the Maestro-32 software. By utilizing the Maestro-32 data processing program, the net area beneath each corresponding peak in the energy spectrum of each sample was calculated. This calculation involved subtracting the count from background sources to obtain the peak's net area. As shown in Figure (3.8), the background spectrum was detected during sample measurements using a polyethylene plastic Marinelli cup and an empty 1 L vessel placed within the detector.

The results obtained were from gamma-rays emitted by ^{238}U and ^{232}Th, which are in secular equilibrium with them. However, the determination of ^{40}K activity was done indirectly using the gamma line at 1460 KeV. This was necessary due to the low resolution of the NaI(Tl) detector, which makes it challenging to accurately measure activity concentrations in peaks with good separation at low gamma energies. Consequently, the gamma line at 1765 KeV was utilized to calculate the specific activity of ^{238}U (^{214}Bi), while the gamma line at 2614 KeV was used to obtain equivalent results for ^{232}Th (^{208}Tl) [171].

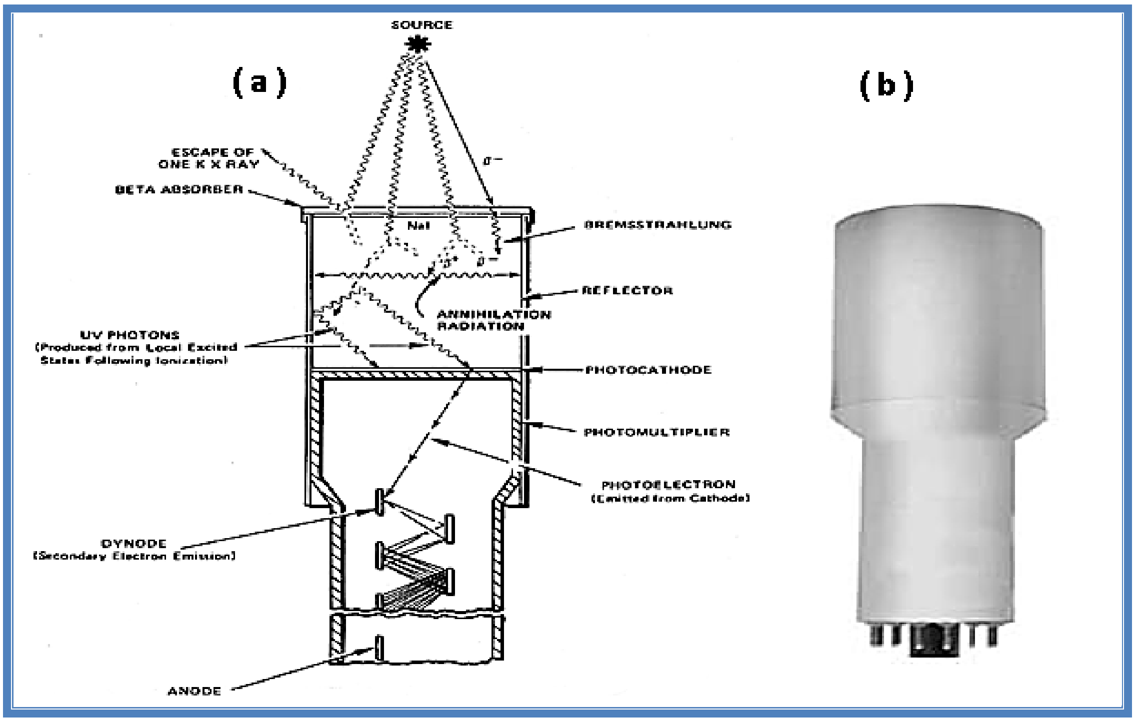

Figure 3.6: Sodium Thulium Activated Iodide Detector NaI (Tl) [170]

Figure 3.7: The sodium iodide detector system in the restaurant consists of a thallium-activated sodium iodide (NaI(Tl)) detector measuring 3" × 3".

Figure 3.8: The samples were placed on the detector.

3.4.2.1 Energy Calibration

The relationship between the gamma ray energy absorbed by the detector (photo peak) and the channels that correspond to it is known as energy calibration [172]. As shown in Table (3.3), the energy of this detector is calibrated using a number of predefined -ray sources from the IAEA (^{137}Cs, ^{60}Co, ^{22}Na, ^{54}Mn, and ^{152}Eu). Figure (3.9) shows the energy calibration curve.

Table 3.4: Properties of radioactive sources consulted for this study [172, 173].

Isotopes	Activity (µCi)	Energy (keV)	Serial number	Production date	I_γ %
^{137}Cs	1	661.66	IRS-126	1/1/2009	85.21
^{60}Co	1	1173.24	IRS-141	1/1/2009	99.9
		1332.5			99.88
		2505.74			20
^{22}Na	1	511	IRS-139	1/2/2009	181
		1274			99.95
^{54}Mn	1	834	IRS-128	1/1/2009	100
^{152}Eu	0.9	1407	IRS-149	1/11/2009	24
		1112			16.4
		1085.8			10
		964			17.3
		778.9			15.2
		344.3			31.4
		121.8			33.2

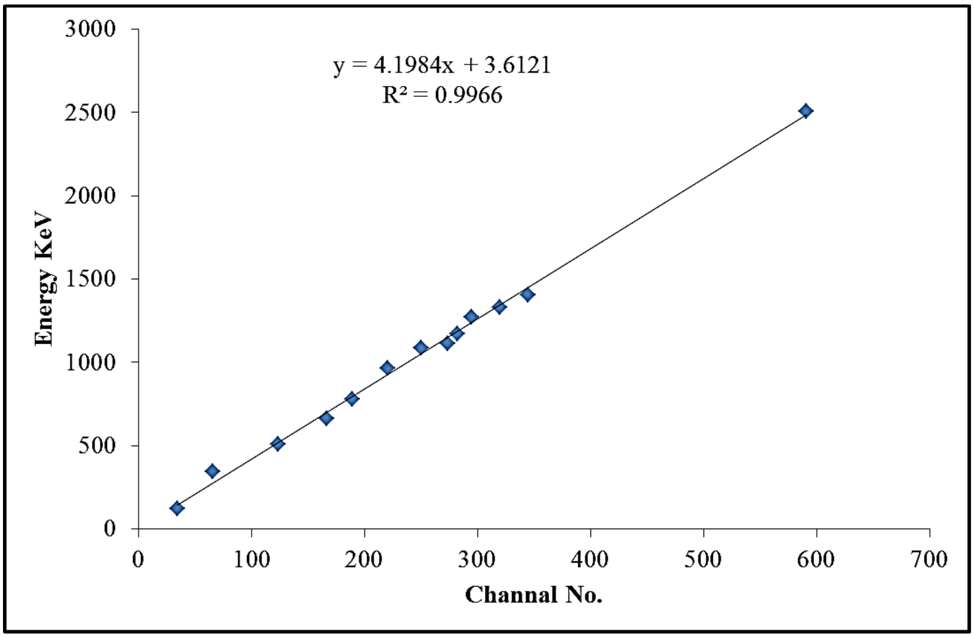

Figure 3.9: The NaI(TI) 3" 3" energy calibration curve

3.4.2.2 Detection Efficiency

The detection efficiency it can be referred to as "detection efficiency (ε)," which can be computed in the current study using equation (3.1). It is the proportion of the radiation count rate between what is recorded and what the detector detects. [174]:

$$\varepsilon = \frac{C}{A.I_{\gamma}.T} \times 100\% \qquad (3.1)$$

Where:

C: (Under the photo peak) is the net area.

T: is the total number of spectra collected.

I_{γ}: Is the probability of gamma rays emitted.

A: Is the stationary source's activity, expressed in units of Bequral or Curi, at the moment of measurement, which is commonly determined using equation (3.2) [175].

$$A = A_{\circ} e^{-\lambda.\Delta t} \quad (3.2)$$

Where:

A: The activity of the sources is measured in becquerels (Bq) at a given time, denoted as "t".

A_o: The starting activity of each source is measured in becquerels (Bq) at a specific initial time, denoted as "to"..

λ: The rate of deterioration.

Δt (Δt= t-t_o): Is time of decay between the product of the stander source (t_o) and time at time measurement (t).

Figure (3.10) shows the calibration of absolute photo-peak detection efficiency with gamma-ray energy using five distinct sources: ^{137}Cs, ^{60}Co, ^{22}Na, ^{54}Mn, and ^{152}Eu. Based on data in Table (3.4) the efficiency of ^{238}U (^{214}Bi; 1765 KeV), ^{232}Th (^{208}Tl; 2614 KeV), and ^{40}K. (^{40}Ar ;1460 KeV) can be found.

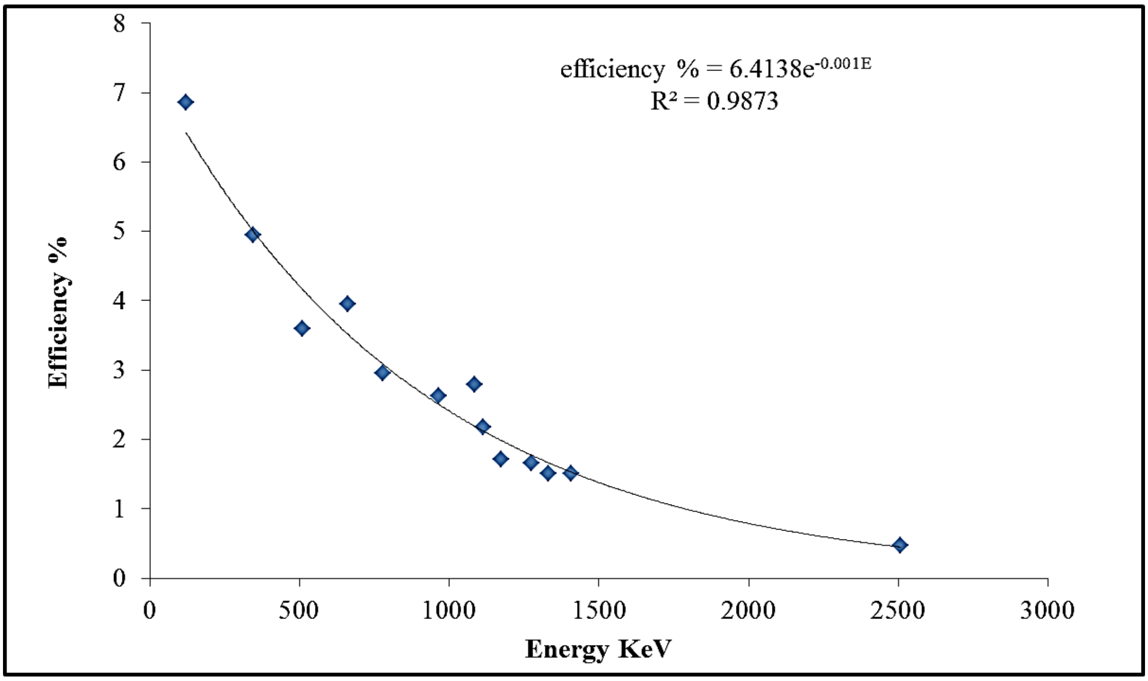

Figure 3.10: The Curve of fficiency for NaI(Tl) detected in present study.

3.4.2.3 Energy Resolution

In Figure (3.11), a detector's energy resolution (R) measures its ability to tell between two peaks where the energy difference is a minimal. The resolution can be calculated using the equation provided below [176,177].

$$R = \frac{FWHM}{Ch} \times 100\% \qquad (3.3)$$

Where:

FWHM (Full Width at Half Maximum) : represents the measurement of the width of the photopeak in the spectrum of a gamma-ray source.

Ch : represents the channel number corresponding to the centroid of the gamma peak.

In this study, the R value was determined to be 7.9%. The energy of the standard source used was 661.66 KeV for ^{137}Cs, as depicted in Figure (3.11).

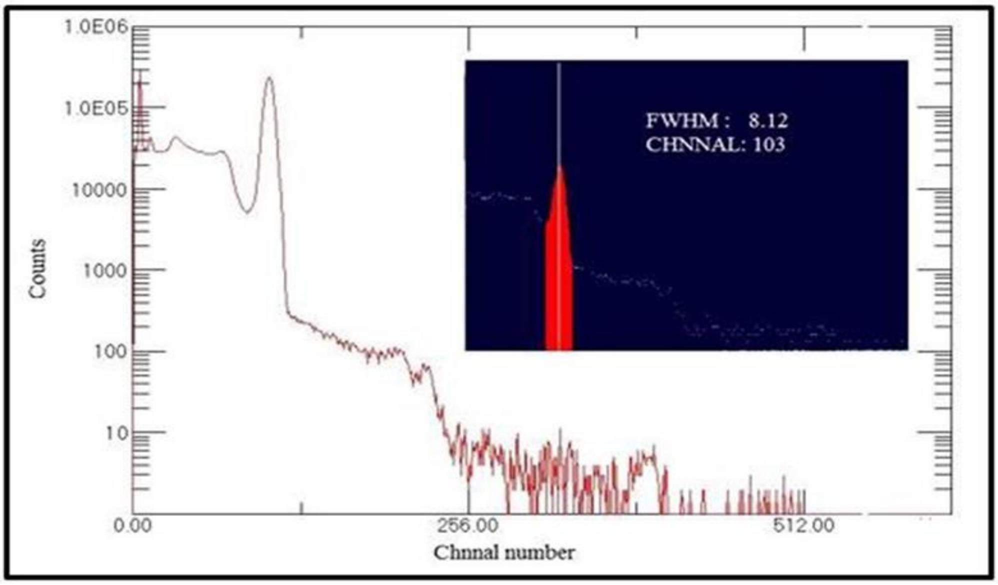

Figure 3.11: The Cs-137 spectrum was analyzed using the Maestro-32 software.

3.4.2.4 Measuring Technique

The MAESTRO-32 data analysis package is utilized to calculate the net count below the respective photo peak within the energy range. This is achieved by subtracting the count obtained from the background radiation measurement. The background range was determined using an empty, 1-liter polyethylene plastic Marinelli. While the accurate evaluation of ^{40}K was achieved using the gamma line at 1460 keV through ^{40}Ar, the specific activity (Bq/kg) can potentially be evaluated at higher energies with well-separated photo-peaks. Our results obtained from gamma rays generated by the progeny of ^{232}Th and ^{238}U demonstrate clear agreement and provide an opportunity for such evaluations.

Consequently, the gamma lines at 1765 KeV were utilized to determine the specific activity of (^{238}U) and (^{214}Bi). Likewise, the gamma-ray lines at 2614 KeV (^{208}Tl), as depicted in Figure (3.12), provided similar results for ^{232}Th [177].

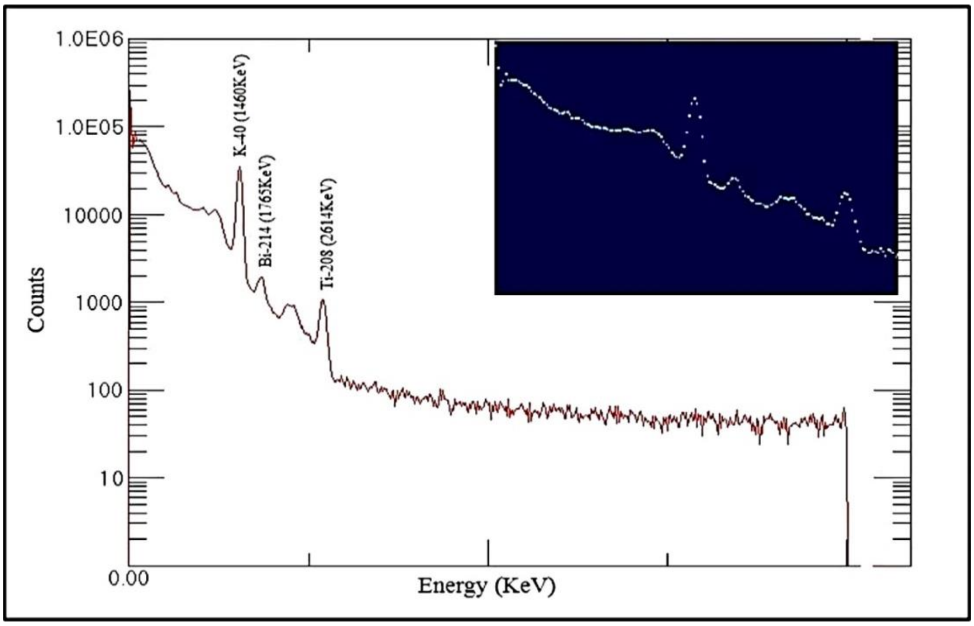

Figure 3.12: Gamma-ray spectrum using MAESTRO-32 soft for NaI(Tl) (3"×3").

3.4.3 CR-39 Detector

The collection and processing of ornamental material samples utilized in the track methodology were identical to those employed in the NaI(Tl) strategy. To distinguish one sample from the others, a special code was given to each one. TASTRAK, Ltd., a United Kingdown (UK) -based analysis system, is the provider of the CR-39 ($C_{12}H_{18}O_7$) detector. The CR-39 detector sheet, measuring 2.5 cm by 2.5 cm and with a thickness of one millimeter, was imprinted with a code specific to the TASL picture system (see Figure 3.13). The sheet has a density of approximately 1.3 g/cm^3[164].

Figure 3.13: The UK-made CR-39 detector (TASTRAK).

3.4.3.1 Sample Container

The sealed plastic cans used in this study had a height of 7 cm and an average diameter of 4.5 cm. The cans were labeled with the sample name and the storage date. Figure (3.14) illustrates the plastic container utilized in this study. Once the containers were filled with samples, a distance of 1 cm (h) and 6 cm (L) was maintained between the sample and the detector CR-39. The detectors were attached to the upper portions of the containers using adhesive tape. The containers' covers were securely sealed with adhesive tape to prevent the escape of radon gas. In this investigation, the samples were stored for a duration of 90 days To obtain radiation balance. A long-term irradiation method was employed in the study. Following the radiation period, the The results are then drawn and analyzed.

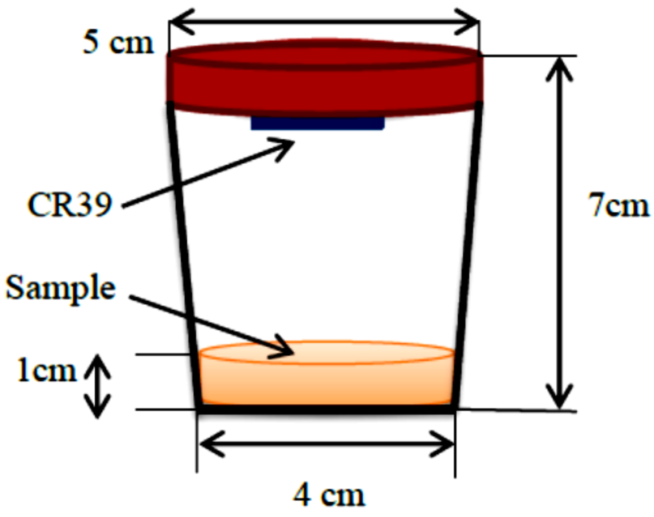

Figure 3.14: Plastic container that used in present study.

3.4.3.2 Chemical Etching

To create sodium hydroxide (NaOH) solution, the formula below was used to dissolve 100 g of NaOH in 0.4 liters of purified water from equation (3.4) [178]:

$$W = W_{eq} \times N \times V \tag{3.4}$$

Where:

W: Denotes the weight of sodium hydroxide (NaOH) necessary to attain the desired normality.

W_{eq}: Rrepresents the weight equivalent of NaOH.

N: Is the desired normality.

V: The volume of distilled water.

Figure (3.15) illustrates the preparation of the etching solution using an HP-3000 magnetic stirrer (Lab Companion Magnetic Stirrer, Ceramic Top, 110 volts, 60 Hz). The solution is allowed to homogenize for fifteen minutes. Subsequently, the detectors were cautiously removed from the plastic containers, taking special precautions to avoid any scratches on the surfaces of the detectors.

Figure 3.15: The magnetic stirrer used in the experiment is the HP-3000 model, manufactured in the USA.

As depicted in Figure (3.16), Pyrex containers were placed in an electric water bath with a temperature range of 0 to 100 °C, which was set to 98 °C within one hour [179]. The following day, CR-39 detectors were immersed in a 6.25 NaOH solution. After thorough cleaning with distilled water and careful drying with soft tissue paper, the detectors were extracted from the solution.

Figure 3.16: Digital water path HH-420.

3.4.3.3. Microscopy Processing of Track

The only need is to count the engraved tracks on a detector. The widths and shapes of etch pit "tracks" naturally vary; circular etch pits are produced by vertically incident alpha particles. The majority of etch pits are elliptical in shape, resulting from alpha particles colliding with the detector surface at lower angles of incidence. Then, any minor etch pits are continuously ignored, and any scratches are readily overlooked [180]. In this investigation, a microscopic procedure was carried out to manually count the amounts of radon present. The optical microscope of the type (Novel, China) was used for manual microscopy processing. The microscope had a 400X magnification, which was used to count the tracks on the item, not 40X. Figure 3.17 shows how the detector surface is divided into 10 areas of view to count the alpha particle. Once the camera program has been installed on the computer, numerous images of each area are shot using a digital camera connected to the computer through a USB cable.

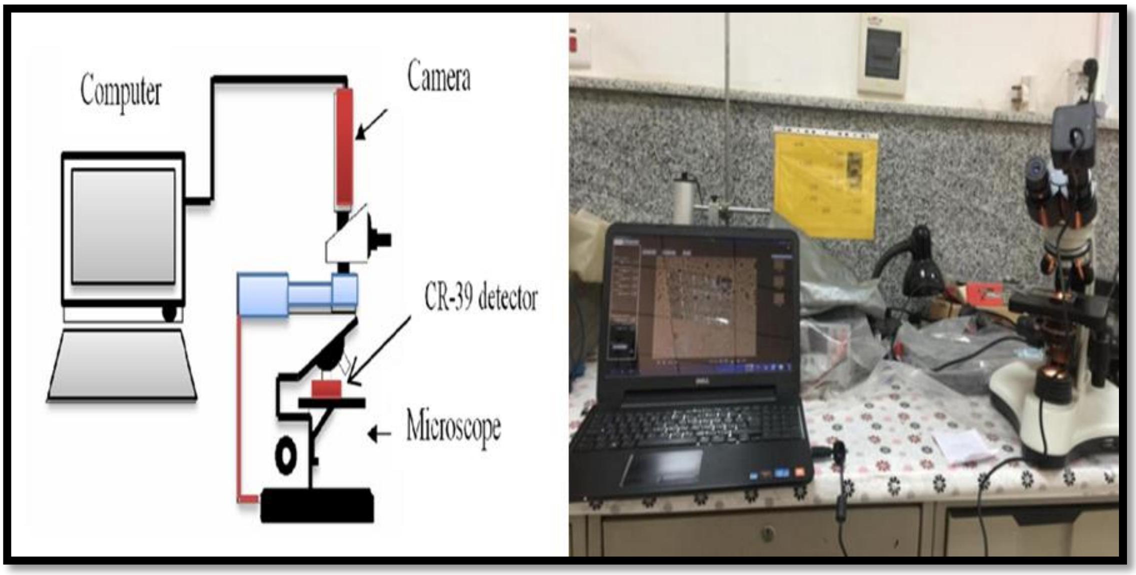

Figure 3.17: Microscopy processing manually.

Chapter Four

Results and

Discussion

4.1 Introduction

This chapter presents the findings regarding radon gas concentrations and natural radioactivity levels, specifically those of ^{238}U, ^{232}Th, and ^{40}K. These measurements were obtained through the application of three distinct techniques. Firstly, radon gas concentrations in both ground and surface waters were assessed in a total of 40 samples. These samples were divided into two sets of 20 each, consisting of groundwater samples and surface water samples, respectively, collected from the study area. The measurements were obtained using an active device known as RAD7.

Furthermore, the natural radioactive activity of gamma emitters was determined in 120 samples. This set comprised 20 soil samples, 20 tomato plants, and 20 tomato fruits, each for both the groundwater and surface water regions. The gamma spectroscopy system NaI (TI) was employed to measure the natural radioactivity concentrations of radionuclides ^{238}U, ^{232}Th, and ^{40}K in these samples. Additionally, the transfer factor was calculated for soil samples, tomato plants,

The tomato fruits to ascertain the concentrations of radon and radium. This calculation was performed using solid-state nuclear track detectors (CR-39). A total of 80 samples, including 20 soil samples, 20 tomato fruits irrigated with groundwater, and 20 soil samples, and 20 tomato fruits irrigated with surface water, were subjected to this measurement.

To evaluate environmental radioactivity and characterize potential radioactive risks, all the obtained results were compared against the global averages established by international organizations and agencies.

4.1.1 Calculating Radon Concentrations in Groundwater and Surface water by using the Rad7 Detector

From Table (4.1) and Table (4.2) and Figures (4.2,4.5) display the results of ^{222}Rn concentrations in groundwater and surface water for the 40 samples analyzed using RAD 7. In general, the predominant range of radon concentration in groundwater was observed to be between 0.109 Bq/L and 0.399 Bq/L, with an average of 0.235±0.02 Bq/L. For surface water, the results ranged from 0.036 Bq/L to 0.144 Bq/L, with an average of 0.074±0.008 Bq/L.

The maps displayed in Figures (4.1) and (4.4), are illustrate the distribution of radon concentrations in the groundwater and surface water samples respectively. These maps were generated using Arc GIS 10.4.1 and a GIS methodology, utilizing distinct colors to differentiate between high, medium, and low levels .

The total of AED (annual effective doses) resulting from, the ingestion or drinking of groundwater and surface water. For groundwater, the average AED for individuals aged one year or less ranged from 0.577 µSv/y to 2.111 µSv/y, with an average of 1.247±0.103 µSv/y. For individuals aged 2 to 17 years, the average AED ranged, from 0.212 µSv/y to 0.777 µSv/y, with an average of 0.459±0.038 µSv/y. For individuals aged 17 years or older, the average AED ranged, from 0.278 µSv/y to 1.019 µSv/y, with average of 0.602±0.05 µSv/y.

Regarding surface water, the average AED ranged from 0.190 µSv/y to 0.762 µSv/y, with average of 0.394±0.040 µSv/y. For individuals aged (2-7) year or less, the average AED ranged, from 0.070 µSv/y to 0.280 µSv/y, with average of 0.145±0.06 µSv/y . For individuals aged ≥17 years, the average AED ranged, from 0.092 µSv/y to 0.368 µSv/y, with average of 0.190±0.051 µSv/y, and all the results in this study were in the normal limit allowed for (1mSv/y) for public [181.182] (UNSCEAR, 2009; WHO, 2012). As shon

Figure (4.3) and Figure (4.6) includes a comparison between the ages of three groundwater and surface water respectively, the largest value was in younger is equal to one year, the older ages or equal to (17) year and ages from (2-17) year, the reason for this is due to the body's highly sensitive tissues of ages younger and equal to one year.

According to the publications of the USEPA: United States Environmental Protection Agency Office of Water [183], all of the results of ^{222}Rn concentrations in water were within the permitted limits of the USEPA (11.1 Bq/L) [183] for ^{222}Rn concentrations in water for human consumption. The fluctuation or discrepancies in ^{222}Rn concentration values for groundwater and surface water samples in the current investigation can be attributed to several things, such as the source of water that was used to collect the samples. One can notice this difference through Figure (4.7) that represents a comparison between the rate of radon concentrations in groundwater and surface water, and their comparison with the rate issued by the USEPA, where it was found that radon concentrations in groundwater are greater than in surface water due to the increase in uranium concentrations in the interior Earth compared to the earth surface.

However, the average of these concentrations of ground and surface water is less than the average of the USEPA [183] due to a variety of factors, including the water sources employed in this study. The difference in radon concentrations of surface water and groundwater can be ascribed to the water sources as well as the research area's geological structure. The geological composition in this study is a very important factor in increasing the radon concentrations in the water[184].

Table 4.1: Radon Concentrations and Annual Effective Dose of Groundwater in Three Age Groups by used Rad7.

No.	Sample Code	Radon Concentrations (Bq/L)	Annual effective dose (µSv/y)		
			≤ 1 y	(2-17) y	≥ 17 y
1	G1	0.203±0.02	1.074	0.395	0.519
2	G2	0.399±0.021	2.111	0.777	1.019
3	G3	0.199±0.022	1.053	0.387	0.508
4	G4	0.12±0.023	0.635	0.234	0.307
5	G5	0.181±0.025	0.957	0.352	0.462
6	G6	0.302±0.027	1.598	0.588	0.772
7	G7	0.211±0.029	1.116	0.411	0.539
8	G8	0.355±0.031	1.878	0.691	0.907
9	G9	0.195±0.034	1.032	0.380	0.498
10	G10	0.13±0.037	0.688	0.253	0.332
11	G11	0.217±0.041	1.148	0.422	0.554
12	G12	0.254±0.046	1.344	0.495	0.649
13	G13	0.362±0.053	1.915	0.705	0.925
14	G14	0.326±0.062	1.725	0.635	0.833
15	G15	0.31±0.074	1.640	0.604	0.792
16	G16	0.145±0.093	0.767	0.282	0.370
17	G17	0.29±0.124	1.534	0.565	0.741
18	G18	0.188±0.186	0.995	0.366	0.480
19	G19	0.109±0.371	0.577	0.212	0.278
20	G20	0.217±0.019	1.148	0.422	0.554
Minimum		**0.109±0.371**	**0.577**	**0.212**	**0.278**
Maximum		**0.399±0.021**	**2.111**	**0.777**	**1.019**
Average ± S.D		**0.235±0.02**	**1.247±0.103**	**0.459±0.038**	**0.602±0.05**
World Wide Average		USEPA[183](11.1 Bq/L)	UNSCEAR [181] (1m Sv/y)		

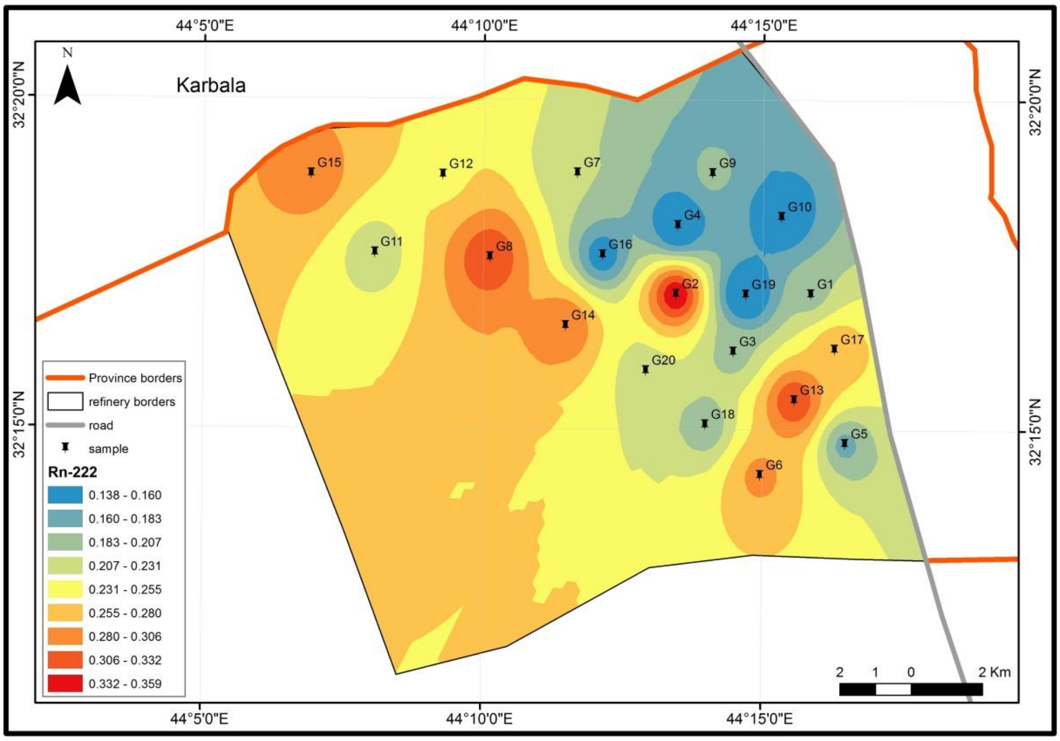

Figure 4.1: The Map of the ^{222}Rn Gas Concentrations of Groundwater.

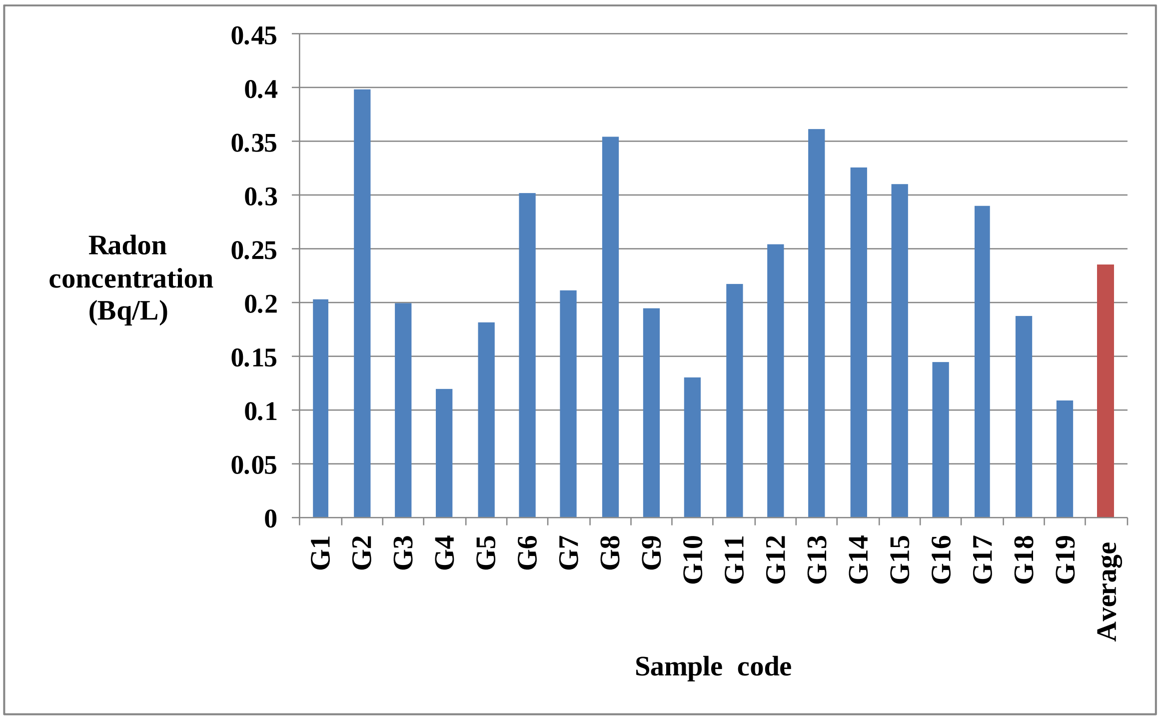

Figure 4.2: Radon Gas Concentration of Groundwater.

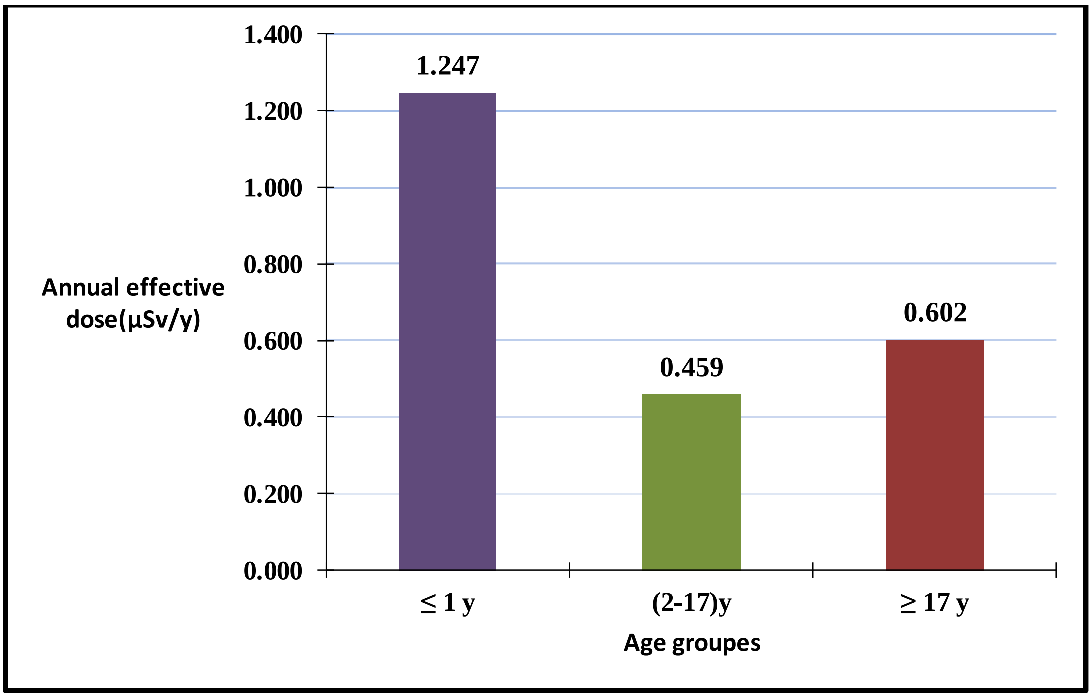

Figure 4.3: Comparison of the Annual Effective Dose in Three Groundwater Age Groups.

Table 4.2: Radon concentrations and Annual effective dose of surfce water in three age groups by used Rad7.

No.	Sample Code	Radon Concentrations (Bq/L)	Annual effective dose (µSv/y)		
			≤ 1 y	(2-17) y	≥ 17 y
1	**S1**	0.036±0.008	0.190	0.070	0.092
2	**S2**	0.055±0.007	0.291	0.107	0.141
3	**S3**	0.039±0.008	0.206	0.076	0.100
4	**S4**	0.065±0.009	0.344	0.127	0.166
5	**S5**	0.041±0.01	0.217	0.080	0.105
6	**S6**	0.123±0.011	0.651	0.239	0.314
7	**S7**	0.077±0.01	0.407	0.150	0.197
8	**S8**	0.063±0.012	0.333	0.123	0.161
9	**S9**	0.075±0.013	0.397	0.146	0.192
10	**S10**	0.122±0.014	0.645	0.238	0.312
11	**S11**	0.072±0.002	0.381	0.140	0.184
12	**S12**	0.144±0.016	0.762	0.280	0.368
13	**S13**	0.031±0.004	0.164	0.060	0.079
14	**S14**	0.071±0.002	0.381	0.140	0.184
15	**S15**	0.044±0.029	0.233	0.086	0.112
16	**S16**	0.039±0.036	0.206	0.076	0.100
17	**S17**	0.083±0.048	0.439	0.162	0.212
18	**S18**	0.102±0.072	0.540	0.199	0.261
19	**S19**	0.096±0.004	0.508	0.187	0.245
20	**S20**	0.114±0.005	0.603	0.222	0.291
Minimum		**0.031±0.004**	**0.577**	**0.212**	**0.278**
Maximum		**0.144±0.016**	**2.111**	**0.777**	**1.019**
Average ± S.D		**0.074±0.008**	**1.247±0.103**	**0.459±0.038**	**0.602±0.05**
World WIDE Average		**USEPA[183](11.1 Bq/L)**	**UNSCEAR [181] (1m Sv/y)**		

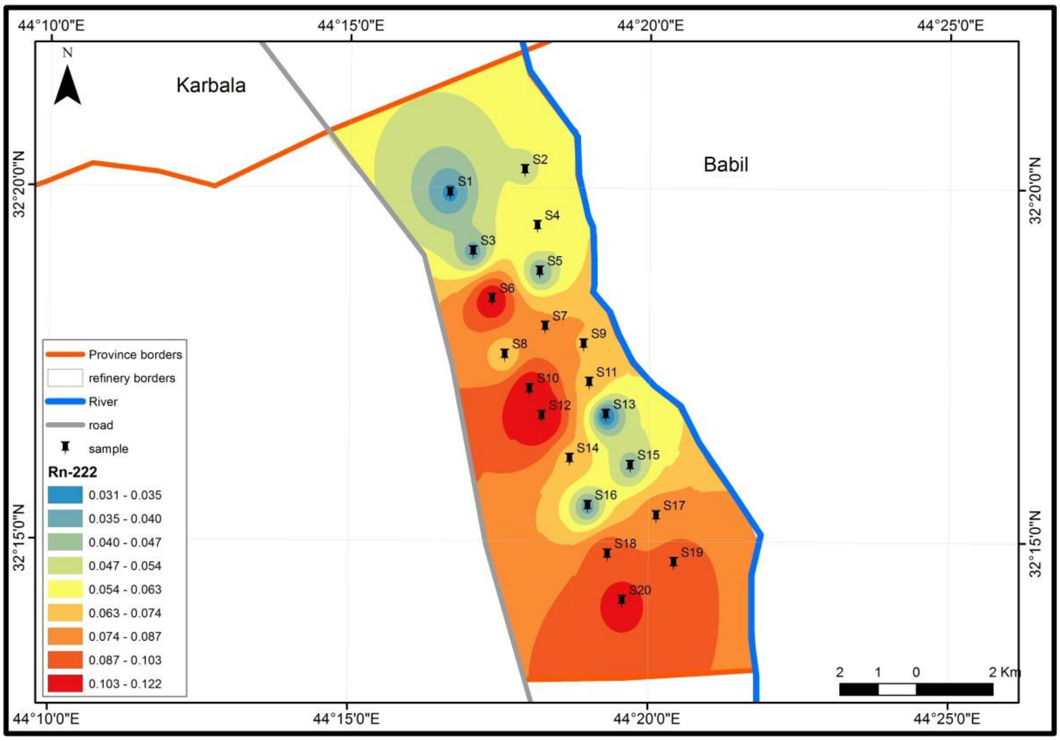

Figure 4.4: The Map of the ^{222}Rn Gas Concentrations of Surface Water.

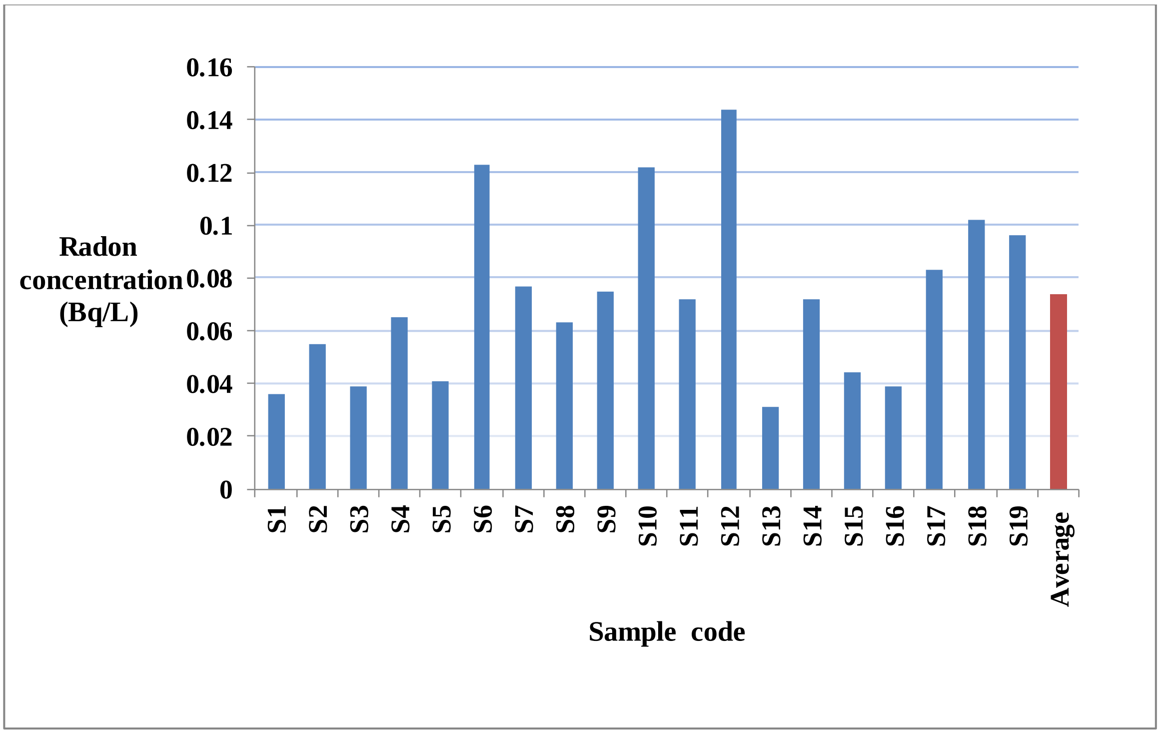

Figure 4.5 : Radon Concentration of Surface water.

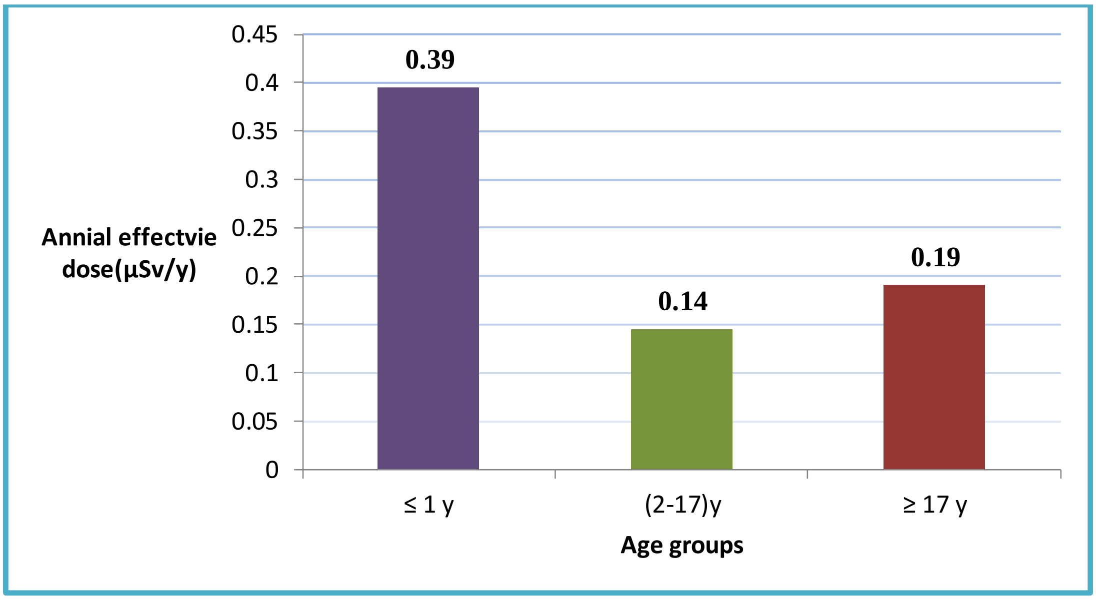

Figure 4.6: Comparison of the Annual Effective Dosage in Three Surface water Age Groups.

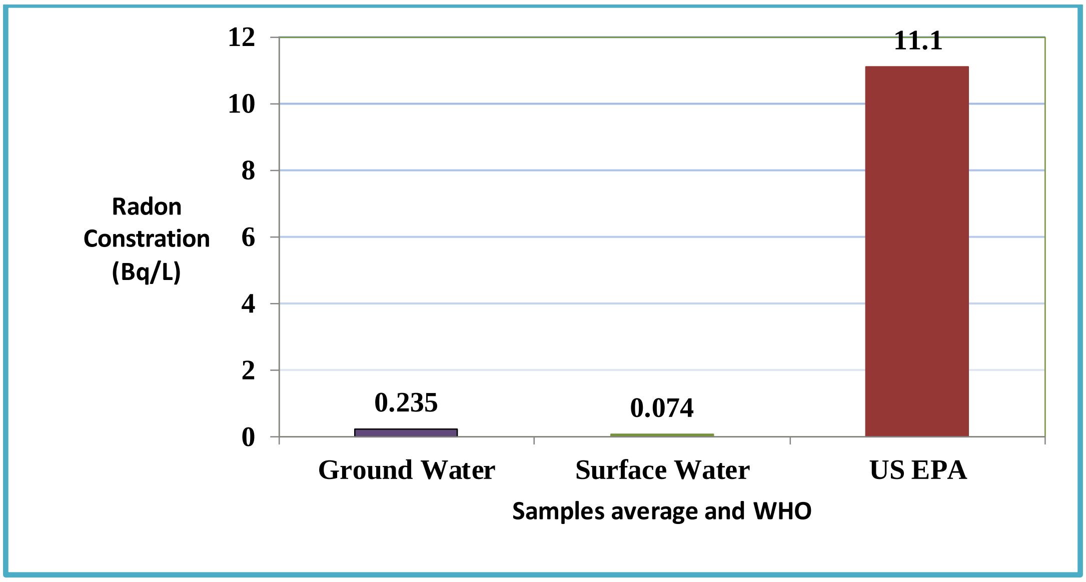

Figure 4.7: Comparison between Groundwater, Surface water with USEPA.

4.1.2 Calculating Gamma Emitters by NaI(TI) detector

4.1.2.1 Results of Gamma Emitters in agricultural soil irrigte with groundwater.

The natural radioactivity levels of selected agricultural soil samples in the study area were measured and compared significantly with the permissible limits provided by UNSCEAR, 2010 [185] for (^{238}U, ^{232}Th , ^{40}K and ^{235}U). The results, shown in Table (4.5), reveals the specific activity of (^{238}U, ^{232}Th , ^{40}K and ^{235}U) as follows: The specific activity range of (^{238}U) was found to be 17.851±0.866 Bq/kg to 49.801±1.505 Bq/kg, with an average of 32.98±1.198 Bq/kg. For (^{232}Th), the specifica activityi ranged from 7.990±0.866 Bq/kg to 16.345±0.397 Bq/kg, with average of 12.815$\pm$0.348 Bq/kg. For (^{40}K) exhibited a specific activity range from 382.731±4.488 Bq/kg to 755.11±8.118 Bq/kg, with average of 606.255±5.893 Bq/kg. Comparing these values with the permissible limits (35, 45, and 412 Bq/kg for (^{238}U, ^{232}Th, and ^{40}K, respectively) set by UNSCEAR [185], it can be observed that the specific activity of (^{238}U) is slightly lower than the global averages, (^{232}Th) is much lower than the global averages, and (^{40}K) is significantly higher than the global averages.

The specific activity range of (^{235}U) was found to be from 0.823±0.038 Bq/kg to 2.295±0.068 Bq/kg, with an average of 1.52±0.022 Bq/kg. These values were higher than the world-wide average [185].

From Table(4.7) it can be found that the value of both Exposure, AEDE, AGED, ELCR, from 126.561 to 235.007 with average 195.517$\pm$9.712 μR/h, from 0.161 to 0.381 with average 0.241$\pm$0.011 mSv/y, from 234.741 562.623 with average 352.212$\pm$17.274, from 0.723 to 1.707 with average 1.079$\pm$0.052. All were less than the World Wide Average except AGED it was a little highe [185].

The maps displayed in Figures (4.10, 4.11, 4.12, 4.13) illustrate the distribution of the average of specific activities for (^{238}U, ^{232}Th and ^{40}K) the average of specific activities in the selected agricultural soil irrigte with groundwater samples, respectively. These maps were generated using Arc GIS 10.4.1 and a GIS methodology, utilizing distinct colors to differentiate between high, medium, and low levels .

Figures (4.14, 4.15, 4.16, 4.17), represent the distributione of the specific activities against the sample positions, for ^{238}U, ^{232}Th , ^{40}K and ^{235}U respectively. Figures (4.14,4.17) show that the highest value of ^{238}U , ^{235}U were in the middle of the study area from the agricultural soil irrigted with groundwater, whereas Figure (4.15) shows that the values of ^{232}Th were found The sample values are close and all are less than the World Wiede Average. Finally, Figure (4.16) show that nearly the high values of the ^{40}K activities were distributed, almost all much higher except for one value only than the World Wiede Average of the study-area [185].

Figure (4.18), represents the a comparison between the specific effectiveness rates of radioactivity of ^{238}U, ^{232}Th , ^{40}K and ^{235}U for agricultural soils irrigated with groundwater. The increasing is noticed in the rate of specific effectiveness of potassium, and it may be due to the use of industrial chemical fertilizers and animal fertilizers for multiple agricultural seasons during one year, In addition to the concentration of naturally occurring radioactive nuclides in soil varies across different locations due to geological and geographical factors.

Table 4.3: The Specific Activity of (^{238}U, ^{232}Th , ^{40}K and ^{235}U) in Agricultural Soil Irrigated with Groundwater.

No.	Samples codes	The specific activity is measured in units (Bq/kg)			
		^{238}U	^{232}Th	^{40}K	^{235}U
1	SA1	31.267±1.182	14.54±0.374	669.9 ± 6.161	1.441±0.053
2	SA2	26.368±1.037	12.663±0.333	566.655±5.417	1.215±0.045
3	SA3	33.801±1.139	13.801±0.338	625.142± 5.516	1.558±0.047
4	SA4	39.834±1.296	16.024±0.381	702.922± 6.134	1.836±0057
5	SA5	32.205±1.199	12.176±0.342	670.127± 6.162	1.484±0.054
6	SA6	24.238±1.015	14.748±0.367	699.516± 6.143	1.117±0.044
7	SA7	41.966±1.37	16.354±0.397	755.11± 8.118	1.934±0.062
8	SA8	29.814±1.137	8.6552±0.284	492.914± 5.209	1.374±0.050
9	SA9	32.934±1.279	12.055±0.359	677.015± 6.532	1.518±0.061
10	SA10	17.851±0.866	13.863±3.54	669.967± 5.975	0.823±0.038
11	SA11	45.077±1.491	15.279±0.403	614.66± 6.201	2.077±0.071
12	SA12	18.523±0.913	10.602±0.32	524.349± 5.469	0.854±0.041
13	SA13	38.307±1.268	13.664±0.351	684.406± 6.039	1.765±0.055
14	SA14	42.892±1.371	16.072±0.389	725.549± 6.35	1.977±0.061
15	SA15	21.015±1.01	10.494±0.331	453.988± 5.287	0.968±0.047
16	SA16	49.801±1.505	13.259±0.36	624.119± 6.001	2.295±0.068
17	SA17	37.595±1.286	12.01±0.337	561.004± 5.597	1.733±0.057
18	SA18	43.707∓1.436	11.861∓0.347	591.909± 5.953	2.014±0.067
19	SA19	26.139±1.115	10.184±0.323	433.108± 5.11	1.205±0.052
20	SA20	26.267±1.044	7.9903±0.267	382.731± 4.488	1.21±0.045
Minimum		**17.851±0.866**	**7.9903±0.267**	**382.731± 4.488**	**0.823±0.038**
Maximum		**49.801±1.505**	**16.354±0.397**	**755.11± 8.118**	**2.295±0.068**
Average ± S.D		**32.98±1.198**	**12.815±0.348**	**606.255±5.893**	**1.52±0.022**
UNSCEAR [185]		**35**	**45**	**412**	**-**

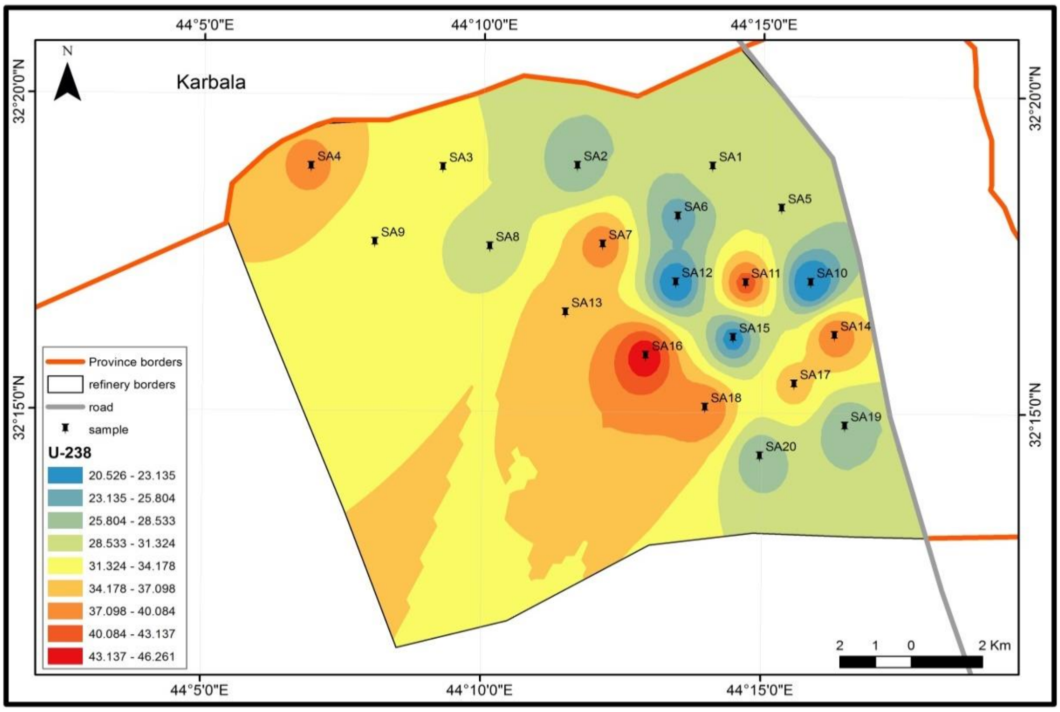

Figure 4.8: The Map of the Average of Specific Activities for ^{238}U in Agricultural Soil Irrigated with Groundwater.

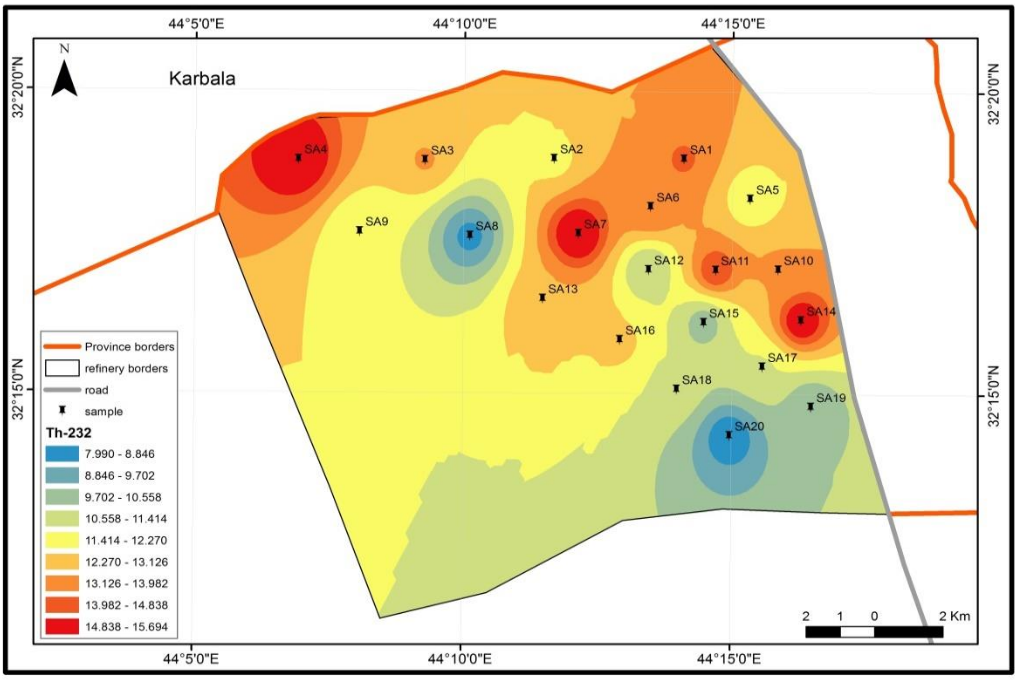

Figure 4.9: The Map of the Average of Specific Activities for ^{232}Th in Agricultural Soil Irrigated with Groundwater.

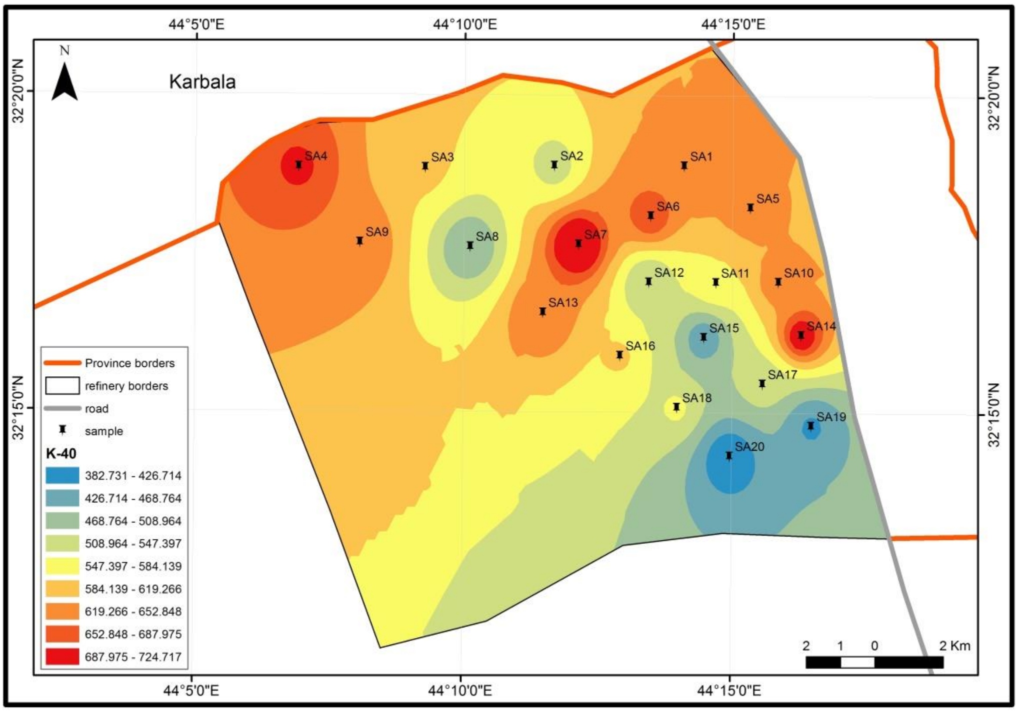

Figure 4.10: The Map of the Average of Specific Activities for ^{40}K in Agricultural Soil Irrigated with Groundwater.

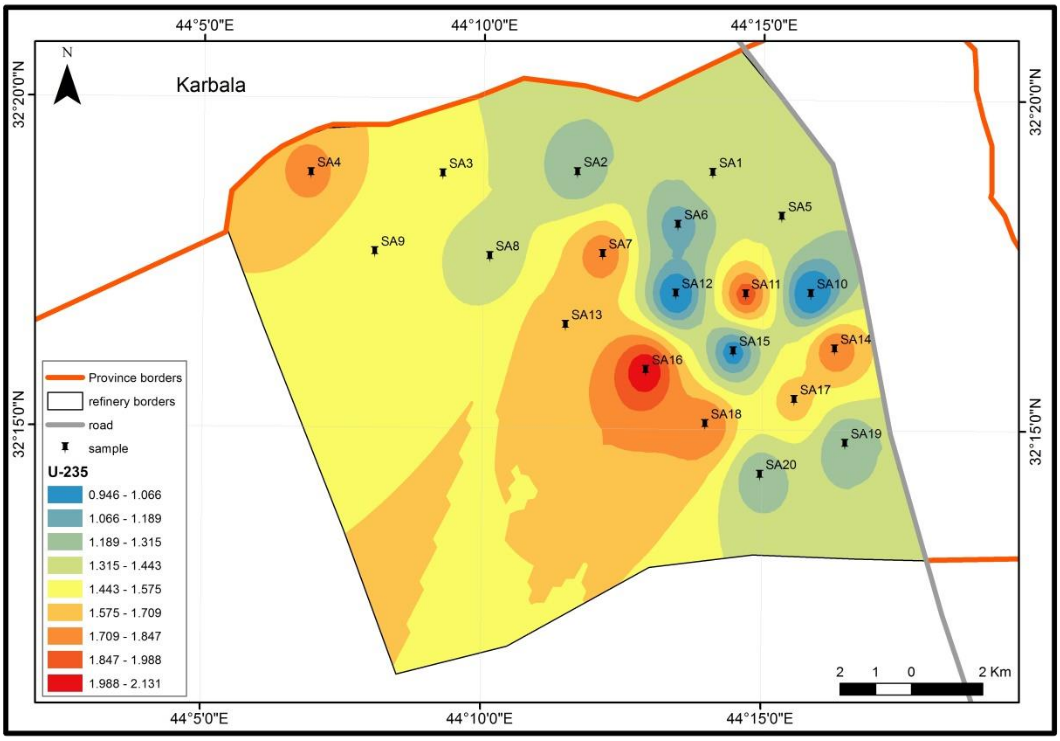

Figure 4.11: The Map of the Average of Specific Activities for ^{235}U in agricultural soil irrigated with groundwater.

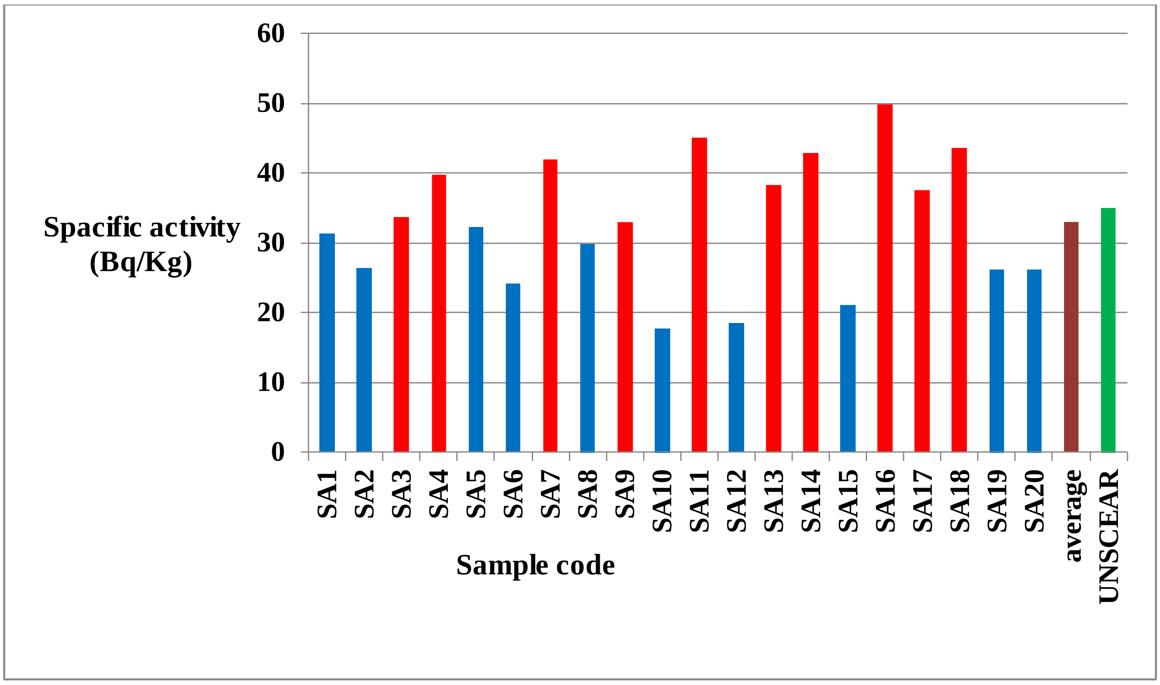

Figure 4.12: Specific Activity in of ^{238}U in Agricultural Soil Irrigated with Groundwater.

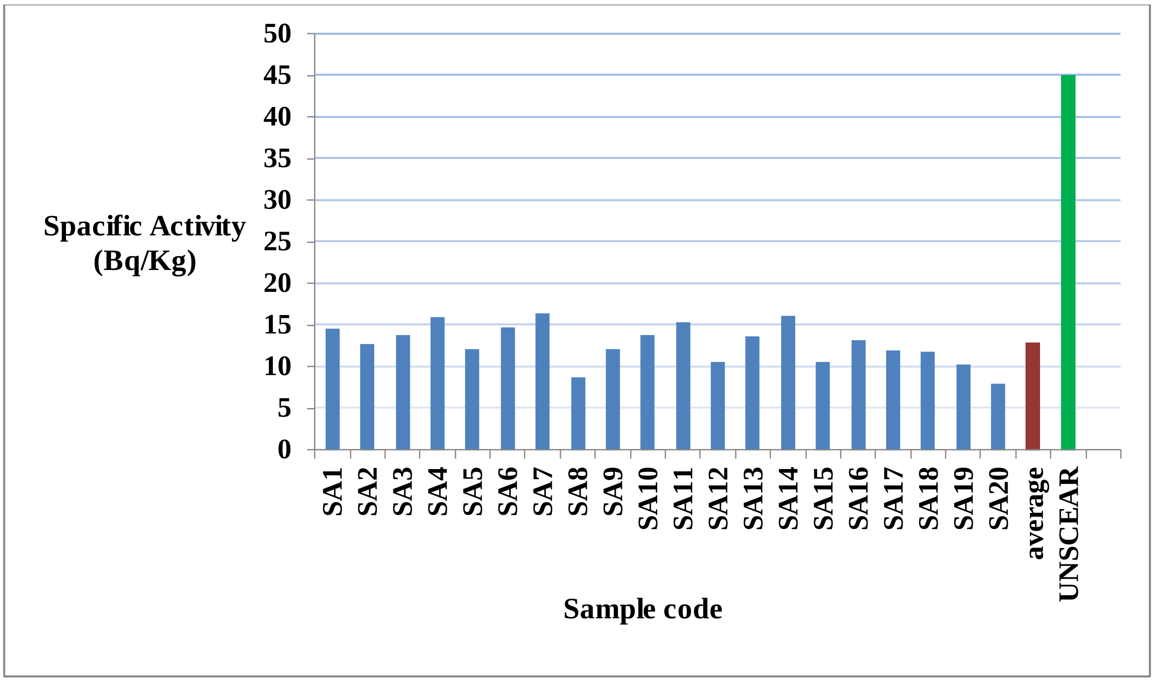

Figure 4.13: Specific Activity of ^{232}Th in Agricultural Soil Irrigated with Groundwater.

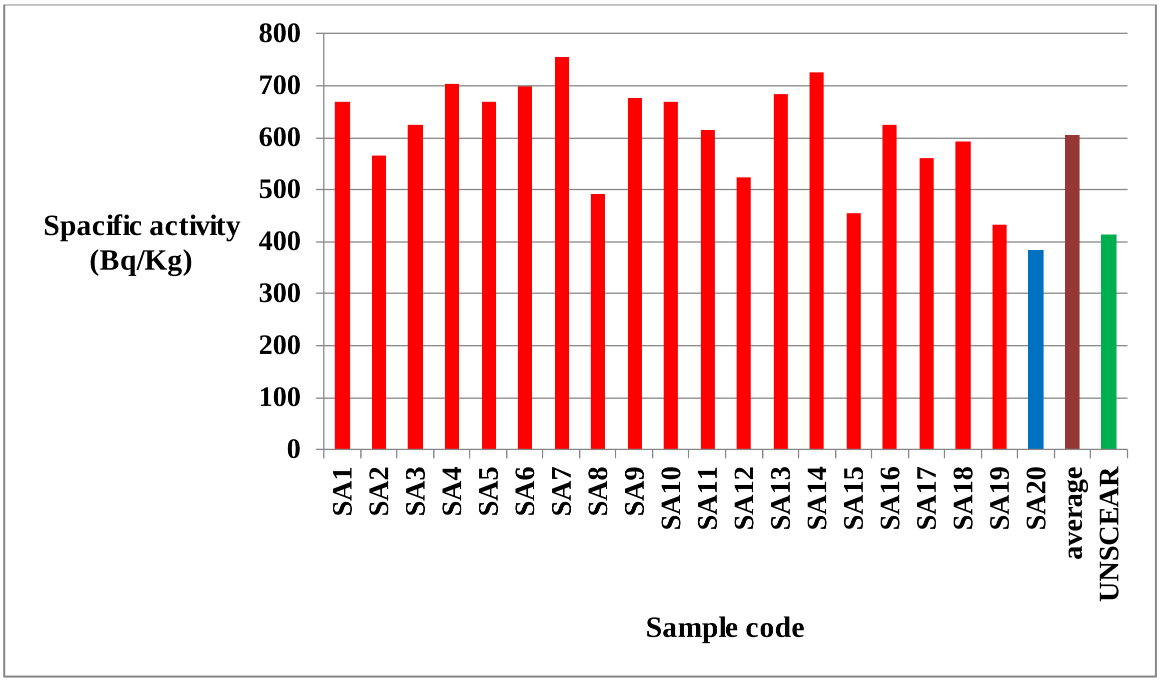

Figure 4.14: Specific Activity of ^{40}K in Agricultural Soil Irrigated with Groundwater.

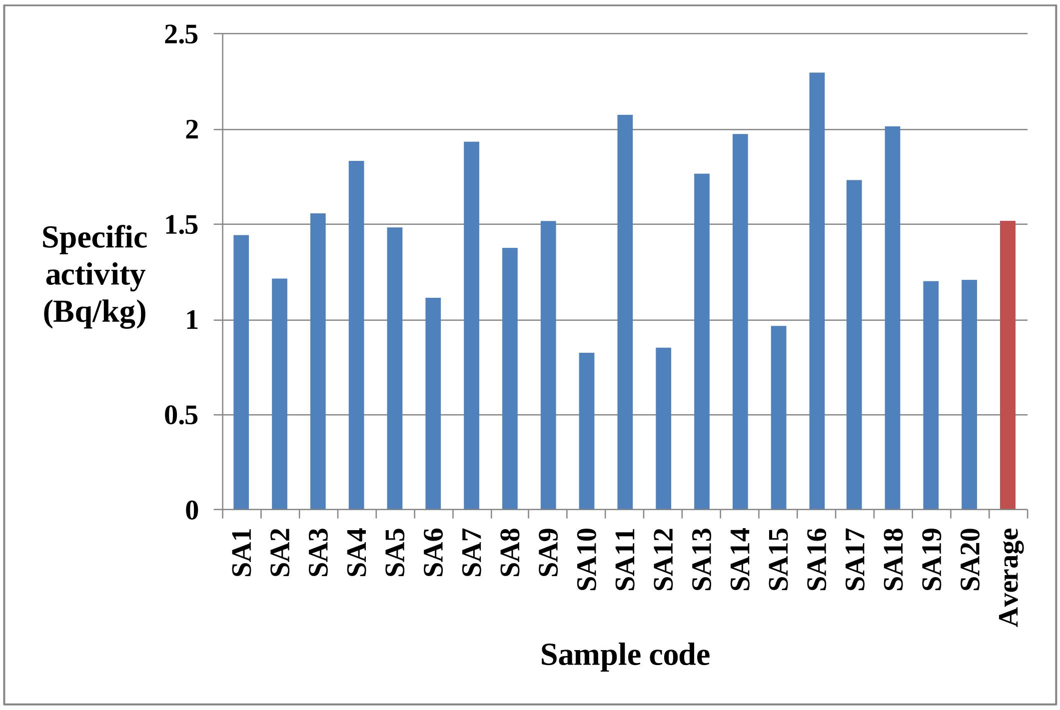

Figure 4.15: Specific Activity of ^{235}U in Agricultural Soil Irrigated with Groundwater.

Table 4.4: Results Ra_{eq}, D_r, H_{in}, H_{ex}, I_γ and I_α in Agricultural soil Irrigated with Groundwater by using NaI(TI).

No.	Sample code	Ra_{eq} (Bq/kg)	D_r (nGy/h)	H_{ex}	Hex	I_γ	I_α
1	SA1	103.641	51.162	0.364	0.28	0.4	0.156
2	SA2	88.109	43.46	0.309	0.238	0.34	0.132
3	SA3	101.672	50.02	0.366	0.275	0.39	0.169
4	SA4	116.873	57.393	0.423	0.316	0.447	0.199
5	SA5	101.216	50.177	0.36	0.273	0.392	0.161
6	SA6	99.190	49.276	0.333	0.268	0.388	0.121
7	SA7	123.495	60.754	0.447	0.334	0.473	0.21
8	SA8	80.144	39.556	0.297	0.216	0.307	0.149
9	SA9	102.304	50.729	0.365	0.276	0.396	0.165
10	SA10	89.262	44.558	0.289	0.241	0.352	0.089
11	SA11	114.255	55.685	0.43	0.309	0.432	0.225
12	SA12	74.058	36.826	0.25	0.2	0.29	0.093
13	SA13	110.546	54.491	0.402	0.299	0.424	0.192
14	SA14	121.741	59.779	0.445	0.329	0.465	0.214
15	SA15	70.978	34.979	0.248	0.192	0.274	0.105
16	SA16	116.818	57.042	0.45	0.316	0.44	0.249
17	SA17	97.966	48.017	0.366	0.265	0.372	0.188
18	SA18	106.245	52.039	0.405	0.287	0.402	0.219
19	SA19	74.0522	36.288	0.271	0.2	0.282	0.131
20	SA20	67.1632	32.921	0.252	0.181	0.255	0.131
Minmum		**67.1632**	**32.921**	**0.248**	**0.181**	**0.255**	**0.089**
Maxmum		**154.757**	**60.754**	**0.271**	**0.329**	**0.609**	**0.249**
Average ±S.D		**99.549±4.805**	**48.258±2.397**	**0.354±0.018**	**0.265±0.013**	**0.376±0.019**	**0.165±0.011**
UNSCEAR [186]		**<370**	**<55**	**≤1**	**≤1**	**≤1**	**≤1**

Table 4.5: Exposure, AEDE, AGED, AGED and ELCR of Agricultural Soil Irrigated with Groundwater by using NaI(TI).

No.	Sample code	Exposure (μR/h)	AEDE (mSv/y)	AGED (mSv/y)	ELCR×10^{-3}
1	**SA1**	207.054	0.251	367.74	1.124
2	**SA2**	176.083	0.213	312.34	0.955
3	**SA3**	198.915	0.245	358.428	1.099
4	**SA4**	227.081	0.282	410.783	1.261
5	**SA5**	201.454	0.246	360.828	1.103
6	**SA6**	205.814	0.242	356.191	1.083
7	**SA7**	320.6	0.381	562.623	1.707
8	**SA8**	154.008	0.194	283.077	0.869
9	**SA9**	203.267	0.249	364.742	1.115
10	**SA10**	190.534	0.219	323.476	0.979
11	**SA11**	213.309	0.273	396.158	1.224
12	**SA12**	153.383	0.181	266.197	0.809
13	**SA13**	215.115	0.267	390.387	1.197
14	**SA14**	235.007	0.293	427.537	1.314
15	**SA15**	141.936	0.172	251.355	0.769
16	**SA16**	214.624	0.28	405.28	1.254
17	**SA17**	185.364	0.236	342.526	1.055
18	**SA18**	197.694	0.255	370.492	1.144
19	**SA19**	142.534	0.178	259.337	0.797
20	**SA20**	126.561	0.161	234.741	0.723
Minmum		**126.561**	**0.161**	**234.741**	**0.723**
Maxmum		**235.007**	**0.381**	**562.623**	**1.707**
Average + S.D		**195.517±9.712**	**0.241±0.011**	**352.212±17.274**	**1.079±0.052**
World Wide Average[187]		**............**	**≤ 1**	**300**	**2.5**

4.1.2.2 Results of Gamma Emitters in in plant Irrigated with groundwater

The natural radioactivity of selected plant samples (tomato fruit) from the study area was measured, and the results were compared to the permissible limits set by UNSCEAR, 2010 [185]. The speicific acttivity of (^{238}U), (^{232}Th) and (^{40}K) was found as follows: The specific activity range of (^{238}U) was found to be 1.023±0.387 Bq/kg to 51.51±2.715 Bq/kg, with average of 17.75±1.467 Bq/kg. For (^{232}Th), the specific activity ranged, from 2.939±0.305 Bq/kg to 22.45±0.761 Bq/kg, with average of 11.35±0.585 Bq/kg. (^{40}K) exhibited a specific activity range, from 287.148±11.603 Bq/kg to 789.171±20.94 Bq/kg, with average of 473.3119 ±16.17 Bq/kg.

Comparing these values with the permissible limits (35, 45 and 412) Bq/kg for (^{238}U, ^{232}Th and ^{40}K respectively) by UNSCEAR [185], it can be observed that the speicific acttivity of (^{238}U) is lower than the global averages, (^{232}Th) is much lower than the global averages, (^{40}K) is a higher than the global averages.

Tabe 4.6: Results of Natural Radioactivity in Plant by Irrigated with Groundwater.

NO.	Sample code	Specific activity in (Bq/kg)		
		^{238}U	^{232}Th	^{40}K
1	SAP1	20.05±2.079	4.159±0.577	411.838±17
2	SAP2	12.51±1.128	6.72±0.384	323.511±11.19
3	SAP3	5.036±0.759	6.821±0.41	422.076±1.355
4	SAP4	18.86±1.673	19.14±0.782	553.649±17.68
5	SAP5	3.085±0.673	2.939±0,305	471.699±16.23
6	SAP6	16.51±1.553	28.83±0.952	789.171±20.94
7	SAP7	9.157±0.965	4.619±0.318	366.101±11.90
8	SAP8	3.894±0.779	2.311±0.365	358.950±13.4
9	SAP9	37.8±2.882	20.05±0.974	664.496±23.57

10	SAP10	3.876±0.808	5.04±0.427	309.769±14.09
11	SAP11	1.536±0.512	11.75±657	452.858±17.14
12	SAP12	51.51±2.715	23.7±0.854	630.138±18.52
13	SAP13	14.98±1.469	3.26±0.417	287.148±11.603
14	SAP14	1.023±0.387	5.219±0.405	385.596±14.64
15	SAP15	4.578±0.809	5.879±0.425	353.908±13.88
16	SAP16	46.62±2.481	21.23±0.777	712.005±18.91
17	SAP17	7.252±1.262	10.54±0.706	563.396±21.70
18	SAP18	38.34±2.705	11.9±0.699	523.824±19.50
19	SAP19	35.27±2.057	22.45±0.761	592.337±16.44
20	SAP20	23.13±1.648	10.48±515	293.761±11.45
Minimum		1.023±0.387	2.311±0.365	287.148±11.603
Maximum		51.51±2.715	28.83±0.952	789.171±20.94
Average ± S.D		17.75±1.467	11.35±0.585	473.311 ±16.17
UNSCEAR [185]		35	45	412

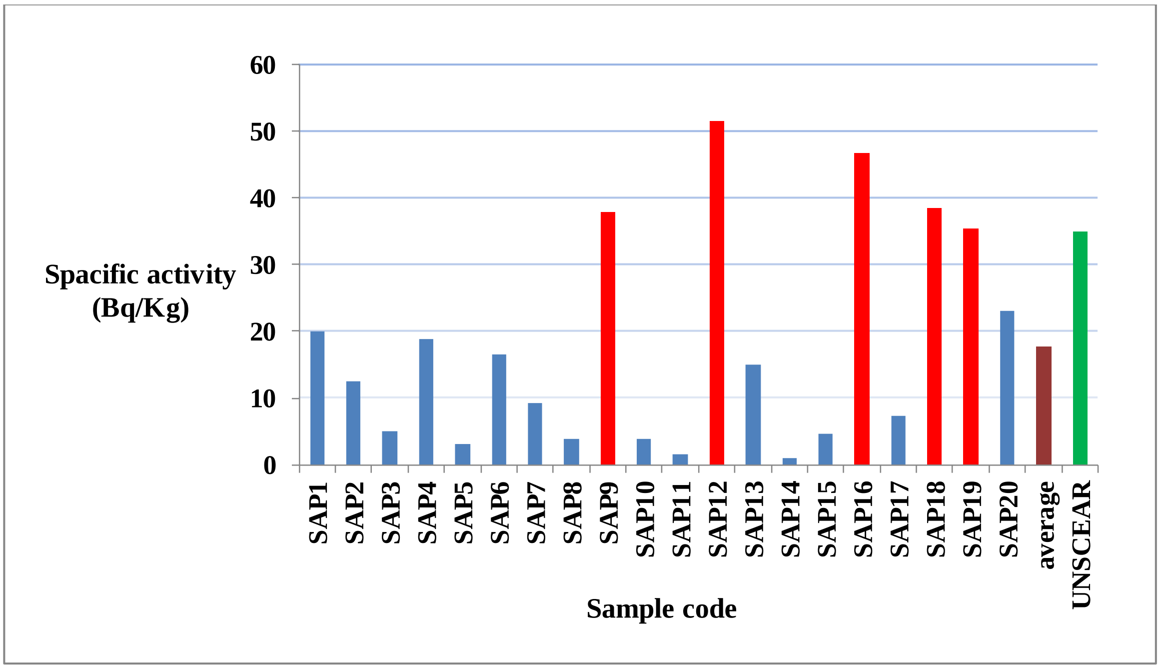

Figure 4.16: Specific Activity in of ^{238}U of Plant Irrigte with Groundwater.

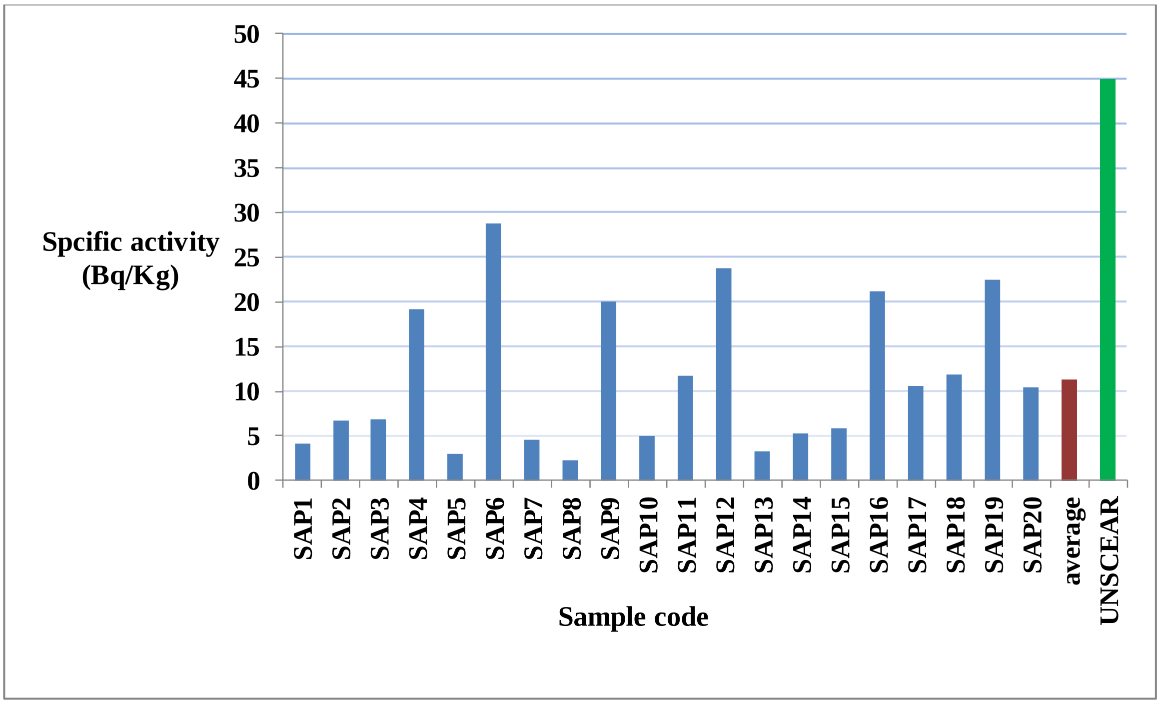

Figure 4.17: Specific Activity in of ^{232}Th of Plant Irrigte with Groundwater.

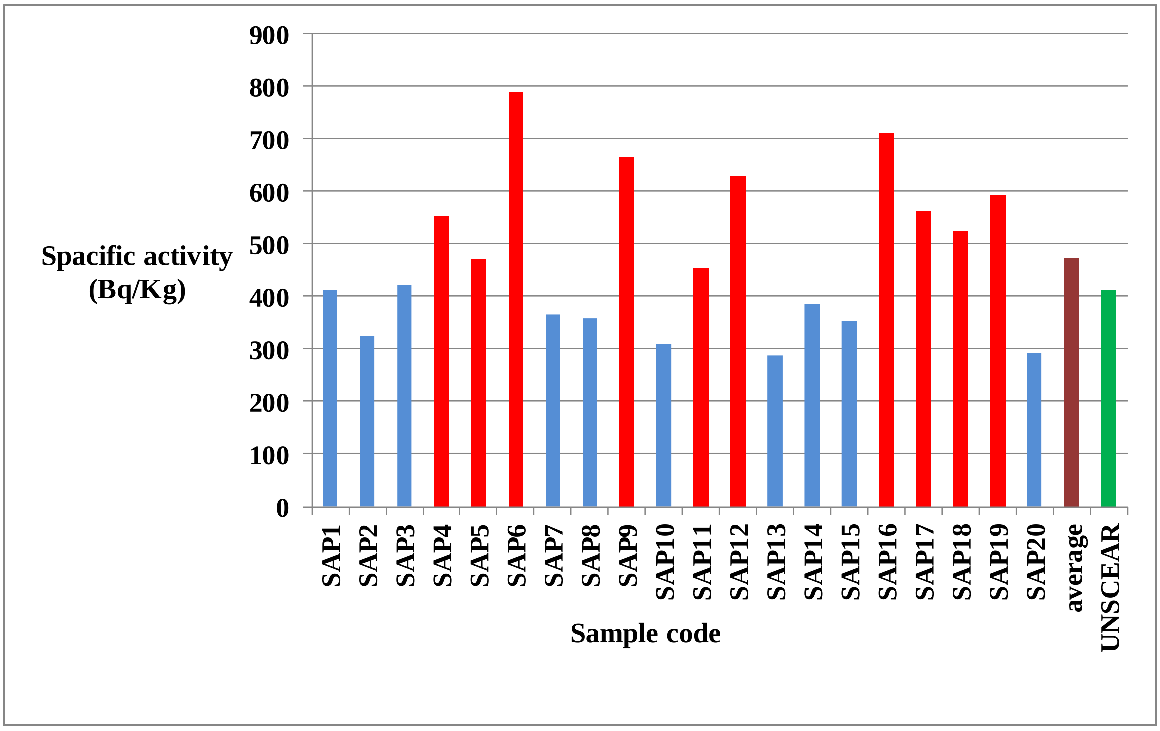

Figure 4.18: Specific Activity in of ^{40}K of Plant Irrigte with Groundwater.

4.1.2.3 Gamma Emitters in Fruit(Tomato Crop) Irrigated with Groundwater

The specific activity of selected fruit samples (tomato crop) in the study area was measured for natural radioactivity. These values were then compared with the peremissible limitses (35, 45 and 412) Bq/kg for ^{238}U, ^{232}Th,^{40}K [206]. The results, presented in Table (4.7), show the following specific activity ranges: (^{238}U) ranged, from 1.621±0.468 Bq/kg to 33.88±1.969 Bq/kg, with average of 14.1±1.29 Bq/kg; (^{232}Th) ranged, from 1.789±0.298 Bq/kg to 20.01±0.795 Bq/kg, with average of 9.705±0.593 Bq/kg; (^{40}K) ranged, from 570.638±20.35 Bq/kg to 818.2±27.61 Bq/kg, with average of 709.007±23.76 Bq/kg. The values of (^{238}U) were lower than the global averages, (^{232}Th) was much lower than the global averages, (^{40}K) was much higher than the worldwide average [185].

Figures (4.19), (4.20) and (4.21) shows the distribution of specific activities for ^{238}U, ^{232}Th and ^{40}K respectively, against the sample positions. Figure (4.19) shows that the highest value for (^{238}U) was found in a sample position, and the values vary significantly in value and position, all of which are lower than the worldwide average. Figure (4.20) illustrates the values of (^{232}Th), which also vary significantly in value and position and are all less than the worldwide average. Figure (4.21) demonstrates that the majority of the high values for (^{40}K) activities were distributed, with most of them being much higher than the worldwide average in the study area [185].

Table 4.7: Spcific Activity in Fruit(Tomato crop) by Irrigated with Groundwater by using NaI(TI).

No.	Sample code	Specific activity in (Bq/Kg)		
		^{238}U	^{223}Th	^{40}K
1	**SAF1**	2.934±0.64	4.924±0.505	630.947±21.86
2	**SAF2**	21.84±1.601	15.33±0.622	721.349±23.17
3	**SAF3**	33.88±1.969	16.65±0.64	687.954±22.34
4	**SAF4**	5.578±0.882	9.12±0.523	770.936±26.11
5	**SAF5**	29.14±1.866	17.29±0.667	787.558±24.42
6	**SAF6**	10.64±1.104	3.792±0.306	570.638±20.35
7	**SAF7**	2.814±0.614	1.789±0.298	650.448±21.74
8	**SAF8**	22.77±1.829	20.01±0.795	818.2±27.61
9	**SAF9**	5.982±0.855	3.021±0.282	691.135±23.13
10	**SAF10**	13.33±1.499	10.2±0.799	803.366±27.11
11	**SAF11**	19.09±1.804	14.8±0.987	756.486±26.44
12	**SAF12**	1.621±0.468	4.711±0.486	651.801±21.85
13	**SAF13**	8.594±1.192	6.744±0.192	763.782±26.16
14	**SAF14**	8.703±1.184	16.08±0.184	686.021±24.4
15	**SAF15**	14.85±1.397	10.52±0.397	655.356±23.9
16	**SAF16**	2.063±0.486	2.807±0.386	624.998±19.71
17	**SAF17**	18.94±1.631	6.715±0.631	708.053±23.21
18	**SAF18**	4.974±0.75	3.061±0.75	637.191±19.76
19	**SAF19**	30.65±2.206	12.2±0.206	778.704±25.9
20	**SAF20**	23.67±1.826	14.34±0.826	754.218±29.5
Minimum		**1.621±0.468**	**1.789±0.298**	**570.638±20.35**
Maximum		**33.88±1.969**	**20.01±0.795**	**818.2±27.61**
Average ± S.D		**14.1±1.29**	**9.705±0.593**	**709.007±23.76**
UNSCEAR [185]		**35**	**45**	**412**

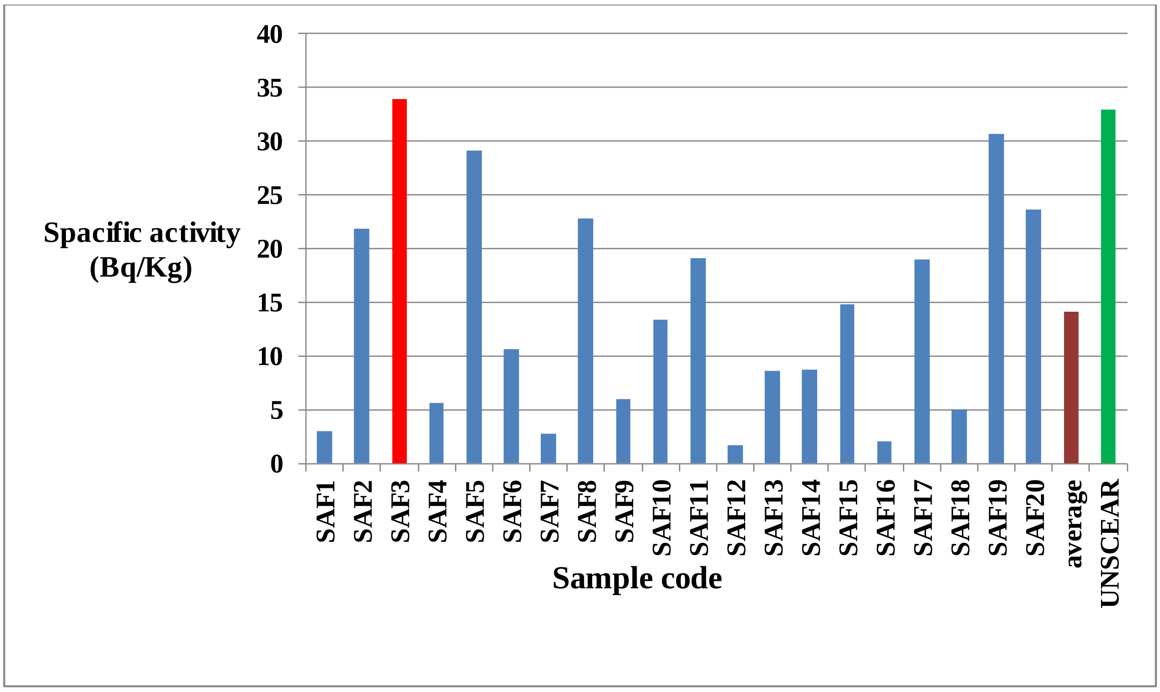

Figure 4.19: The Peacific Activitey of ^{238}U in Fruit Irrigated with Groundwater.

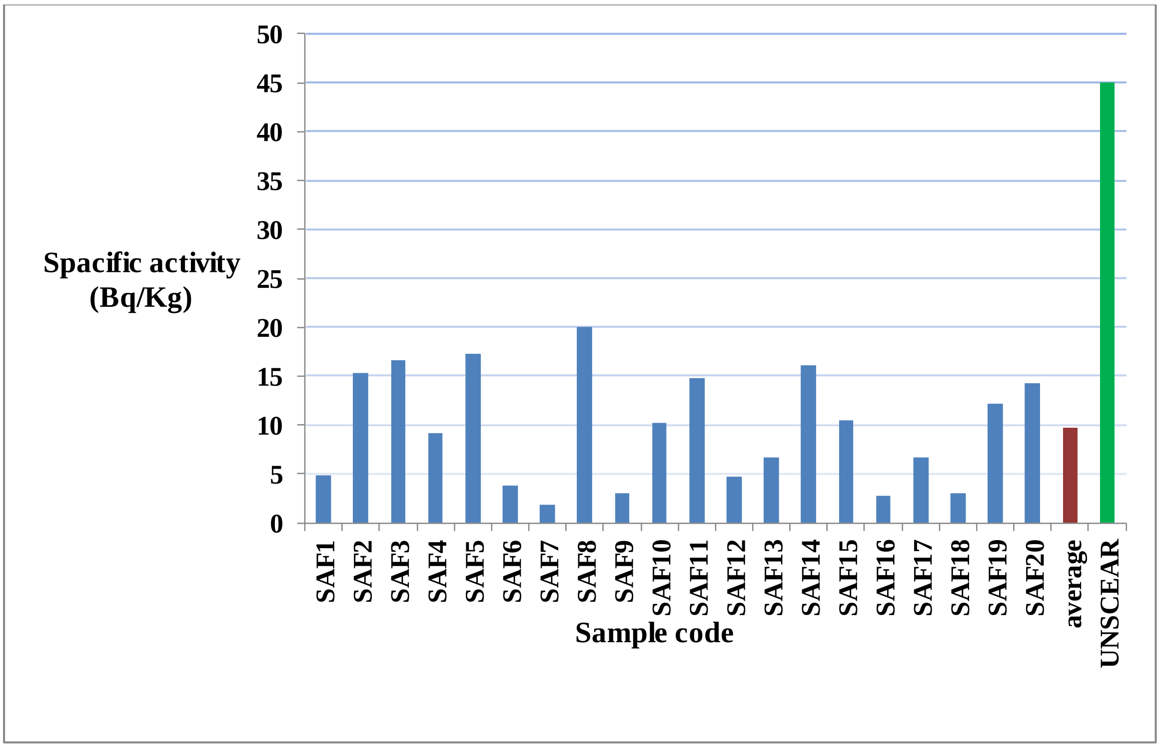

Figure 4.20: Specific Activity of ^{232}Th in Fruit Irrigated with Groundwater.

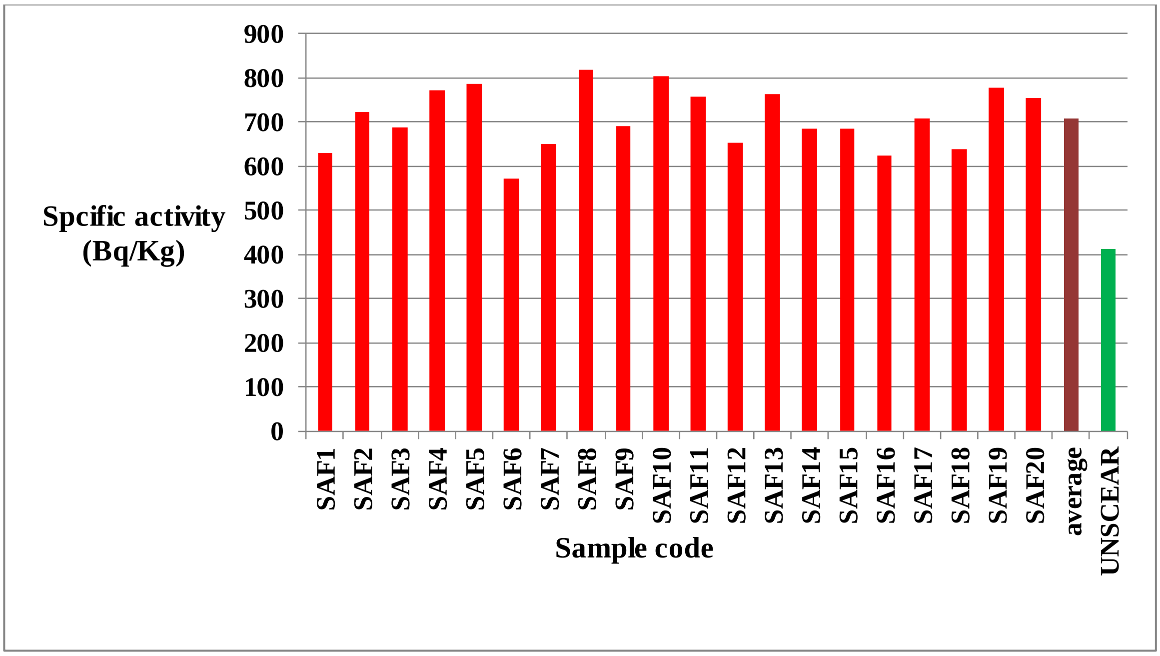

Figure 4.21: The Sapecific Activitey of ^{40}K in Fruit Irrigated with Groundwater.

4.1.2.4 Compared btween the Average values of the Agricultural Soil, Tomato Plant and Fruit(Tomato Crop) which Irrigated with Groundwater

Figures (4.22), (4.23),and (4.24) present a comparison among the average specific activity of radioactive elements ^{238}U, ^{232}Th and ^{40}K in agricultural soil, plants, and tomato crop irrigated with groundwater.

From Figure (4.22), it is evident that the average specific activity of (^{238}U) in agricultural soil is higher compared to that in plants and fruits. Similarly, from Figure (4.23), it can be observed that the specific activity of (^{232}Th) in agricultural soils is greater than that in plants and tomato crop. This difference in specific activity could be attributed to various factors, such as the nature of the soil, the excessive use of chemical fertilizers, the type of water used for irrigation, and the absorption mechanisms of plants and fruits of tomato.

As for the figure (4.24), we can notice that the specific effectiveness of the ^{40}K element in the fruit (tomatoes) is much higher than that of plants and agricultural soils. This is due to the high absorption of the fruit (tomato) of ^{40}K, which is used in agricultural fertilizers in a large and sometimes used excessive manner. ^{40}K is considered one of the light elements compared to the elements ^{238}U, ^{235}U and thus it has the ability to move higher than ^{238}U, ^{232}Th , so the plant absorbs it easily and its concentration becomes higher, and the fruit can absorb it from the plant and its concentration becomes higher than the plant[187-190].

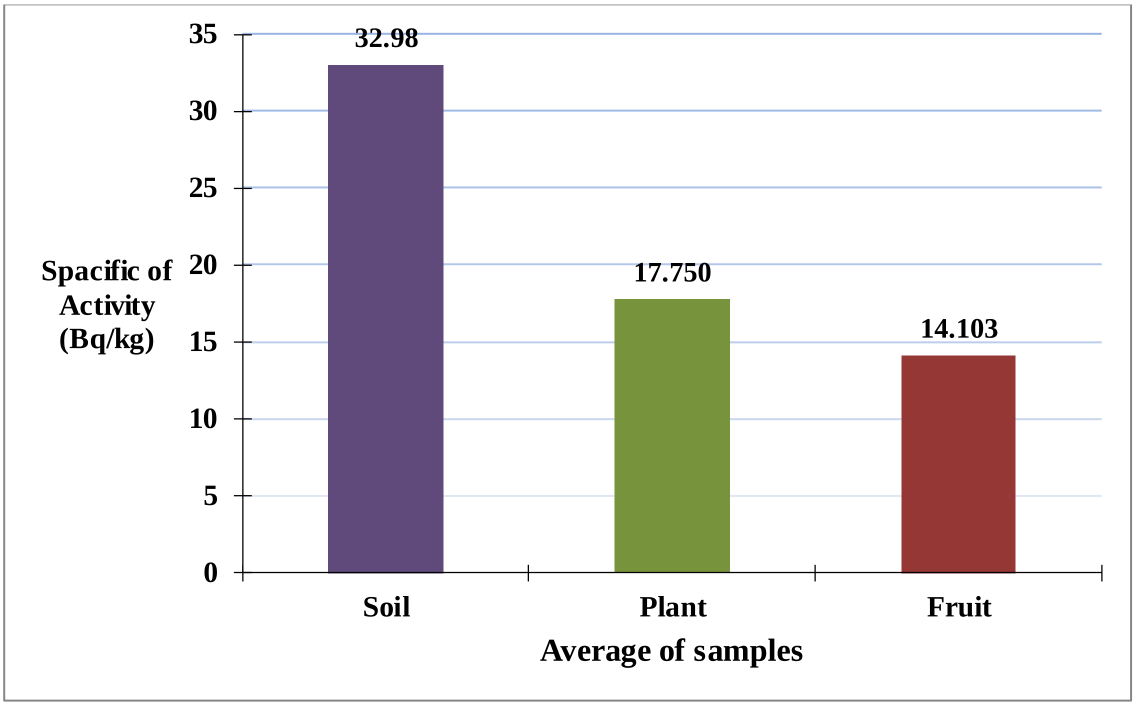

Figure 4.22: Compared the Average of Specific Activity of ^{238}U for Agricultural Soil, Plant and Fruit which Irrigation with Groundwater.

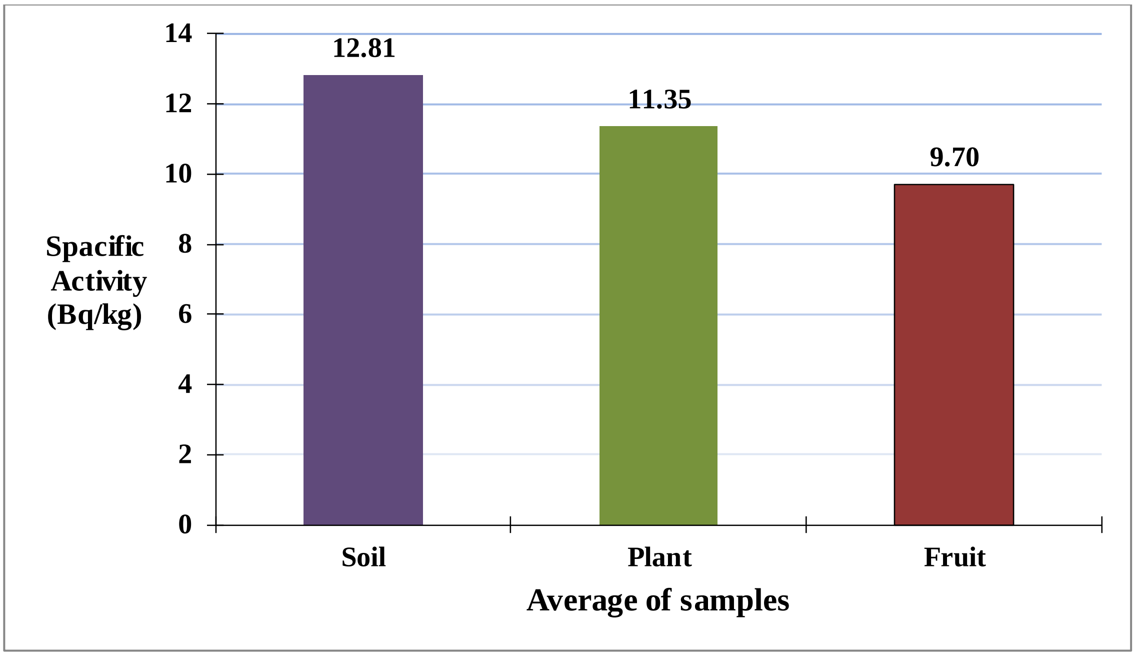

Figure 4.23: Compared the Average of Specific Activity of ^{232}Th for Agricultural Soil, Plant and Fruit which Irrigation with Groundwater.

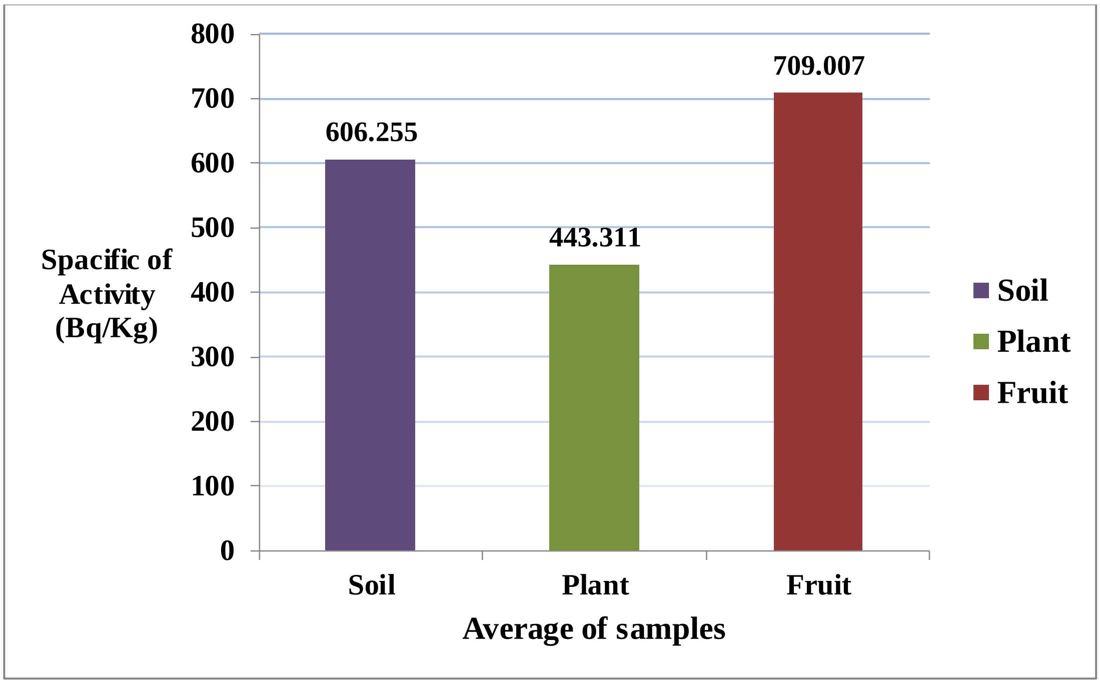

Figure 4.24: Compared the Average of Specific Activity of ^{40}K for Agricultural Soil, Plant and Fruit which Irrigation with Groundwater.

4.1.2.5 Gamma Emitters in Agricultural Soil Irrigated with Surface Water

Table (4.8) presents the results of measuring the natural radioactivity in selected agricultural soil samples irrigated with surface water in the study area. These values were compared to the allowable limits for specific activity, which are 35, 45 and 412 Bq/kg for (^{238}U), (^{232}Th) and (^{40}K) respectively [185].

The specific activity of (^{238}U), (^{232}Th) and (^{40}K) were found within the following ranges: (^{238}U) ranged from 5.4291±0.502 Bq/kg to 73.903±1.769 Bq/kg, with average of 34.799±1.188 Bq/kg; (^{232}Th) ranging from 8.8752±0.298 Bq/kg to 15.118±0.374 Bq/kg, with average of 12.205±0.336 Bq/kg; and (^{40}K) ranged from 603.426±5.905 Bq/kg to 922.167±7.037 Bq/kg, with average of 699.975±6.216.766 Bq/kg. The spaecific acteivity of (^{235}U) ranged from 0.25±0.023 Bq/kg to 3.406±0.078 Bq/kg, with an average of 1.604±0.059 Bq/kg.

It is noteworthy that the values of (^{238}U) exceed the global averages, while the specific activity of (^{232}Th) is considerably lower than the global averages. Additionally, the specific activity of (^{40}K) is significantly higher than the worldwide average [185].

Table (4.9) provides the values of various parameters obtained from the measurement of natural radioactivity in selected agricultural soil samples irrigated with surface water. The parameters include Ra_{eq} (Radium equivalent activity) in Bq/Kg, D_r (absorbed dose rate) in nGy/h, H_{in} (Internal hazard index), H_{ex} (external hazard dose), I_{γ} (Gamma index), and I_{α} (Alpha Index). The recorded values ranged from 63.068 to 170.03 Bq/Kg for Ra_{eq}, from 33.153 to 83.208 nGy/h for D_r, from 0.19 to 0.659 for H_{in}, from 0.17 to 0.459

for H_{ex}, from 0.254 to 0.642 for I_{γ}, and from 0.027 to 0.284 for I_α. The average values were 106.15±7.001 Bq/Kg for Ra_eq, 52.638±3.337 nGy/h for D_r, 0.381±0.031 for H_{in}, 0.287±0.019 for H_{ex}, 0.41±0.025 for I_{γ}, and 0.174±0.022 for Iα. These average values are comparable to the worldwide average, and all values were lower than the worldwide average [186].

Table (4.10) presents the values of exposure Exposure, AEDE (Annual Effective Dose Equivalent), AGED (Annual Gonadal Equivalent Dose), and ELCR (Excess Lifetime Cancer Risk). The recorded values ranged from 148.076 to 371.62 μR/h for exposure, from 0.157 to 0.408 mSv/y for AEDE, from 233.752 to 513.344 for AGED, and from 0.702 to 1.829 for ELCR. The average values were 238.43±14.539 μR/h for exposure, 0.258±0.016 mSv/y for AEDE, 378.336±23.225 for AGED, and 1.157±0.073 for ELCR. These average values are comparable to the worldwide average, and all values were lower than the worldwide average [187].

The maps displayed in Figures (4.25, 4.26, 4.27 and 4.28) are illustrate the distribution of the average of specific activities for (^{238}U, ^{232}Th , ^{40}K and ^{235}U) the average of specific activities in the selected agricultural soil irrigte with surface water samples, respectively. These maps were generated using Arc GIS 10.4.1 and a GIS methodology, utilizing distinct colors to differentiate between high, medium, and low levels .

Figures (4.29, 4.30 , 4.31 and 4.32) illustrate the distribution of specific activities for (^{238}U), (^{232}Th), (^{40}K), and (^{235}U) against the sample positions, respectively. Figure (4.29) and Figure (4.32) indicate that the highest values for (^{238}U) and (^{235}U), respectively, are lower than the worldwide average. The samples show significant variation in value and position, which can be attributed to fruit irrigation with groundwater. Figure (4.30) demonstrates that the specific activity values of (^{232}Th) were found to be lower than the worldwide average, with significant variation in value and position. Finally, Figure (4.31) shows that the specific activity of (^{40}K) is generally much higher than the worldwide average in the study area.

During a a comparison between the average sapecific acttivities of (^{238}U), (^{232}Th), and (^{40}K). It is evident that the average specific activity of (^{40}K) is significantly higher compared to (^{238}U) and (^{232}Th). This difference can be attributed to the excessive use of chemical fertilizers and the nature of the soil.

Tabe 4.8: Specific activity in Agricultural Soil Irrigated with Surface water.

No.	Sample code	Specific activity in (Bq/Kg)			
		^{238}U	^{232}Th	^{40}K	^{235}U
1	SB1	63.72±1.809	13.687±0.389	793.715±7.19	2.936±0.088
2	SB2	44.554±1.471	11.277±0.343	694.772±6.54	2.053±0.069
3	SB3	55.618±1.642	17.772±0.43	850.94±7.232	2.563±0.077
4	SB4	30.295±1.175	9.9875±0.313	603.426±5.905	1.396±0.053
5	SB5	24.175±1.017	11.378±0.324	634.345±5.868	1.114±0.045
6	SB6	5.4291±0.502	8.8752±0.298	606.338±5.974	0.25±0.023
7	SB7	73.903±1.769	17.567±0.4	922.167±7.037	3.406±0.078
8	SB8	44.134±1.384	14.715±0.371	803.448±6.651	2.034±0.061
9	SB9	27.821±1.105	12.689±0.346	757.881±6.495	1.282±0.049
10	SB10	49.278±1.438	18.949±0.413	889.407±6.879	2.271∓0.063
11	SB11	16.141±0.829	10.143±0.305	640.957±5.885	0.744±0.036
12	SB12	8.805±0.566	8.924±0.264	538.988±4.988	0.406±0.023
13	SB13	33.859±1.174	12.074±0.325	694.036±5.986	1.560±0.050
14	SB14	23.142±1.027	10.634±0.223	619.953±5.985	1.066±0.047
15	SB15	26.18±1.098	8.9743±0.298	637.876±6.107	1.206±0.050
16	SB16	17.87±0.802	9.399±0.27	573.277±5.113	0.824±0.032
17	SB17	52.45±1.475	12.579±0.335	701.98±6.079	2.417±0.064
18	SB18	18.506±0.874	10.309±0.303	649.872±5.836	0.853±0.038

19	**SB19**	56.706±1.563	15.118±0.374	735.597±6.339	2.613±0.069
20	**SB20**	23.385±1.048	9.042±0.302	650.525±6.225	1.078±0.048
Minimum		**5.4291±0.502**	**8.8752±0.298**	**603.426±5.905**	**0.25±0.023**
Maximum		**73.903±1.769**	**15.118±0.374**	**922.167±7.037**	**3.406±0.078**
Average ± S.D		**34.799±1.188**	**12.205±0.336**	**699.975±6.216**	**1.604±0.059**
UNSCEAR [185]		**35**	**45**	**412**	**-**

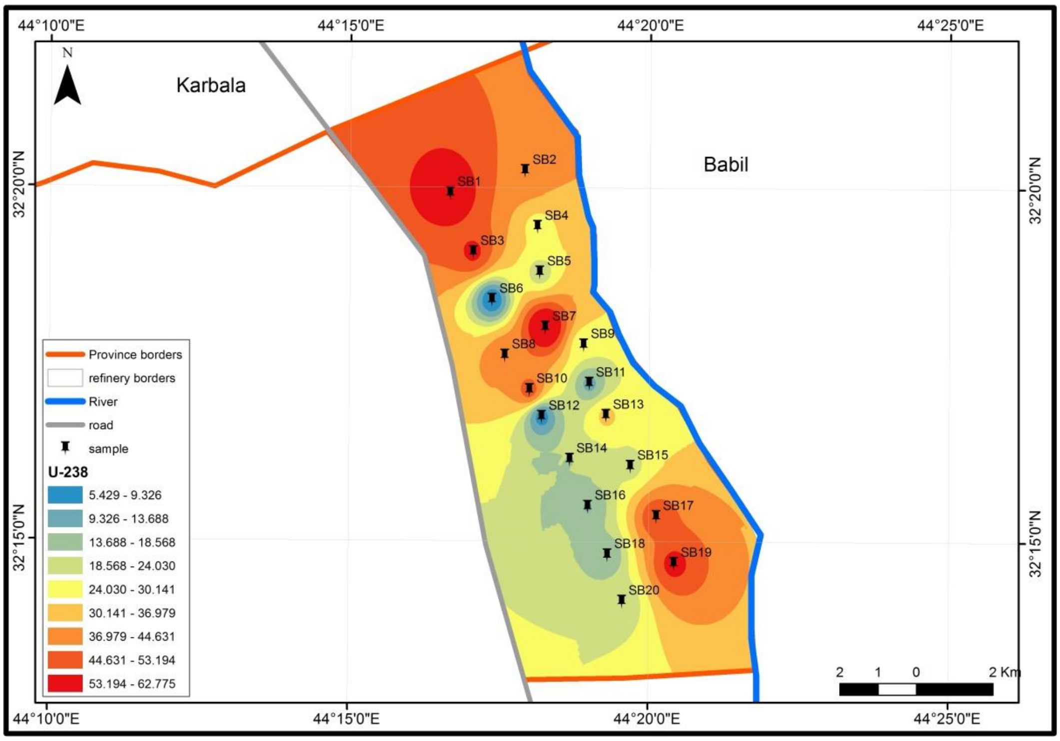

Figure 4.25: The Map of the Average of Specific Activities for ^{238}U in Agricultural Soil Irrigatde with Surface water.

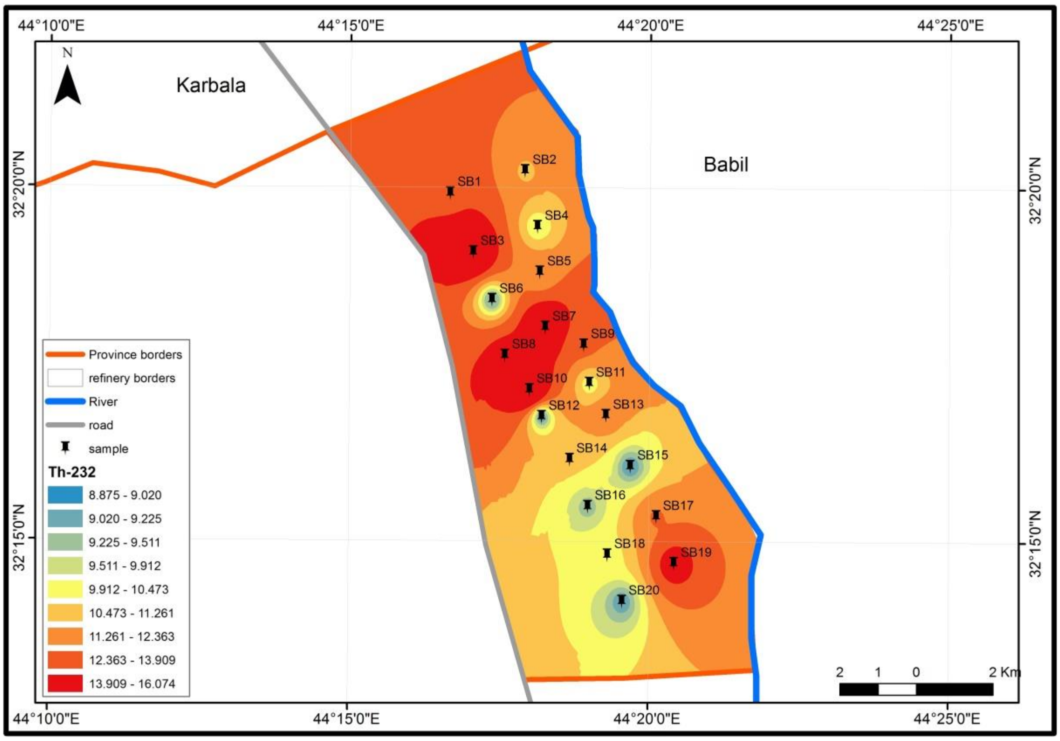

Figure 4.26: The Map of the Average of Specific Activities for ^{232}Th in Agricultural Soil Irrigatde with Surface water.

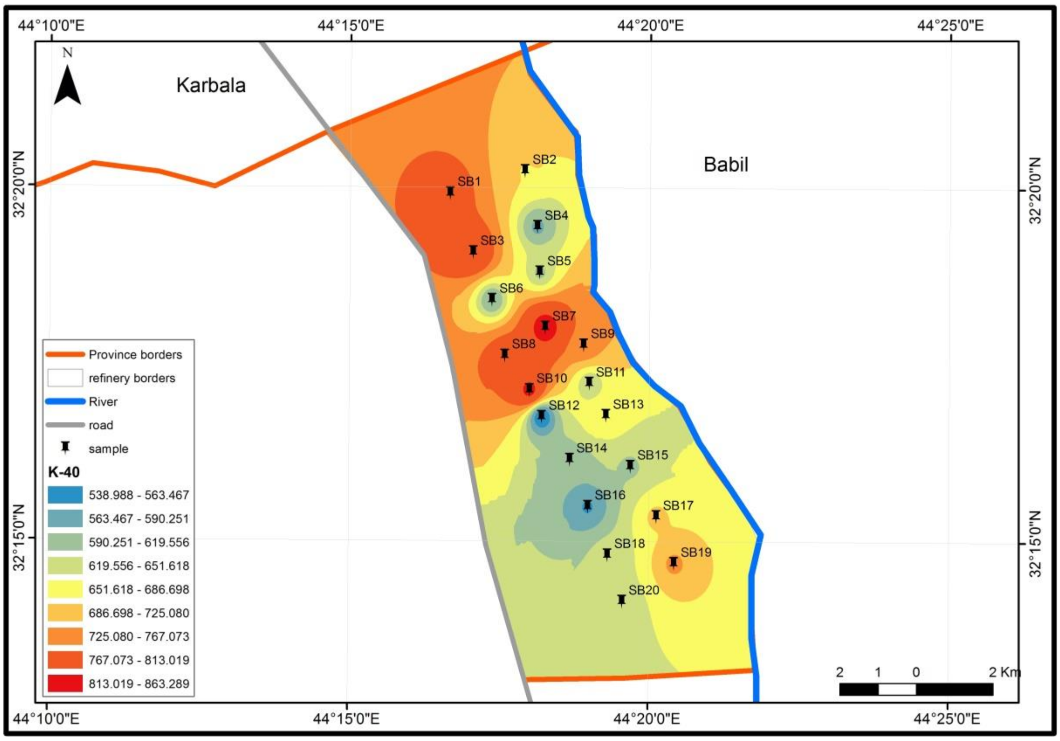

Figure 4.27: The Map of the Average of Specific Activities for ^{40}K in Agricultural Soil Irrigatde with Surface water.

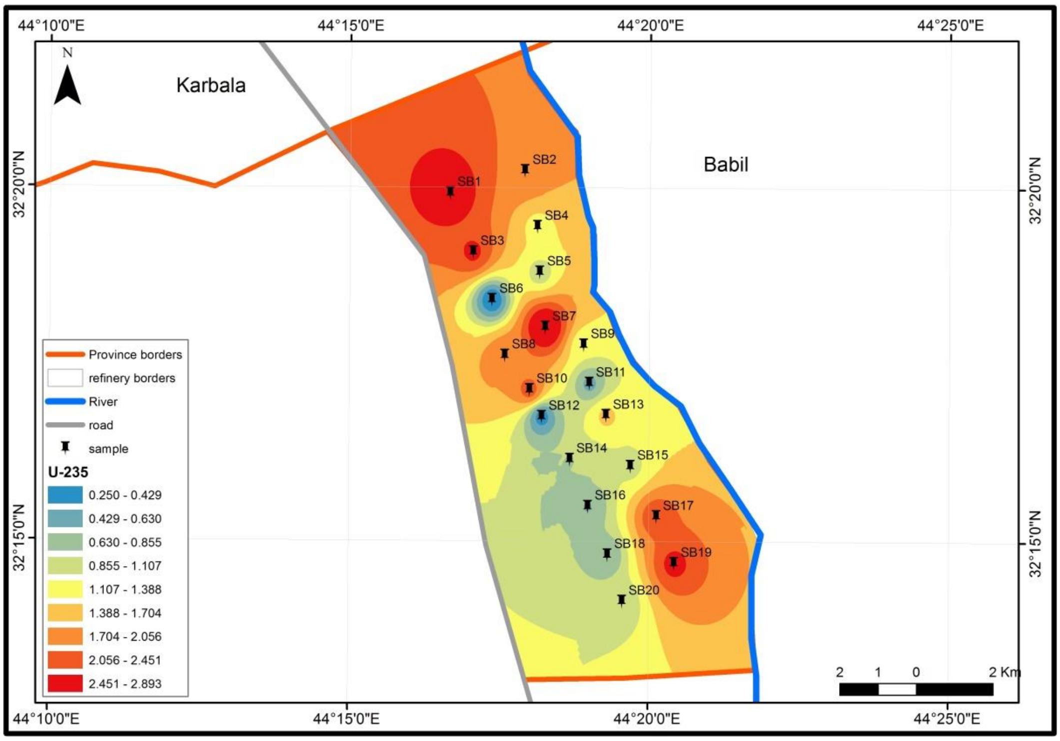

Figure 4.28: The Map of the Average of Specific Activities for ^{235}U in Agricultural Soil Irrigatde with Surface water.

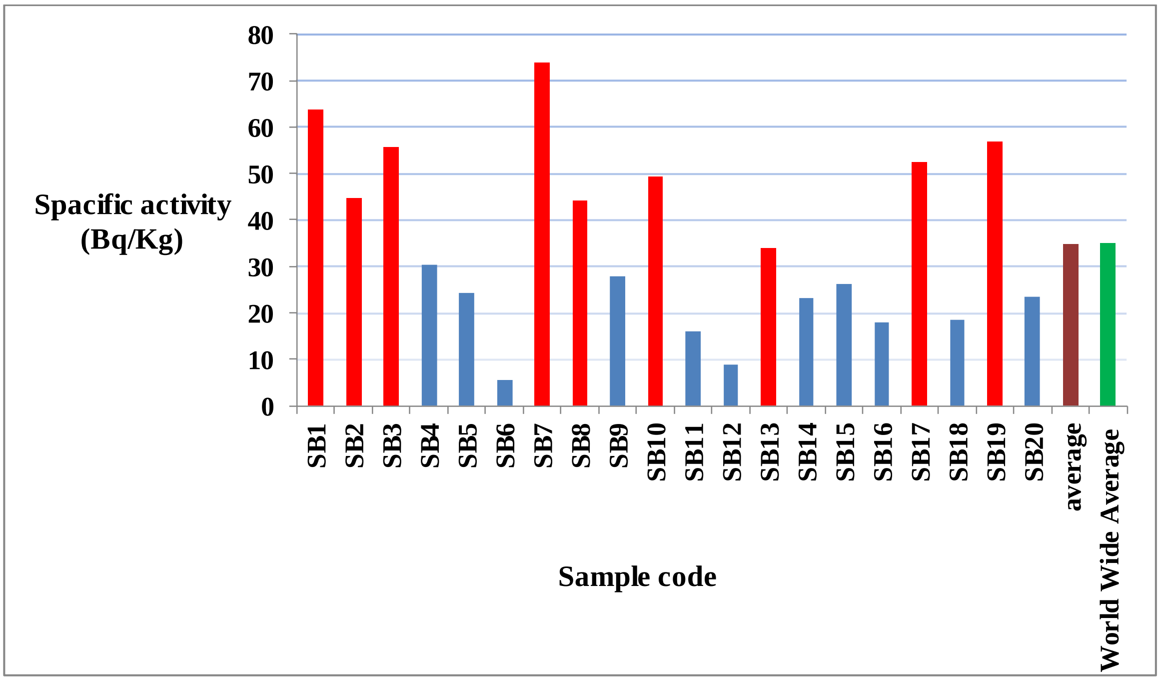

Figure 4.29: The Specific Activity of ^{238}U in Agricultural Soil Irrigated with Surface water.

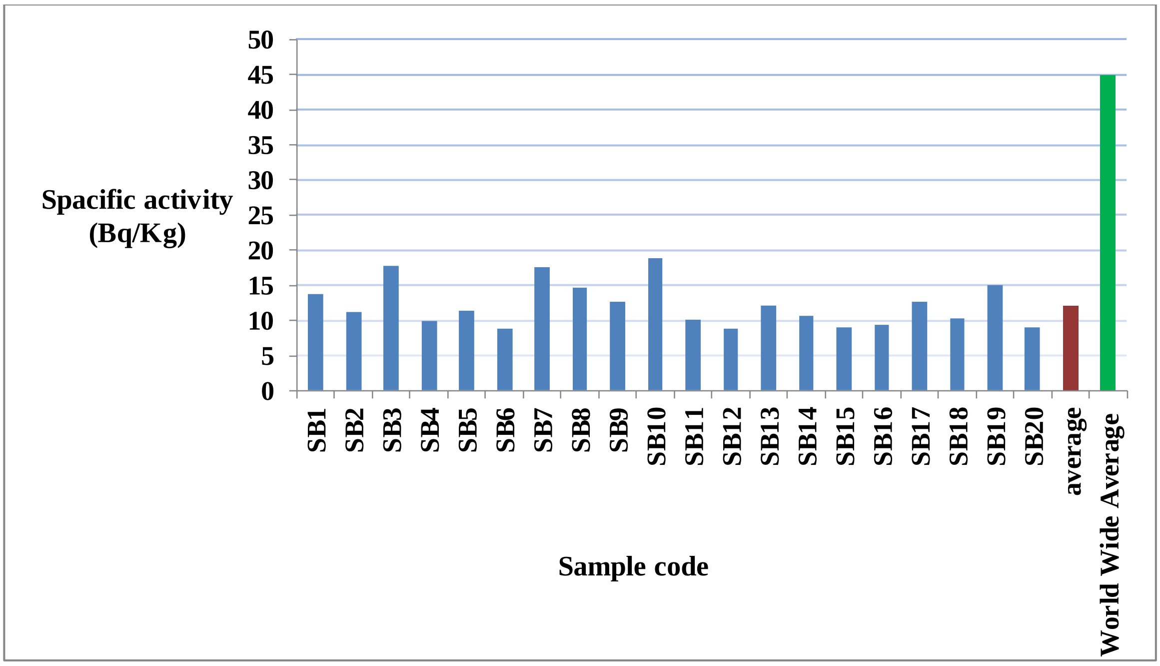

Figure 4.30: The Specific Activity of ^{40}Th in Agricultural Soil Irrigated with Surface water.

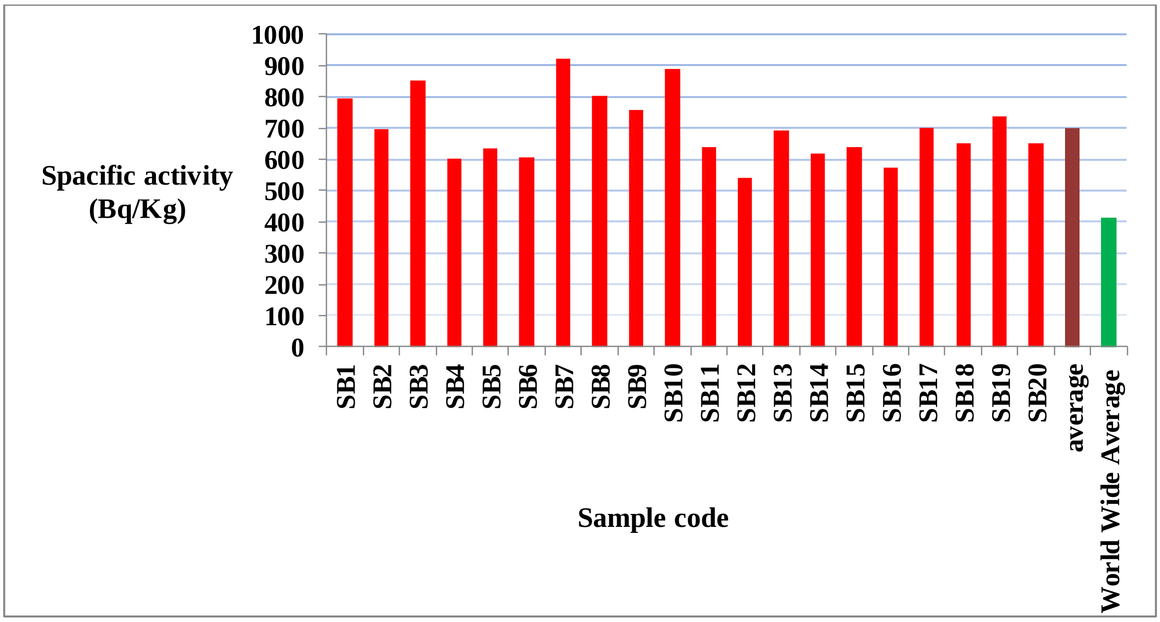

Figure 4.31: The Specific Activity of ^{40}K in Agricultural Soil Irrigated with Surface water.

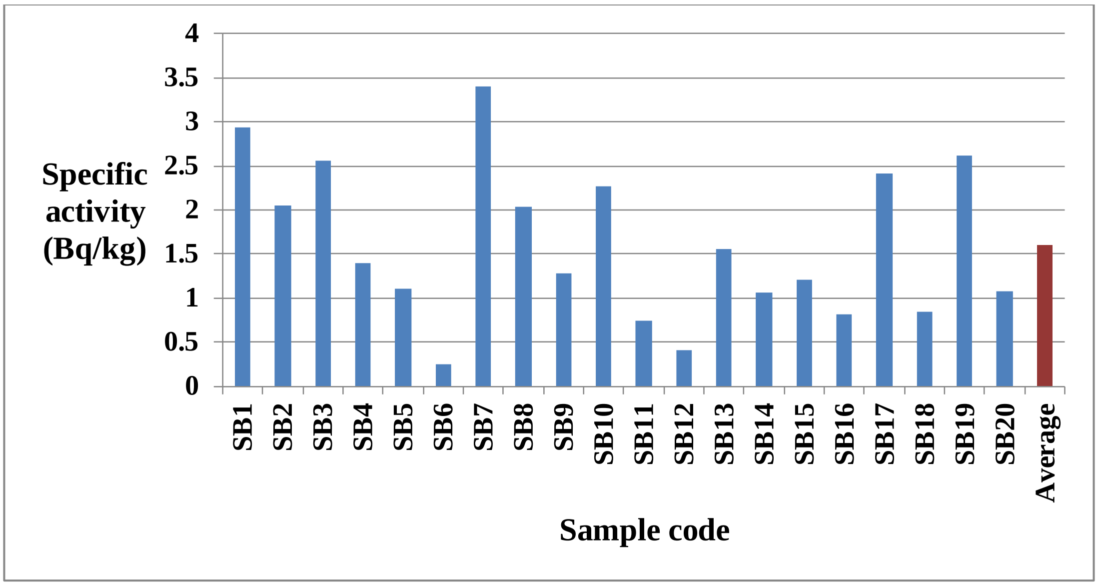

Figure 4.32: The Specific Activity of ^{235}U in Agricultural Soil Irrigated with Surface water.

Tabe 4.9: Results Ra_{eq}, D_r, H_{in}, H_{ex}, I_γ and I_α in Agricultural Soil Irrigatde with Surface water.

No.	Sample code	Ra_{eq} (Bq/kg)	D_r (nGy/h)	H_{in}	H_{ex}	I_γ	I_α
1	**SB1**	144.409	70.804	0.562	0.39	0.545	0.319
2	**SB2**	114.178	56.367	0.429	0.308	0.436	0.223
3	**SB3**	146.555	71.914	0.546	0.396	0.558	0.278
4	**SB4**	91.0405	45.191	0.328	0.246	0.352	0.151
5	**SB5**	89.291	44.494	0.306	0.241	0.349	0.121
6	**SB6**	64.808	33.153	0.19	0.175	0.265	0.027
7	**SB7**	170.03	83.208	0.659	0.459	0.642	0.37
8	**SB8**	127.042	62.782	0.462	0.343	0.489	0.221
9	**SB9**	104.323	52.121	0.357	0.282	0.409	0.139
10	**SB10**	144.859	71.3	0.524	0.391	0.555	0.246
11	**SB11**	80.000	40.312	0.26	0.216	0.318	0.081

12	**SB12**	63.068	31.934	0.194	0.17	0.254	0.044
13	**SB13**	104.566	51.877	0.374	0.282	0.405	0.169
14	**SB14**	86.085	42.967	0.295	0.232	0.337	0.116
15	**SB15**	88.129	44.115	0.309	0.238	0.345	0.131
16	**SB16**	75.452	37.839	0.252	0.204	0.298	0.089
17	**SB17**	124.491	61.103	0.478	0.336	0.472	0.262
18	**SB18**	83.288	41.876	0.275	0.225	0.33	0.093
19	**SB19**	134.965	66.004	0.518	0.365	0.51	0.284
20	**SB20**	86.405	43.392	0.297	0.233	0.34	0.117
Minmum		**63.068**	**33.153**	**0.19**	**0.17**	**0.254**	**0.027**
Maxmum		**170.03**	**83.208**	**0.659**	**0.459**	**0.642**	**0.284**
Average + S.D		**106.15± 7.001**	**52.638± 3.337**	**0.381± 0.031**	**0.287± 0.019**	**0.41± 0.025**	**0.174± 0.022**
UNSCEAR [186]		**<370**	**<55**	**≤1**	**≤1**	**≤1**	**≤1**

Tabe 4.10: Exposure, AEDE, AGED and ELCR of Agricultural Soil Irrigatde with Surface water.

No.	Sample code	Exposure (μR/h)	AEDE (mSv/y)	AGED (mSv/y)	ELCR×10^{-3}
1	**SB1**	316.029	0.347	503.335	1.556
2	**SB2**	253.325	0.277	402.97	1.239
3	**SB3**	323.428	0.353	513.344	1.58
4	**SB4**	204.599	0.222	324.834	0.993
5	**SB5**	202.986	0.218	321.448	0.978
6	**SB6**	154.792	0.163	244.265	0.729
7	**SB7**	371.62	0.408	591.348	1.829
8	**SB8**	283.63	0.308	450.166	1.38
9	**SB9**	237.945	0.256	376.982	1.145
10	**SB10**	322.277	0.35	510.749	1.567

11	**SB11**	185.542	0.198	293.537	0.886
12	**SB12**	148.076	0.157	233.752	0.702
13	**SB13**	235.108	0.254	373.023	1.14
14	**SB14**	196.09	0.211	310.627	0.944
15	**SB15**	200.71	0.216	318.7	0.969
16	**SB16**	173.394	0.186	274.515	0.832
17	**SB17**	273.419	0.3	435.075	1.343
18	**SB18**	192.259	0.205	304.337	0.92
19	**SB19**	295.286	0.324	469.391	1.45
20	**SB20**	198.083	0.213	314.32	0.954
Minmum		**148.076**	**0.157**	**233.752**	**0.702**
Maxmum		**371.62**	**0.408**	**513.344**	**1.829**
Average + S.D		**238.43± 14.539**	**0.258±0.016**	**378.336±23.225**	**1.157±0.073**
World Wide average[187]		**............**	**≤ 1**	**300**	**2.5**

4.1.2.6 Gamma Emitters in Plant Irrigtated with Surface Water

Table (4.11) presents the results of measuring the natural radioactivity in selected plant samples irrigated with surface water in the study area. These values were compared with the allowable limits for ^{238}U, and ^{40}K , which are 35, 45 and 412 [186].

The results are as follows: The spaecific acttivity of (^{238}U), ranging from 1.446±0.2 Bq/kg to 94.47±4.19 Bq/kg, with average of 27.08±1.89 Bq/kg. The spaecific activity of (^{232}Th), ranging from 0.832±0.186 Bq/kg to 66.6±2.38 Bq/kg, with average of 14.21±0.688 Bq/kg. The spaecific activity of (^{40}K), ranged from 97.2692±3.458 Bq/kg to 967.053±25.964 Bq/kg, with average of 416.053±15.321 Bq/kg.

The recorded values for (^{238}U), were lower than the global averages, while the values for (^{232}Th) were much lower than the global averages. On the other hand, the spaecific acttivity of (^{40}K), was a higher than the global averages. These values deviate from the worldwide average [186].

Figures (4.33, 4.34 and 4.35), illustrate the distribution of specific activities across different sample positions for (^{238}U), (^{232}Th) and (^{40}K) respectively. In Figure (4.33) was evident that the majority of samples values for (^{238}U) was below the worldwide average. These values are primarily located at the beginning and end of the study area. However, there is a few samples with higher values that are dispersed within the study area, both in terms of position and magnitude. These elevated values are in relation to the study area near the plant irrigation with surface water.

Moving on to Figure (4.34), it can be noted that the distribution of (^{232}Th) values, which exhibit divergent values and positions across the samples. Notably, two sample values exceed the worldwide average for (^{232}Th).

Figure (4.35) focuses on the distribution of (^{40}K) activities. It reveals that the majority of sample values are higher than the worldwide average and exhibit significant variability, particularly in the middle of the study area. This observation can be attributed to the excessive use of chemical fertilizers and the characteristics of the soil. (^{40}K) is a lighter element compared to (^{238}U) and (^{232}Th), which enables it to move more easily. Consequently, plants readily absorb (^{40}K), leading to higher concentrations.

Lastly, a comparison between the average specific activities of (^{238}U), (^{232}Th) and (^{40}K). It is evident that the average specific activity of (^{40}K) is considerably higher than that of (^{238}U) and (^{232}Th). This disparity can be attributed to the excessive use of chemical fertilizers and the nature of the soil. (^{40}K), being a lighter element compared to (^{238}U), exhibits a higher mobility, which facilitates its absorption by plants and results in higher concentrations.

Tabe 4.11: Specific Activity in Plant Irrigated with Surface water.

No.	Sample code	Specific activity in (Bq/Kg)		
		^{238}U	^{232}Th	^{40}k
1	SBP1	5.417±1.02	0.832±0.186	454.311±18.288
2	SBP2	9.541±1.25	12.92±0.676	454.324±16.864
3	SBP3	11.44±1.19	4.894±0.362	358.45±13.021
4	SBP4	4.15±0.91	4.039±0.414	294.899±14.893
5	SBP5	66.34±3.69	52.56±1.998	831.179±23.535
6	SBP6	80.32±4.15	43.86±1.867	967.053±25.964
7	SBP7	21.72±2.01	4.632±0.43	396.574±16.737
8	SBP8	38.01±2.56	10.07±0.612	427.945±16.774
9	SBP9	23.18±1.76	10.55±0.552	322.06±12.815
10	SBP10	15.12±1.79	1.741±0.282	401.499±18.038
11	SBP11	18±1.85	2.242±0.302	397.409±16.927
12	SBP12	77.27±4.21	66.6±2.38	941.962±26.512
13	SBP13	12.09±1.38	9.355±0.562	129.496±8.795
14	SBP14	19.15±1.92	6.951±0.538	426.909±17.728
15	SBP15	94.47±4.19	27.35±1.045	663.101±21.642
16	SBP16	4.963±0.39	1.431±0.098	41.6044±2.2231
17	SBP17	1.446±0.2	1.114±0.083	44.3466±2.2091
18	SBP18	4.796±1.02	13.56±0.797	401.471±18.251
19	SBP19	26.93±1.9	5.418±0.396	269.205±11.745
20	SBP20	7.336±0.49	4.095±0.196	97.2692±3.4587
Minimum		**1.446±0.2**	**0.832±0.186**	**97.2692±3.4587**
Maximum		**94.47±4.19**	**66.6±2.38**	**967.053±25.964**
Average ± S.D		**27.08±1.89**	**14.21±0.688**	**416.053±15.321**
UNSCEAR [185]		**35**	**45**	**412**

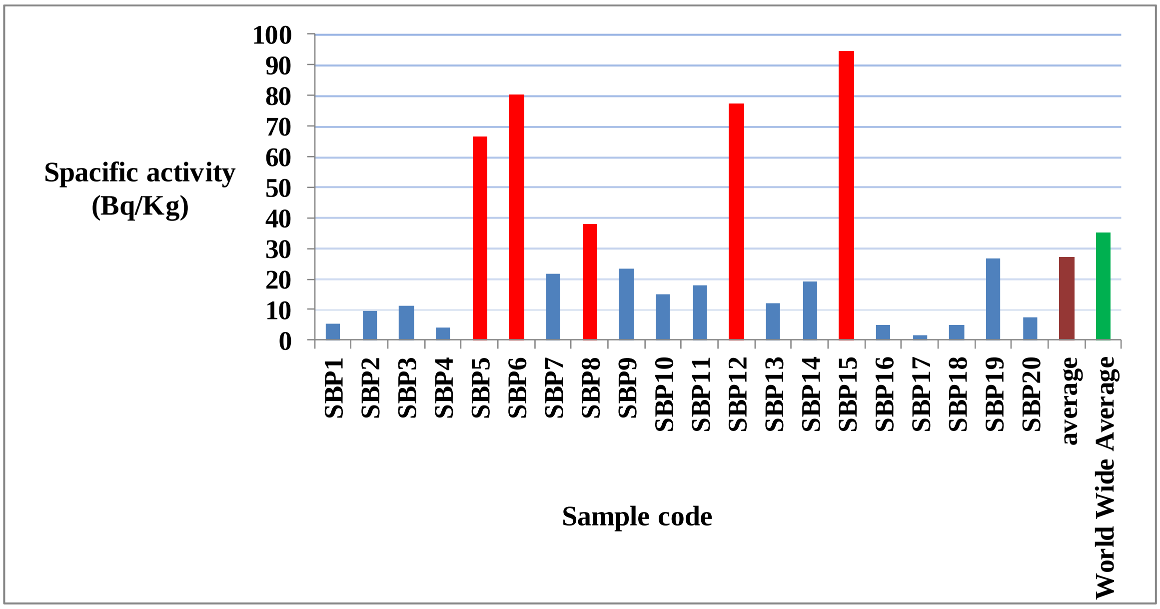

Figure 4.33: The Specific Activity of ^{238}U in Plants Irrigated with Surface water was Measured.

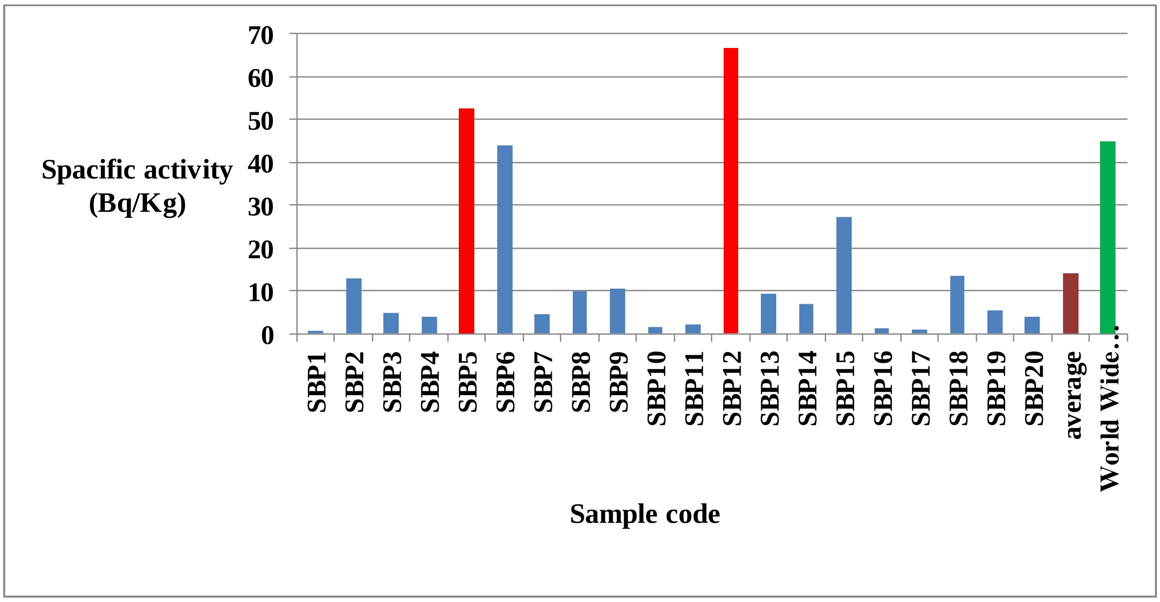

Figure 4.34: The Specific Activity of ^{232}Th in Plants Irrigated with Surface water was Measured.

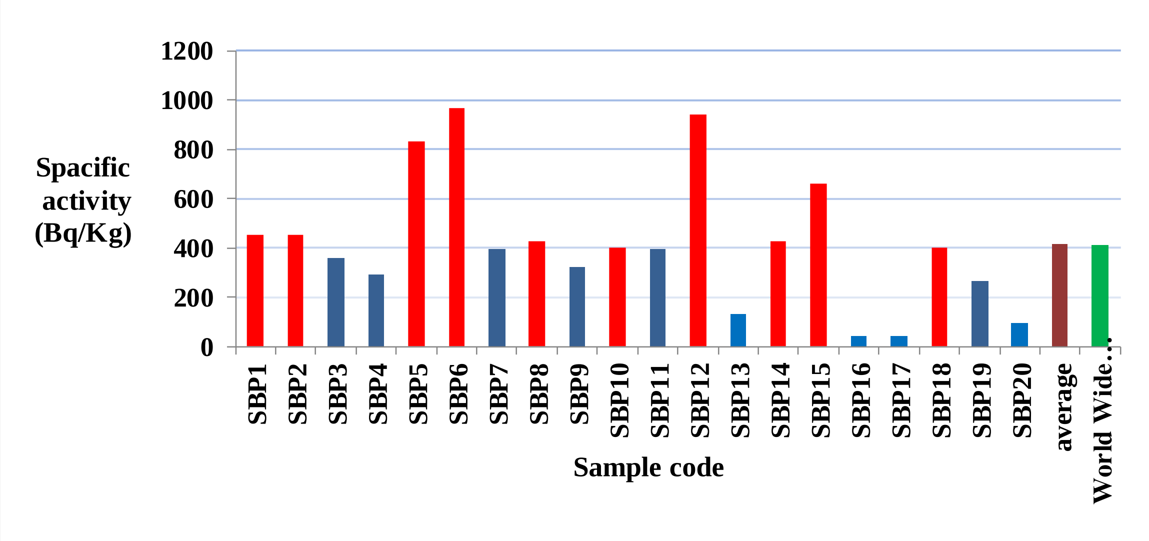

Figure 4.35: The Specific Activity of ^{40}K in Plants Irrigated with Surface water was Measured by NaI(TI).

4.1.2.7 Results of Gamma Emitters in Fruit Irrigtated with Surface Water

The natural radioactivity of specific fruits irrigated with surface water samples in the study area was measured and campared to the permissible limits for ^{238}U, and ^{40}K, as indicated in references [185]. The results, presented in Table (4.12), illustrate the specific activities of (^{238}U), (^{232}Th) and (^{40}K). For (^{238}U), the spaecific activity ranged, from 1.822±0.47 Bq/kg to 32.03±1.935 Bq/kg, with average of 14.77±1.276 Bq/kg. Regarding (^{232}Th), the spaecific activity ranged, from 1.650±0.268 Bq/kg to 20.044±0.748 Bq/kg, with average of 9.157±0.535 Bq/kg. The spaecific activity of (^{40}K) ranged, from 350.891±11.42 Bq/kg to 734.626±18.516 Bq/kg, with average of 501.38±14.611 Bq/kg. Lastly,

Comparing these values to global averages[185], it can be observed that the spaecific acttivities of (^{238}U) is lower, while (^{232}Th) is significantly lower than the global averages. On the other hand, (^{40}K) exhibits significantly higher specific activity compared to the worldwide average [185].

Figures (4.36, 4.37 and 4.38) depict the distribution of specific activities against sample positions for (^{238}U), (^{232}Th) and (^{40}K) respectively. In Figure (4.36) the values for (^{238}U) in the samples are below the worldwide average. The positions and values of the samples from fruit irrigation with surface water exhibit variation and contrast. Figure (4.37) demonstrates that the values of (^{232}Th) in the samples exhibit diverse positions and close values. Finally, Figure (4.38) illustrates the distribution of (^{40}K) activities, with most sample values surpassing the worldwide average and being close in proximity, particularly in the middle of the specified area.

Moving on to a comparison between the average specific activities of (^{238}U), (^{232}Th) and (^{40}K). Notably, the average specific activity of (^{40}K) is significantly higher compared to (^{238}U) and (^{232}Th). This disparity can be attributed to the excessive use of chemical fertilizers and the soil's characteristics. (^{40}K) is considered a lighter element compared to (^{238}U), allowing it to move more freely. As a result, plants easily absorb (^{40}K), leading to higher concentrations, particularly in fruits such as tomatoes. This higher concentration of (^{40}K) in fruits compared to other elements has been reported in references [187-190].

Table 4.12: Results of Specific Activity in Fruit Irrigated with Surface water.

No.	Sample code	Specific activity in (Bq/Kg)		
		^{238}U	^{232}Th	^{40}K
1	SBF1	7.138±0.879	14.147±0.574	658.422±16.462
2	SBF2	10.73±1.037	10.569±0.477	526.425±14.172
3	SBF3	32.03±1.935	13.857±0.59	605.239±16.409
4	SBF4	4.45±0.722	1.650±0.268	417.111±12.609
5	SBF5	24.69±1.654	11.543±0.689	397.535±11.97
6	SBF6	9.46±1.078	8.431±0.62	436.374±13.209
7	SBF7	9.229±1.001	1.985±0.215	442.581±13.523
8	SBF8	21.83±1.636	14.327±0.615	734.626±18.516
9	SBF9	25.38±2.012	14.505±0.927	542.042±16.779
10	SBF10	10.02±1.017	5.8879±0.362	460.295±13.45
11	SBF11	6.968±0.892	11.103±0.686	350.891±11.422
12	SBF12	6.694±0.879	5.0162±0.353	489.216±14.659
13	SBF13	1.822±0.47	4.8219±0.466	463.471±13.537
14	SBF14	7.148±1.001	8.5034±0.506	479.73±15.996
15	SBF15	20.6±1.634	20.044±0.748	730.568±19.032
16	SBF16	21.26±1.766	11.86±0. 803	506.207±15.544
17	SBF17	11.02±1.175	3.205±386	422.034±13.115
18	SBF18	27.68±1.993	5.426±0.537	418.4±13.975
19	SBF19	7.564±0.868	7.687±0.406	433.139±12.808
20	SBF20	29.69±1.863	8.576±0.464	509.301±15.052
Minimum		**1.822±0.47**	**1.650±0.268**	**350.891±11.42**
Maximum		**32.03±1.935**	**20.044±0.748**	**734.626±18.516**
Average ± S.D		**14.77±1.276**	**9.157±0.535**	**501.38±14.611**
UNSCEAR [185]		**35**	**45**	**412**

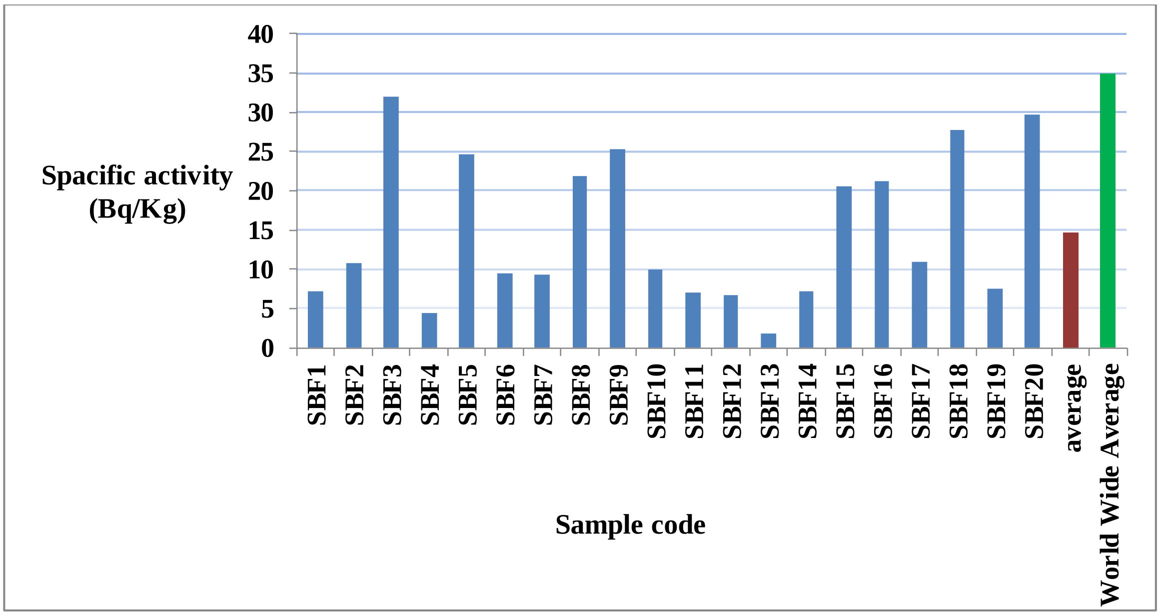

Figure 4.36: The Specific Activity of ^{238}U in Fruits Irrigated with Surface water.

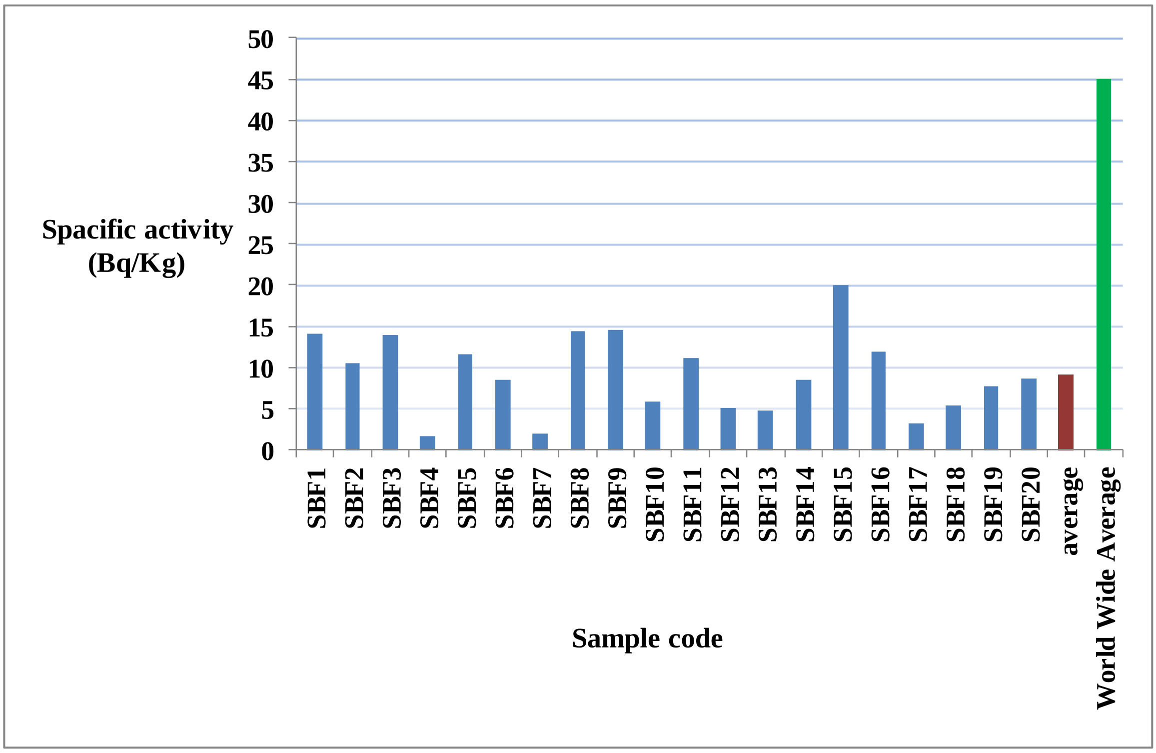

Figure 4.37: The Specific Activity of ^{232}Th in Fruits Irrigated with Surface water.

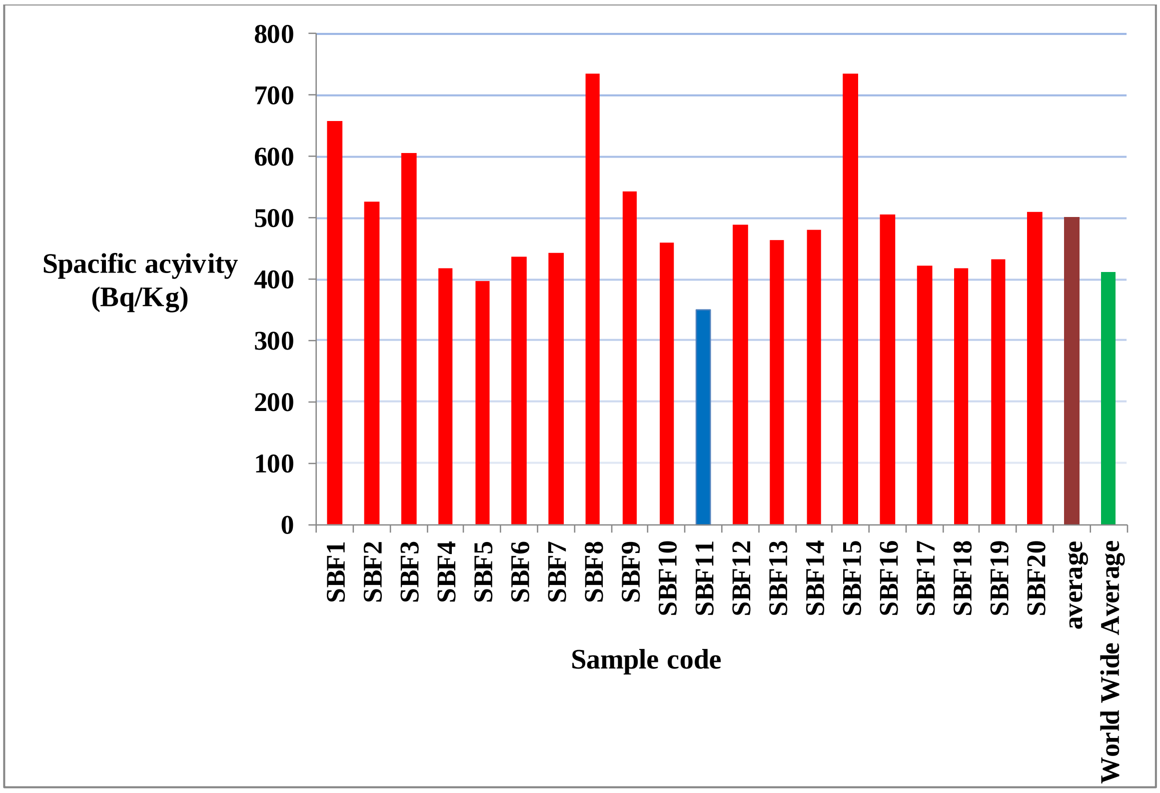

Figure 4.38: The Specific Activity of ^{40}K in Fruits Irrigated with Surface water.

4.1.2.8 Acomparison the average values of the agricultural soil, plant and fruit which irrigation with surfacewater

The average specific activity values of radioactive elements, including (^{238}U), (^{232}Th), (^{40}K) , were compared between agricultural soil, plants, and fruits irrigated with surface water, as shown in Figure (4.39), Figure (4.40), and Figure (4.41).

Figure (4.39), it is evident that the average of spaecific acttivity values, of (^{238}U) in agricultural soil are higher compared to plants and fruits (specifically tomato crops). This difference may be attributed to the nature of the soil, the use of animal and chemical fertilizers, and the type of water utilized for irrigation. It can be observed that plants exhibit lower absorption of (^{238}U) compared to fruits (tomatoes).

Furthermore, Figure (4.40) demonstrates that the average specific activity value of (^{232}Th) in plants is higher than that in agricultural soil and fruits (tomatoes). This discrepancy could be due to the plant's greater capacity for absorbing (^{232}Th), compared to fruits (tomatoes).

Also from the Figure (4.41), it can be noted that, the average specific activity value of (^{40}K) is higher than agricultural soil and fruits (tomatoes). This may be due to This is due to the high absorption of the fruit (tomato) of (^{40}K), which is used in agricultural fertilizers in a large and sometimes used excessive manner.

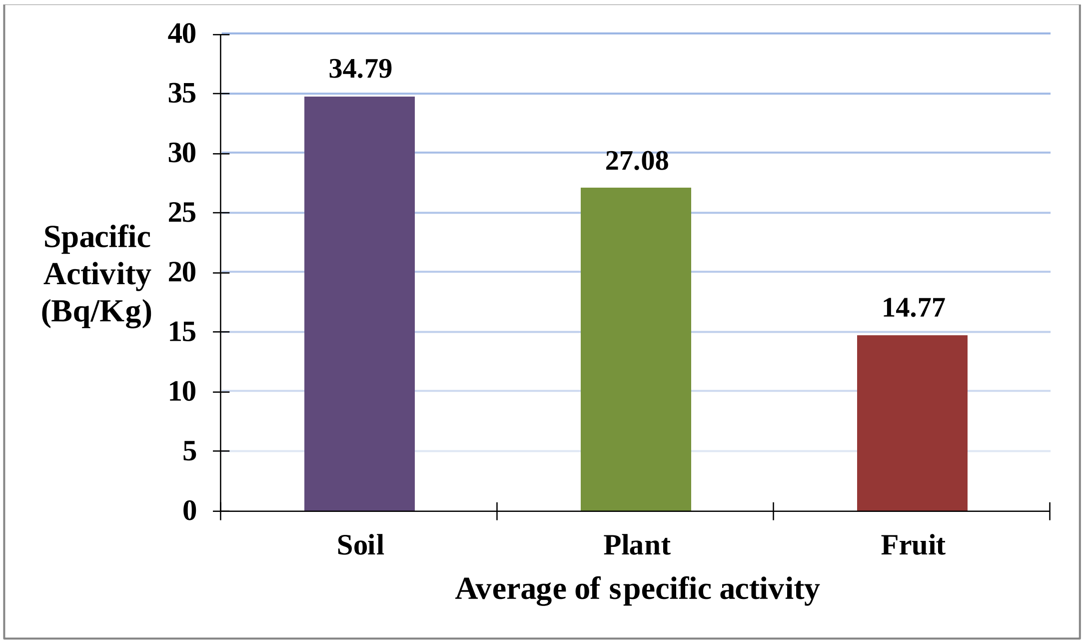

Figure 4.39: Compared the Average of Specific Activity of ^{238}U for Agricultural Soil, Plant and Fruit which Irrigation with Surface water.

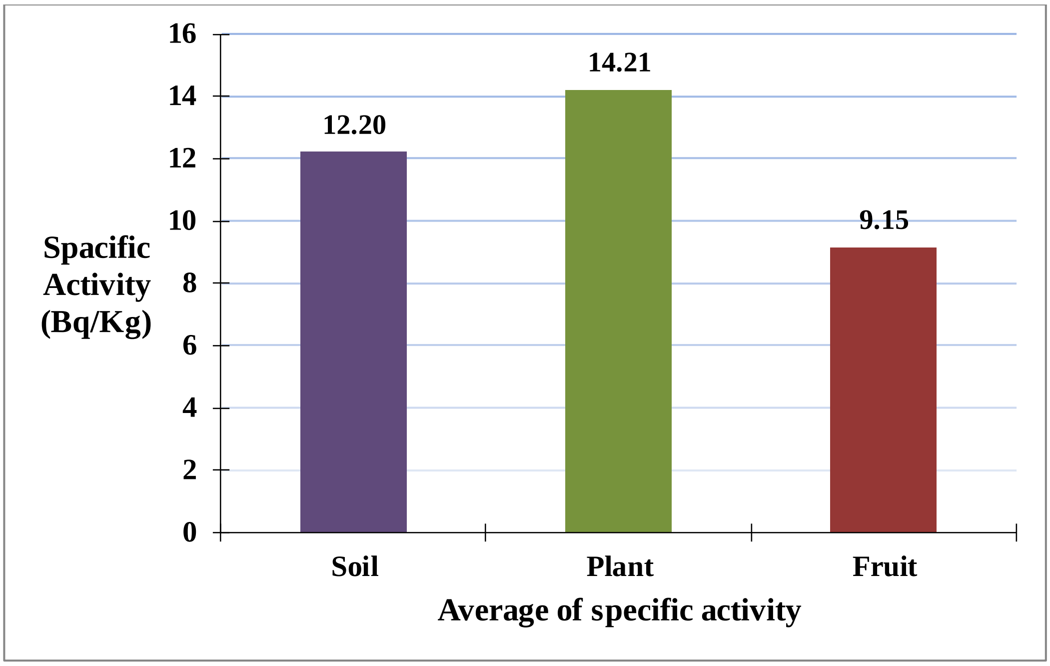

Figure 4.40: Compared the Average of Specific Activity of ^{232}Th for Agricultural Soil, Plant and Fruit which Irrigation with Surface water.

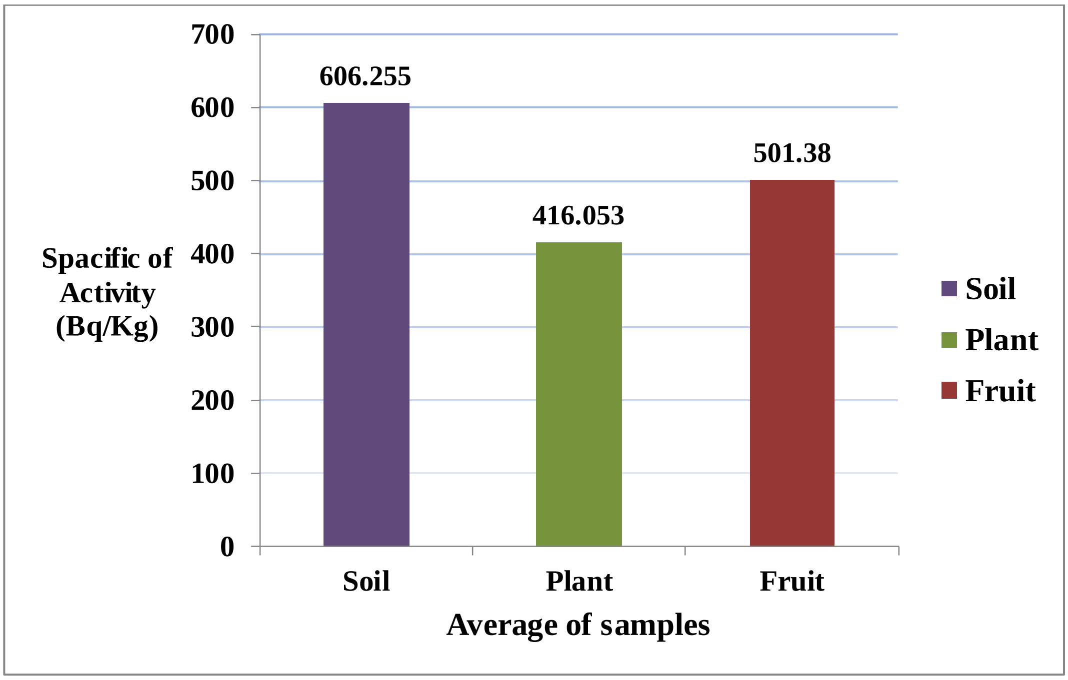

Figure 4.41: Compared the Average of Specific Activity of ^{40}K for Agricultural Soil, Plant and Fruit which Irrigation with Surface water.

4.1.3 Results of Alpha Emitters by Using CR-39

In this section of the study was to measure radon concentrations in selected samples from agricultural soil which irrigation with groundwater at depth (15cm) and measured by CR-39. The results of the radon concentration in soil for (20) samples in agricultural soil which irrigation with groundwater, and (20) samples in agricultural soil which irrigation with surfacewater. Also the results of the radon concentration in fruit (tomato crop) for (20) samples in fruit which irrigation with groundwater, and (20) samples in fruit (tomato crop) which irrigation with surfacewater. Was measured Radon in air space , Radon concentration within the sample , Activity concentration of radium and it was compared with World wide average [191-192].

4.1.3.1 Results of alpha Emitters in agricultural soil irrigtation with groundwater

The results are presented in Table (4.13), which provides a summary of the findings. It is evident that the measurements of (^{222}Rn) in the air space indicate certain observations from 8.97 Bq/m^3 to 35.81 Bq/m^3 with the average 16.997$\pm$2.188 Bq/m^3, and ^{222}R concentration within samples from 366.02 Bq/m^3 to 1196.13 Bq/m^3 with the average 680.527$\pm$89.3086 Bq/m^3, activity concentration of ^{226}R from 58.586 mBq/Kg to 210.841 mBq/Kg with the average 107.484$\pm$13.323 mBq/Kg. The all results, were compared with the Worldwiede average[191-193].

Based on Figure (4.42), it is evident that the Radon concentration in the air space is lower than the worldwide average [291]. Figure (4.43) shows that the Radon concentration within the sample is also lower than the worldwide average [292]. Additionally, Figure (4.44) indicates that the activitys concenttration of radium, is lower than the worldwide average [193].

Table 4.13: Radon Concentrations, Radon in Air Space, Activity Concentration of Radium of Agricultural Soils Irrigated with Groundwater.

No.	Sample code	Radon in air space (Bq/m^3)	Radon concentrations within the sample (Bq/m^3)	Activity concentration of radium (mBq/kg)
1	**SA1**	20.92	854.05	109.361
2	**SA2**	17.94	732.04	110.280
3	**SA3**	35.81	2196.13	210.841
4	**SA4**	16.44	671.04	101.090
5	**SA5**	25.41	1037.06	165.995
6	**SA6**	16.44	671.04	114.569
7	**SA7**	14.95	610.03	97.644
8	**SA8**	10.46	427.02	68.351
9	**SA9**	11.96	488.03	73.520
10	**SA10**	23.91	976.06	147.040
11	**SA11**	20.92	854.05	121.513
12	**SA12**	8.97	366.02	58.586
13	**SA13**	14.20	579.53	106.013
14	**SA14**	13.45	549.03	82.710
15	**SA15**	10.46	427.02	68.351
16	**SA16**	16.44	671.04	107.408
17	**SA17**	15.69	640.54	109.361
18	**SA18**	13.45	549.03	87.880
19	**SA19**	19.43	793.05	135.400
20	**SA20**	12.70	518.73	73.775
Minmum		**8.97**	**366.02**	**58.586**
Maxmum		**35.81**	**1196.13**	**210.841**
Average + S.D		**16.997±2.18**	**680.527±89.30**	**107.484±13.32**
World Wide average		**100(Bq/m^3) [191]**	**200(Bq/m^3) [192]**	**30 (Bq/kg) [193]**

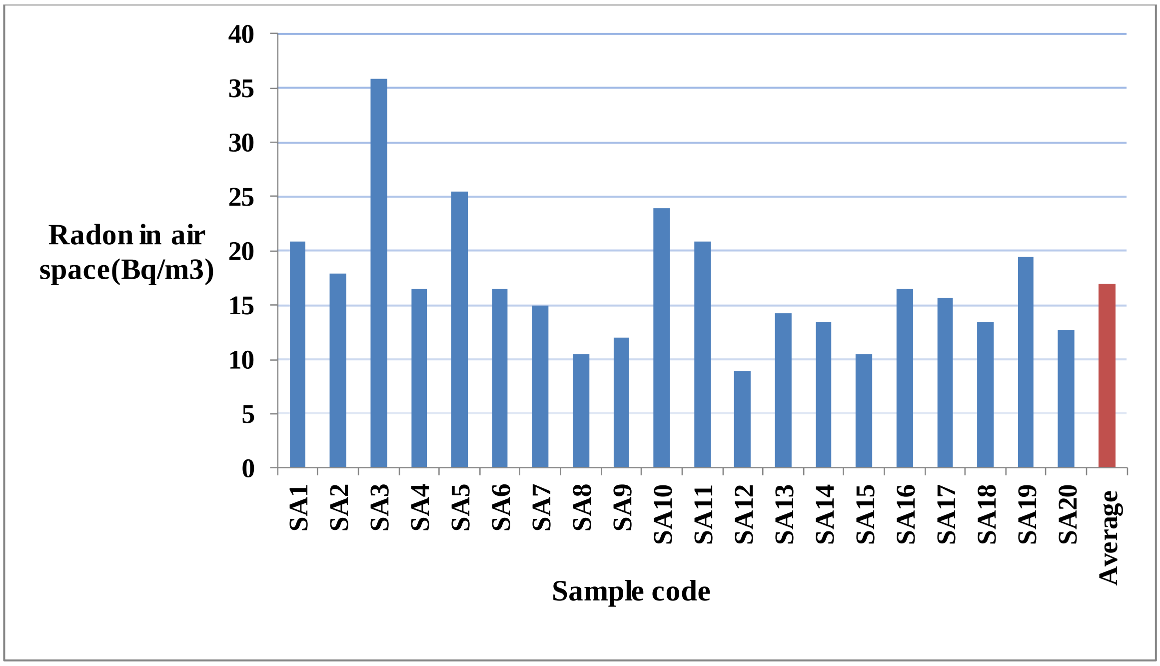

Figure 4.42: Radon in Air Space of Agricultural Soils Irrigated with Groundwater.

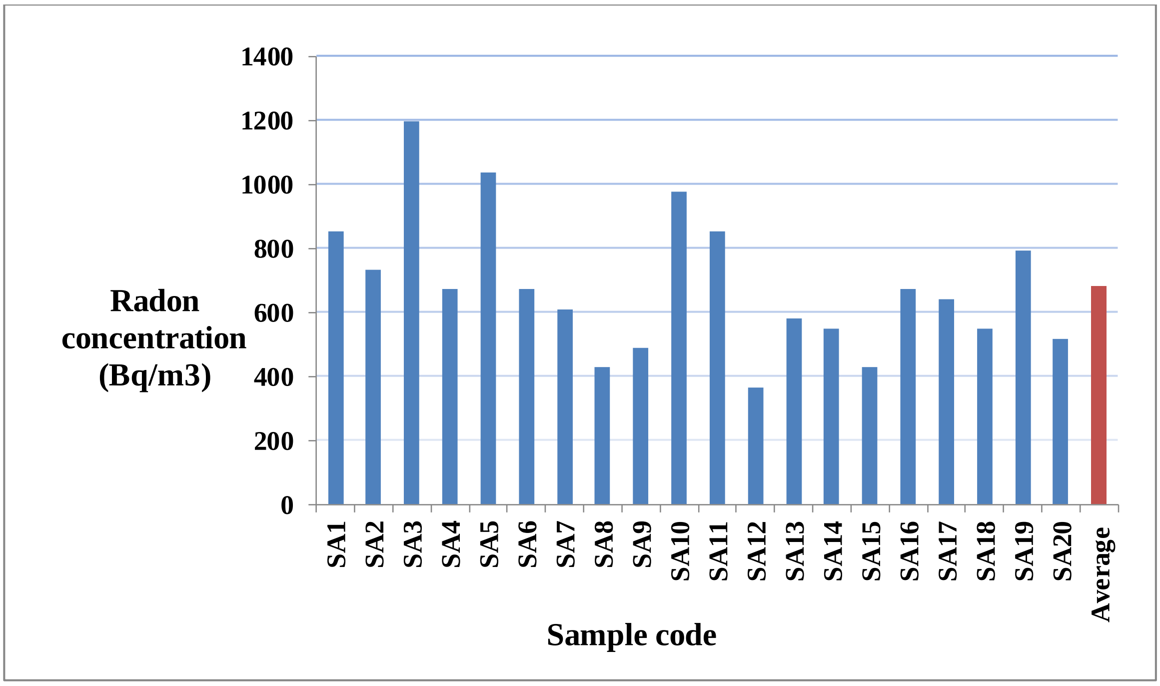

Figure 4.43: Radon Concentration of Agricultural Soil Irrigated with Groundwater.

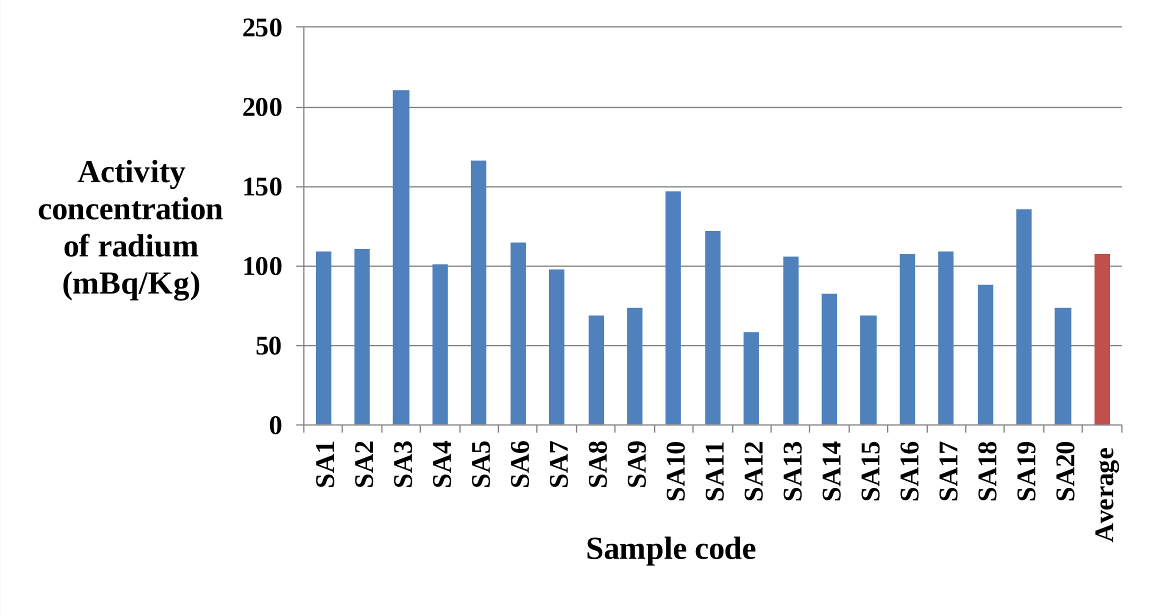

Figure 4.44: Activity Concentration of Radium of Agricultural Soil Irrigated with Groundwater.

4.1.3.2 Alpha Emitters in Fruit Irrigated with Groundwater

From Table (4.14) it can observable that, the results of ^{222}R in air space from 10.46 Bq/m^3 to 31.39 Bq/m^3 with the average 17.8985$\pm$1.282 Bq/m^3, and ^{226}R concentration within sample from 427.02 Bq/m^3 to 1281.07 Bq/m^3 with the average 730.516$\pm$52.339 Bq/m^3, Activity concentration of radium from 156.230 mBq/Kg to 468.691 mBq/Kg with the average 285.771$\pm$21.747 mBq/Kg.

The results obtained were compared with the worldwide average. Figure (4.45) illustrates that the radon concentration in the air space is lower than the worldwide average [191]. Figure (4.46) indicates that the radon concentration within the sample is higher or lower than the worldwide average [192]. Lastly, Figure (4.47) demonstrates that the activityes concenttration of radium, is lower than the worldwide average [193].

Table 4.14: Radon concentration, ^{222}Rn in Air Space, Activity Concentration of ^{226}Ra of Fruit(tomato) Irrigated with Groundwater.

No.	Sample code	Radon in air space (Bq/m^3)	Radon concentration within the sample (Bq/m^3)	Activity concentration of radium (mBq/kg)
1	SAF1	10.46	427.02	156.230
2	SAF2	11.96	488.03	208.307
3	SAF3	14.20	579.53	212.027
4	SAF4	14.95	610.03	223.186
5	SAF5	13.45	549.03	200.868
6	SAF6	12.70	518.53	221.326
7	SAF7	11.96	488.03	208.307
8	SAF8	17.94	732.04	312.461
9	SAF9	16.44	671.04	245.505
10	SAF10	14.95	610.03	223.186
11	SAF11	15.69	640.54	234.346
12	SAF12	26.90	1098.06	468.691
13	SAF13	25.41	1037.06	442.653
14	SAF14	19.43	793.05	338.499
15	SAF15	16.44	671.04	245.505
16	SAF16	31.39	1281.07	468.691
17	SAF17	17.94	732.04	267.824
18	SAF18	23.91	976.06	357.098
19	SAF19	19.43	793.05	290.142
20	SAF20	22.42	915.05	390.576
Minmum		**10.46**	**427.02**	**156.230**
Maxmum		**31.39**	**1281.07**	**468.691**
Average + S.D		**17.898±1.282**	**730.516±52.339**	**285.771±21.747**
World Wide average		**100(Bq/m^3) [191]**	**200(Bq/m^3) [192]**	**30 (Bq/kg)[193]**

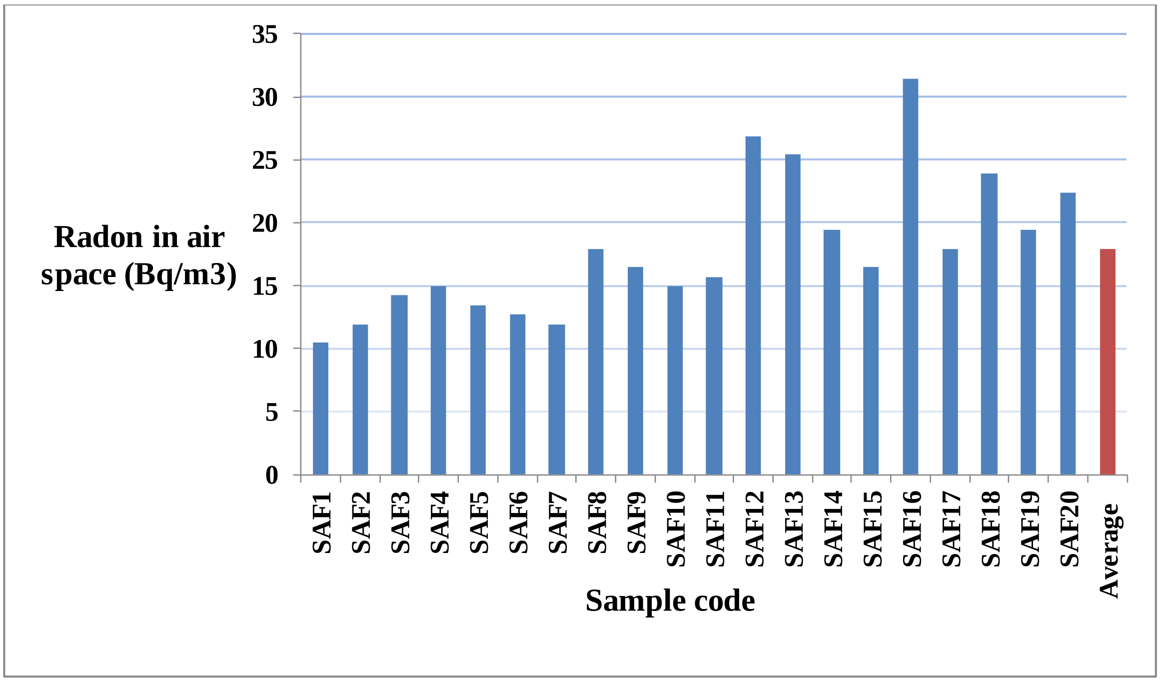

Figure 4.45: Radon in Air Space of Fruit Irrigated with Groundwater.

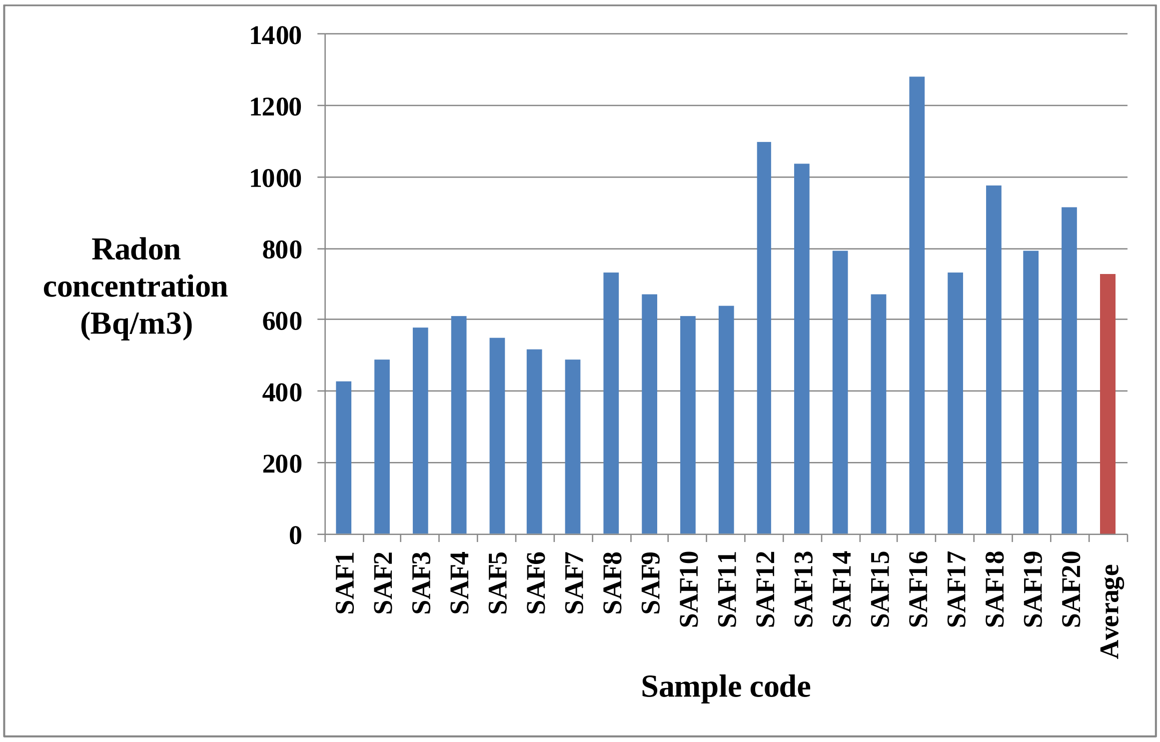

Figure 4.46: Radon Concentration of Fruit Irrigated with Groundwater.

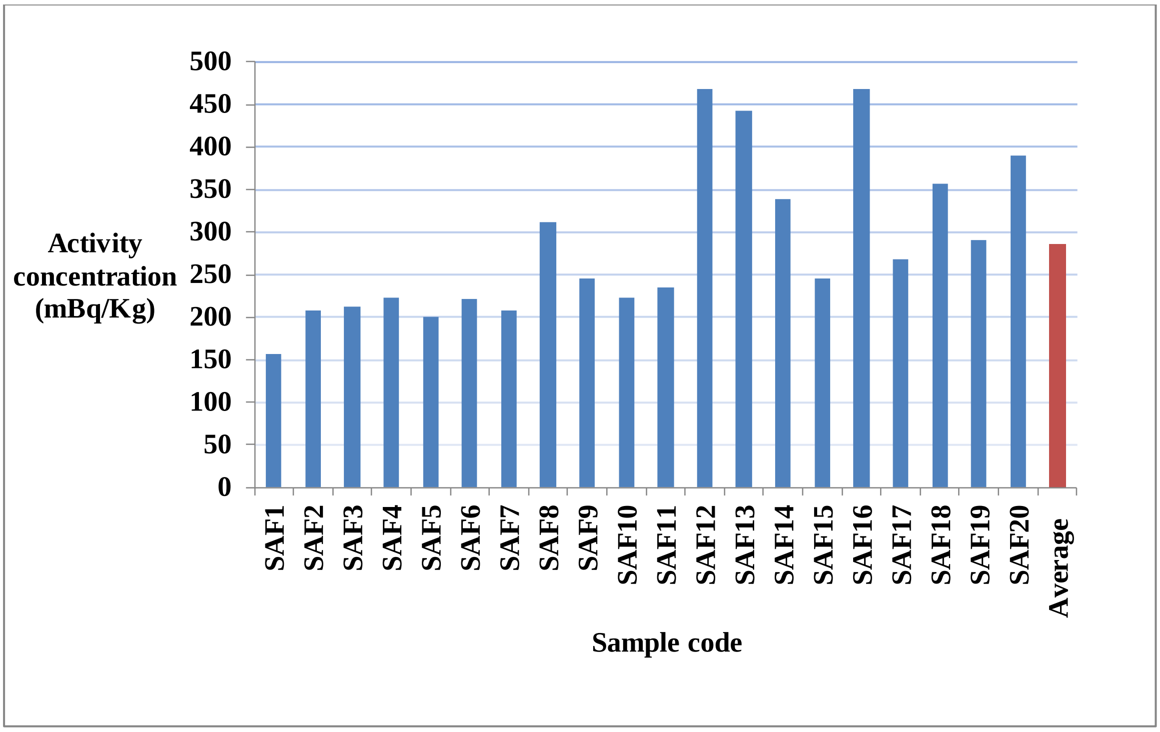

Figure 4.47: Activity Concentration of Radium of Fruit Irrigated with Groundwater.

4.1.3.3 Alpha Emitters in agricultural soil which irrigated with surface water

From Table (4.15) it can observable that, the results of Radon in air space from 11.96 Bq/m^3 to 34.38 Bq/m^3 with the average 23.241 ± 1.378 Bq/m^3, and Radon concentration from 488.03 Bq/m^3 to 1281.07 Bq/m^3 with the average 948.605 ± 56.251 Bq/m^3, Activity concentration of radium from 96.142 Bq/Kg to 256.664 Bq/Kg with the average 182.751 ± 10.525 Bq/Kg. Al the results, were compared with the world wide average.

Based on Figure (4.48), it is evident that the Radon concentration in the air space is lower than the worldwide average [191]. Figure (4.49) reveals that the radon concentration within the sample is significantly higher than the worldwide average [192]. Furthermore, Figure (4.50) demonstrates that the activityes concenttration of radium, is lower than the worldwide average [193].

Table 4.15: Radon Concentration, ^{222}Rn in Air Space, Activity Concentration of ^{226}Ra of Agricultural Soils Irrigated with Surface water.

No.	Sample code	Radon in air space (Bq/m^3)	Radon concentration within the sample (Bq/m^3)	Activity concentration of radium (mBq/kg)
1	**SB1**	20.92	854.05	168.248
2	**SB2**	27.65	1128.56	206.447
3	**SB3**	26.16	1067.56	195.288
4	**SB4**	13.45	549.03	117.173
5	**SB5**	23.91	976.06	227.244
6	**SB6**	11.96	488.03	96.142
7	**SB7**	20.18	823.55	162.239
8	**SB8**	20.92	854.05	156.230
9	**SB9**	31.39	1281.07	234.346
10	**SB10**	17.94	732.04	144.213
11	**SB11**	34.38	1403.08	256.664
12	**SB12**	25.41	1037.06	177.061
13	**SB13**	26.90	1098.06	200.868
14	**SB14**	19.43	793.05	156.230
15	**SB15**	23.91	976.06	208.307
16	**SB16**	25.41	1037.06	189.708
17	**SB17**	28.40	1159.07	212.027
18	**SB18**	29.15	1189.57	253.874
19	**SB19**	23.91	976.06	192.284
20	**SB20**	13.45	549.03	100.434
Minmum		**11.96**	**488.03**	**96.142**
Maxmum		**34.38**	**1281.07**	**256.664**
Average + S.D		**23.241±1.378**	**948.605±56.251**	**182.751±10.525**
World Wide average		**100(Bq/m^3) [191]**	**200(Bq/m^3) [192]**	**30 (Bq/kg)[193]**

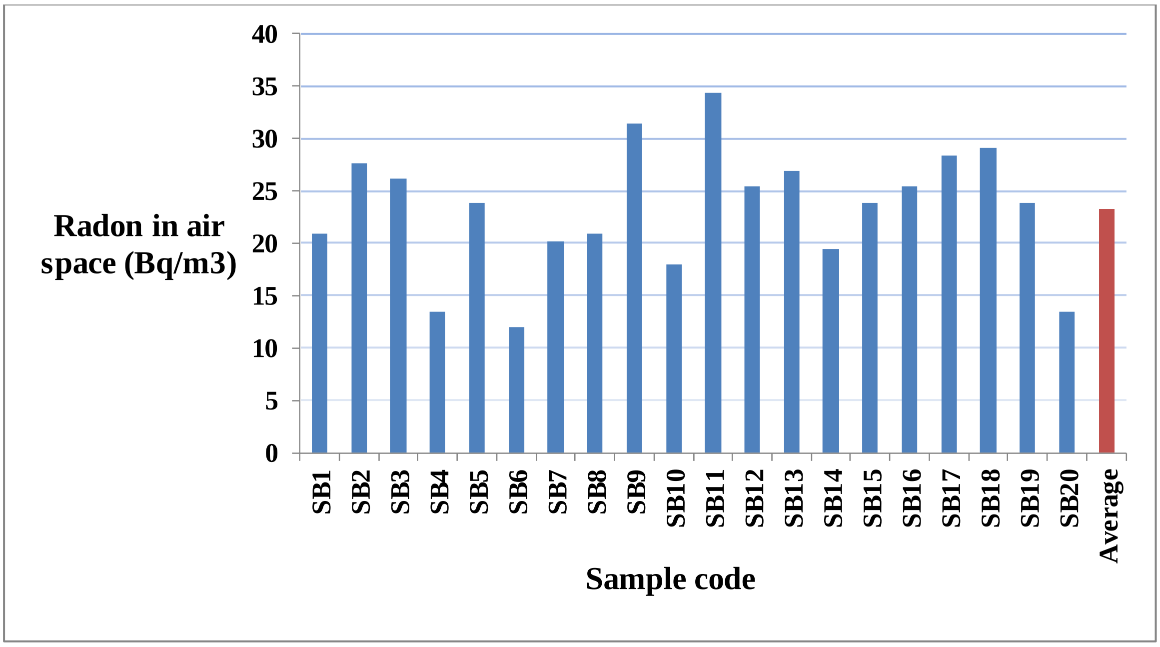

Figure 4.48: Radon in Air Space of Agricultural Soil Irrigated with Surface water.

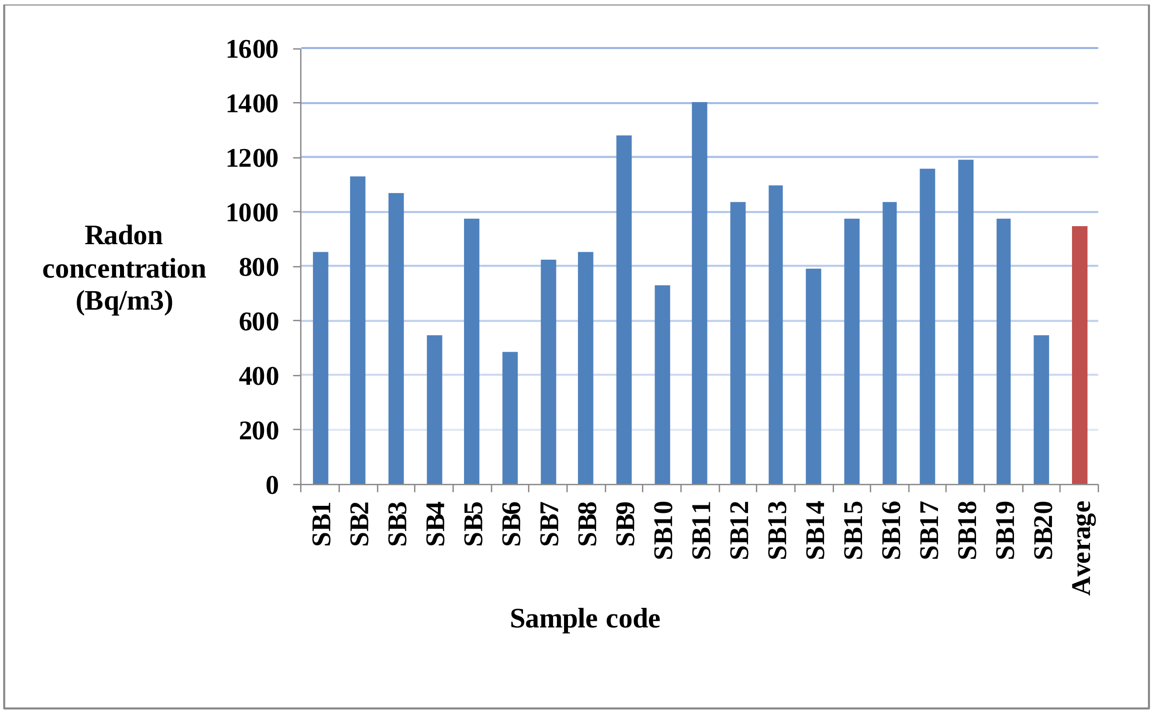

Figure 4.49: Radon Concentration within Sample of Agricultural Soil Irrigated with Surface water.

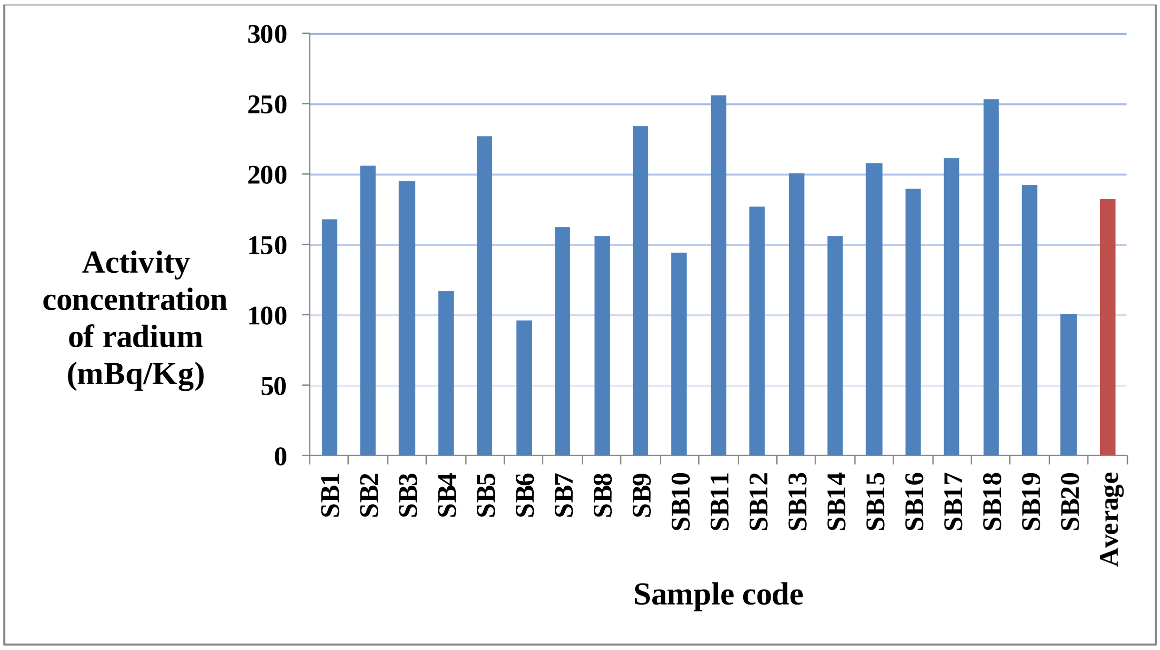

Figure 4.50: Activity Concentration of Radium of Agricultural Soil Irrigated with Surface water.

4.1.3.4 Results of Alpha Emitters in Fruit which Irrigtation with Surface Water

From Table (4.16) and Figures (4.51, 4.52, 4.53) observable that, the results of radon in air space from 10.46 to 21.67 with the average 15.058±0.827 Bq/m^3, and radon concentration from 366.02 to 884.55 with the average 756.92±33.771 Bq/m^3, activity concentration of radium from 133.912 to 312.461 with the average 198.15±12.371 mBq/Kg. All the results were compared with the worldwide average.

Based on Figure (4.51), it is observed that the radon concentration in the air space is lower than the worldwide average [191]. In Figure (4.52), it is noteworthy that the radon concentration within the sample is significantly higher than the world wide average [192]. Additionally, Figure (4.53) demonstrates that the activityes concenttration of radium, is hight than the worldwide average [193].

Table 4.16: Radon Concentration, ^{222}Rn in Air Space, Activity Concentration of ^{226}Ra of Fruit (tomato) Irrigated with Surface water.

No.	Sample code	Radon in air space (Bq/m^3)	Radon concentration within the sample (Bq/m^3)	Activity concentration of radium (mBq/kg)
1	**SBF1**	20.18	823.55	301.302
2	**SBF2**	14.20	579.53	212.027
3	**SBF3**	11.96	488.03	178.549
4	**SBF4**	13.45	549.03	200.868
5	**SBF5**	11.96	488.03	178.549
6	**SBF6**	12.70	518.53	147.551
7	**SBF7**	14.95	610.03	173.589
8	**SBF8**	17.94	732.04	267.824
9	**SBF9**	11.21	457.53	167.390
10	**SBF10**	17.19	701.54	256.664
11	**SBF11**	15.69	640.54	234.346
12	**SBF12**	17.94	732.04	267.824
13	**SBF13**	18.68	762.54	278.983
14	**SBF14**	19.43	793.05	290.142
15	**SBF15**	8.97	366.02	133.912
16	**SBF16**	13.45	549.03	200.868
17	**SBF17**	10.46	427.02	156.230
18	**SBF18**	21.67	884.55	283.168
19	**SBF19**	16.44	671.04	245.505
20	**SBF20**	11.96	488.03	178.549
Minmum		**10.46**	**366.02**	**133.912**
Maxmum		**21.67**	**884.55**	**312.461**
Average + S.D		**15.02±0.827**	**756.92±33.771**	**218.25±12.371**
World Wide average		**100(Bq/m^3) [191]**	**200(Bq/m^3) [192]**	**30 (Bq/Kg) [193]**

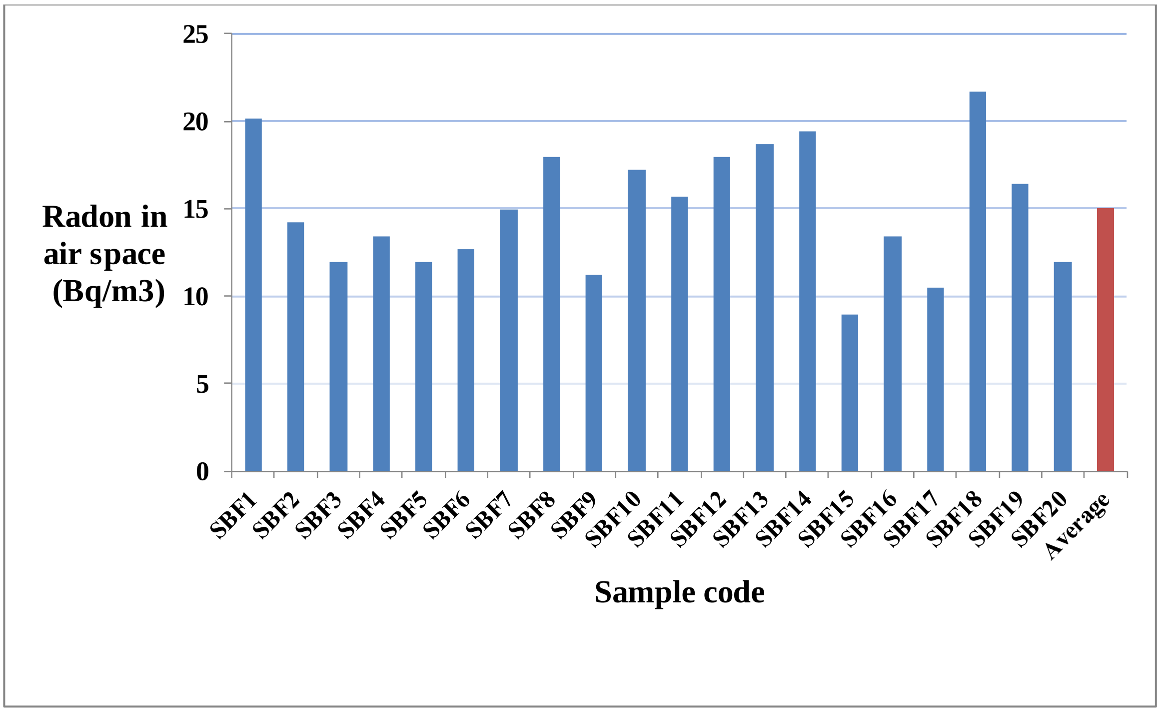

Figure 4.48: Radon in Air Space of Fruit (tomato crop) which Irrigated with Surface water.

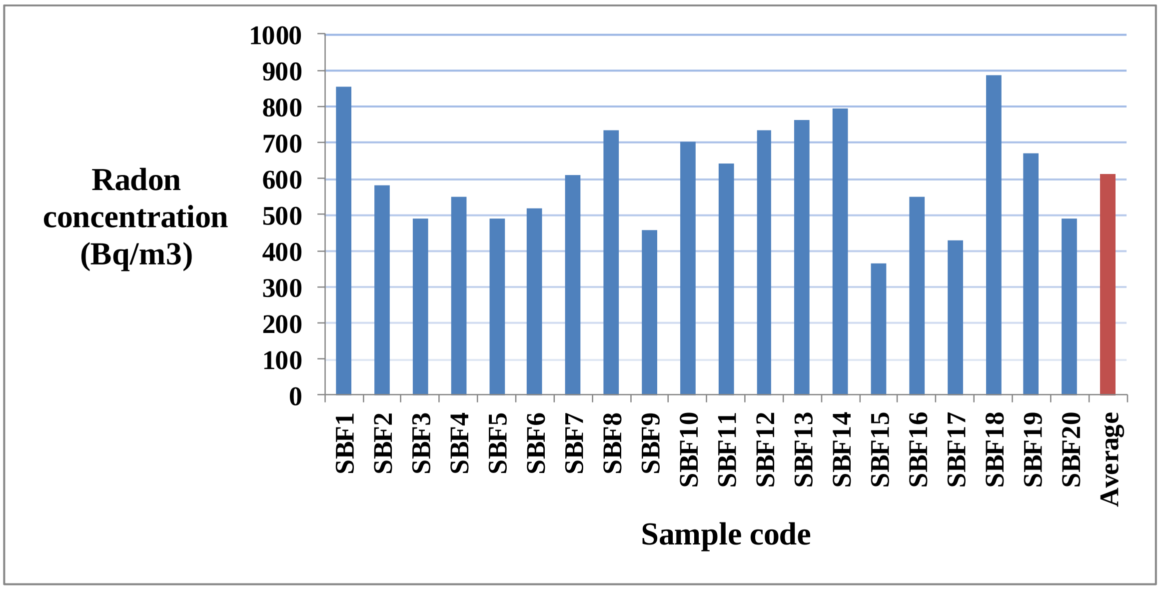

Figure 4.49: Radon Concentration within Sample of Fruit (tomato crop) which Irrigated with Surface water.

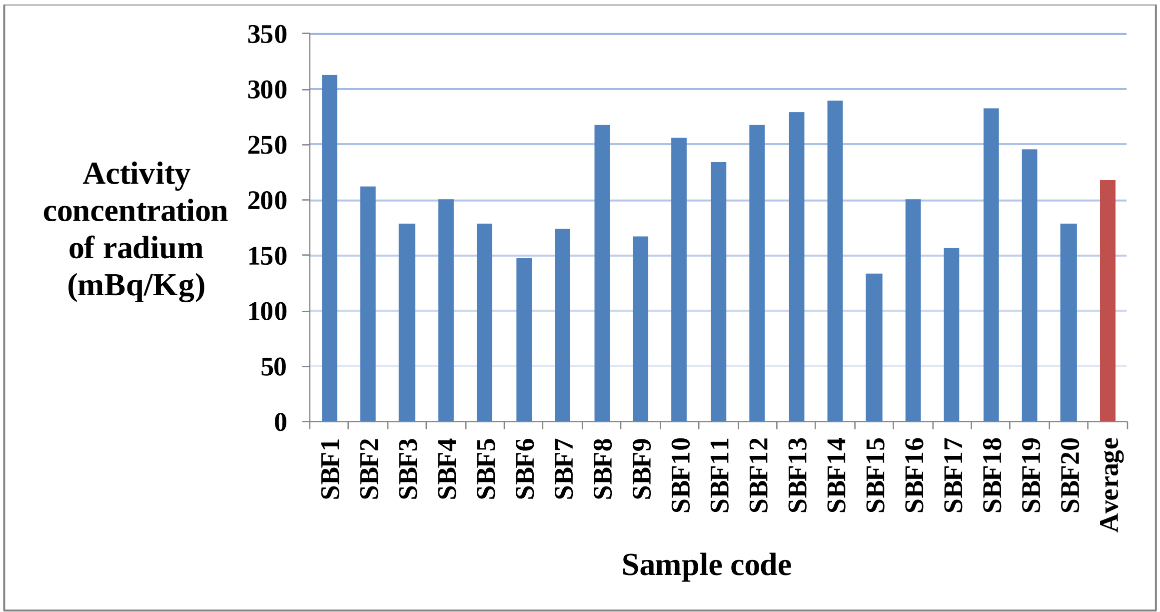

Figure 4.50: Activity Concentration of Radium of Fruit (tomato crop) which Irrigated Surface water.

4.1.4 Transfer Factor (TF)

The average specific activity concentrations of ^{238}U, ^{232}Th and ^{40}K were calculated and compared in two regions: agricultural soil, plant, and fruit irrigated with surface water, and agricultural soil, fruit, and plant irrigated with groundwater. Additionally, the soil-to-plant and soil-to-fruit transfer factors for both regions were determined and reported.

4.1.4.1 The Transfer Factor from Agricultural Soil to Plant which Irrigte with Groundwater

The results are presented in Table (4.17), indicating the transfer factors (TF) for ^{238}U, ^{232}Th and ^{40}K. The ranges of TF values for each element are as follows: ^{238}U ranged from 0.034 to 1.349, with an average of 0.538±0.147.

^{232}Th ranged from 0.239 to 2.205, with an average of 0.885±0.158. ^{40}K ranged from 0.462 to 1.368, with an average of 0.781±0.182.

The research findings of this study indicate, that the transfer factors (TF) of ^{238}U, ^{232}Th and ^{40}K as shown in Figure (4.54), are mostly less than 1. This implies that the average spaecific activityes concenttrations of ^{238}U and ^{232}Th in plants are low than those in the soil. On the other hand, the transfer factors of ^{40}K in the agricultural soil exhibit higher values compared to ^{238}U, and ^{232}Th. In fact, all the transfer factors of ^{40}K in this area were found to be greater than 1.

This can be interpreted as ^{40}K is classified as a light element, whereas ^{238}U and ^{232}Th are considered heavy elements. As a result, ^{40}K exhibits greater mobility than ^{238}U and ^{232}Th, and ^{232}Th has greater mobility than ^{238}U. Furthermore, the water solubility of ^{40}K is greater than that of ^{238}U and ^{232}Th [187-190].

The average spaecific activityes concenttrations of ^{238}U, ^{232}Th and ^{40}K, in plant crops were found, to be largely independent of their concentrations in the soil. This can be attributed to various physiochemical characteristics of the soil that affect the transfered of radioactives nucalides froms the soil to plants. Factors such as the soil's organic matter content, availability of nuclides to the plant, K (potassium) contentes, cationes exchange capacity, Ca (Calcium) content, and organicce mattere contente play significant roles in this transfer process [194,195].

Tabe 4.17: Transfer Factor of ^{238}U, ^{232}Th and ^{40}K from Agricultural Soil to Plant which Irrigte with Groundwater.

No.	Sample code	Transition Factor		
		^{238}U	^{232}Th	^{40}K
1	**SAPT1**	0.641	0.286	0.615
2	**SAPT2**	0.475	0.531	0.571
3	**SAPT3**	0.149	0.494	0.675
4	**SAPT4**	0.473	1.194	0.788
5	**SAPT5**	0.096	0.241	0.704
6	**SAPT6**	0.681	1.955	1.128
7	**SAPT7**	0.218	0.282	0.485
8	**SAPT8**	0.131	0.267	0.728
9	**SAPT9**	1.148	1.663	0.982
10	**SAPT10**	0.217	0.364	0.462
11	**SAPT11**	0.034	0.769	0.737
12	**SAPT12**	2.781	2.236	1.202
13	**SAPT13**	0.391	0.239	0.42
14	**SAPT14**	0.024	0.325	0.531
15	**SAPT15**	0.218	0.56	0.78
16	**SAPT16**	0.936	1.601	1.141
17	**SAPT17**	0.193	0.878	1.004
18	**SAPT18**	0.877	1.003	0.885
19	**SAPT19**	1.349	2.205	1.368
20	**SAPT20**	0.88	1.312	0.768
Minimum		**0.034**	**0.239**	**0.462**
Maximum		**1.349**	**2.205**	**1.368**
Average ± S.D		**0.538±0.147**	**0.885±0.158**	**0.781±0.182**

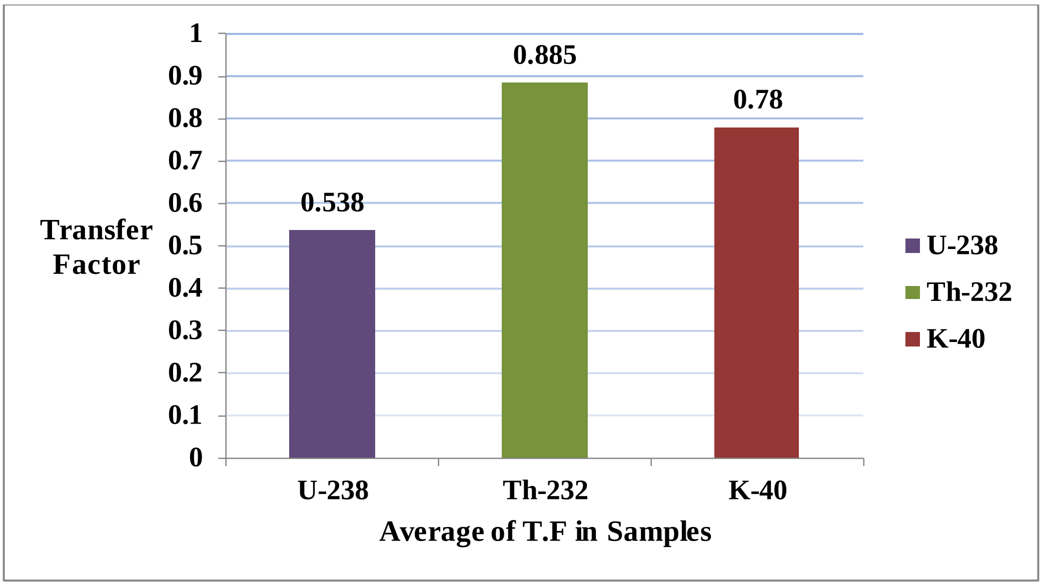

Figure 4.54: Comparison Average TF of ^{238}U , and ^{232}Th from Agricultural Soil to Plant which Irrigated with Groundwate.

4.1.4.2 Transfer Factor from Agricultural Soil to Fruit which Irrigated with Groundwater

The results are summarized in the Table (4.18) The resulte in this table show that the ranges of TF of ^{238}U, ^{232}Th and ^{40}K respectively, were from 0.094 to 1.173 with the average 0.427±0.084, from 0.109 to 2.311 with the average 0.757±0.134 and from 0.816 to 1.971 with the average 1.169±0.350, respectively.

The findings of this study indicate that the transfer factors of ^{238}U and ^{232}Th in most samples were found to be less than 1. This suggests that the average specific activity concentrations of ^{238}U and ^{232}Th in plants are lower than those in the soil. In contrast, the transfer factors of ^{40}K in the agricultural soil showed higher values compared to ^{238}U and ^{232}Th. In fact, all the transfer factors of ^{40}K in this area were greater than one, as depicted in Figure (4.55).

This can be interpreted as ^{40}K being classified as a light element, while ^{238}U and ^{232}Th are considered heavy elements. Consequently, ^{40}K exhibits higher mobility compared to $^{238}U$and ^{232}Th, and ^{232}Th has greater mobility than ^{238}U. Additionally, ^{40}K has greater water solubility compared to ^{238}U, and ^{232}Th [187-190].

Table 4.18: The Transfer Factor of ^{238}U , ^{232}Th and ^{40}K from Agricultural soil to Fruit which Irrigated with Groundwater.

No.	Sample code	Transition factor		
		^{238}U	^{232}Th	^{40}K
1	**SAFT1**	0.094	0.339	0.942
2	**SAFT2**	0.828	1.211	1.273
3	**SAFT3**	1.002	1.206	1.1
4	**SAFT4**	0.14	0.569	1.097
5	**SAFT5**	0.905	1.42	1.175
6	**SAFT6**	0.439	0.257	0.816
7	**SAFT7**	0.067	0.109	0.861
8	**SAFT8**	0.764	2.311	1.66
9	**SAFT9**	0.182	0.251	1.021
10	**SAFT10**	0.747	0.736	1.199
11	**SAFT11**	0.424	0.968	1.231
12	**SAFT12**	0.088	0.444	1.243
13	**SAFT13**	0.224	0.494	1.116
14	**SAFT14**	0.203	1.001	0.946
15	**SAFT15**	0.707	1.002	1.512
16	**SAFT16**	0.041	0.212	1.001
17	**SAFT17**	0.504	0.559	1.262
18	**SAFT18**	0.114	0.258	1.077
19	**SAFT19**	1.173	1.197	1.798
20	**SAFT20**	0.901	1.794	1.971
Minimum		**0.094**	**0.109**	**0.816**

Maximum	**1.173**	**2.311**	**1.971**
Average ± S.D	**0.427±0.084**	**0.757±0.134**	**1.169±0.350**

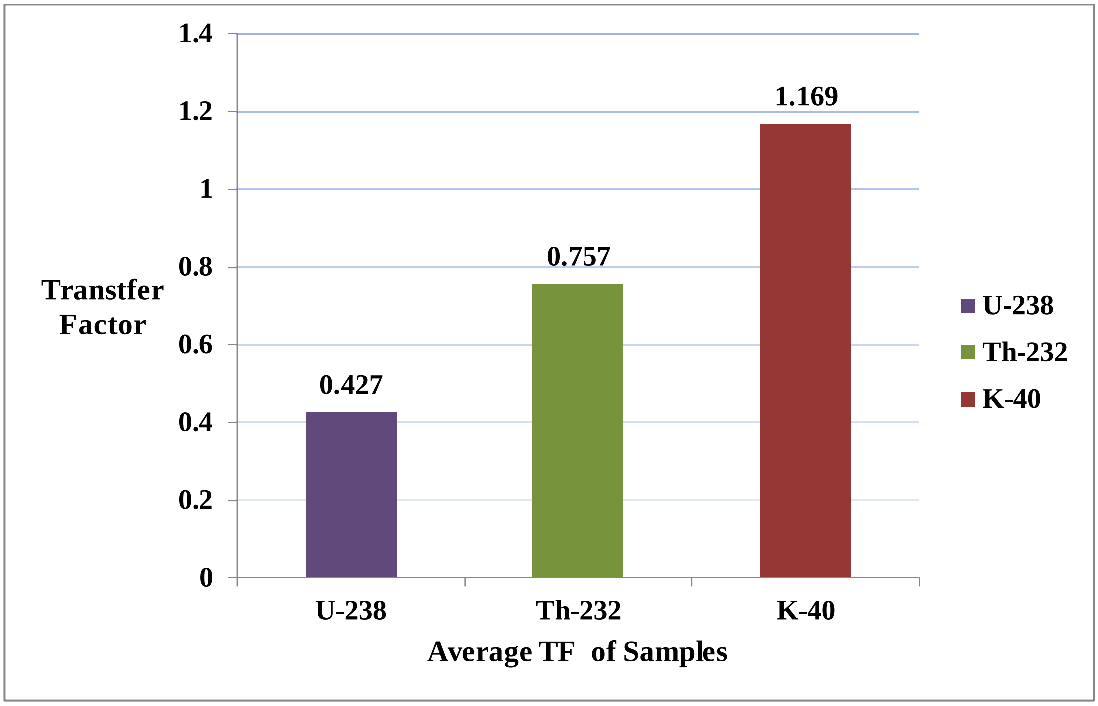

Figure 4.55: Comparison Average TF of ^{238}U , and ^{232}Th from Agricultural Soil to Fruit which Irrigated with Groundwate.

4.1.4.3 The Transfer Factor from Agricultural soil to plant which Irrigated with Surface Water

The results are summarized in Table (4.19). The table shows the ranges and average transfer factors (TF) for ^{238}U, ^{232}Th and ^{40}K . The TF ranges were from 0.085 to 4.79 with an average of 1.651±0.838 for ^{238}U, from 0.061 to 7.463 with an average of 1.392±0.464 for ^{232}Th, from 0.19 to 1.748 with an average of 0.621±0.320 for ^{40}K .

The findings of this study indicate that the transfer factors of ^{238}U, ^{232}Th and ^{40}K had high values. This suggests that the average specific activity concentrations of ^{238}U and ^{232}Th in plants are higher than in the soil and greater than one. Figure (4.56) illustrates this trend.

The (TF) from agricultural soil to plant crops for, ^{238}U and ^{232}Th, were higher compared to those for ^{40}K . This can be attributed to the mobility of thorium, which is absorbed by cell walls in plants [192].

Tabe 4.19: Transfer Factor of ^{238}U , ^{232}Th and ^{40}K from Agricultural Soil to Plant which Irrigated with Surface water.

No.	Sample code	Transition Factor		
		^{238}U	^{232}Th	^{40}K
1	SBPT1	0.085	0.061	0.572
2	SBPT2	0.214	1.145	0.654
3	SBPT3	0.206	0.275	0.421
4	SBPT4	0.137	0.404	0.489
5	SBPT5	2.744	4.62	1.31
6	SBPT6	4.79	4.942	1.595
7	SBPT7	0.294	0.264	0.43
8	SBPT8	0.861	0.685	0.533
9	SBPT9	0.833	0.832	0.425
10	SBPT10	0.307	0.092	0.451
11	SBPT11	1.115	0.221	0.62
12	SBPT12	8.775	7.463	1.748
13	SBPT13	0.357	0.775	0.187
14	SBPT14	0.828	0.654	0.689
15	SBPT15	3.609	3.048	1.04
16	SBPT16	0.278	0.152	0.073
17	SBPT17	0.028	0.089	0.063
18	SBPT18	0.259	1.315	0.618

19	SBPT19	0.475	0.358	0.366
20	SBPT20	0.314	0.453	0.15
Minimum		0.085	0.061	0.063
Maximum		4.79	7.463	1.748
Average ± S.D		1.651±0.838	1.392±0.464	0.621±0.320

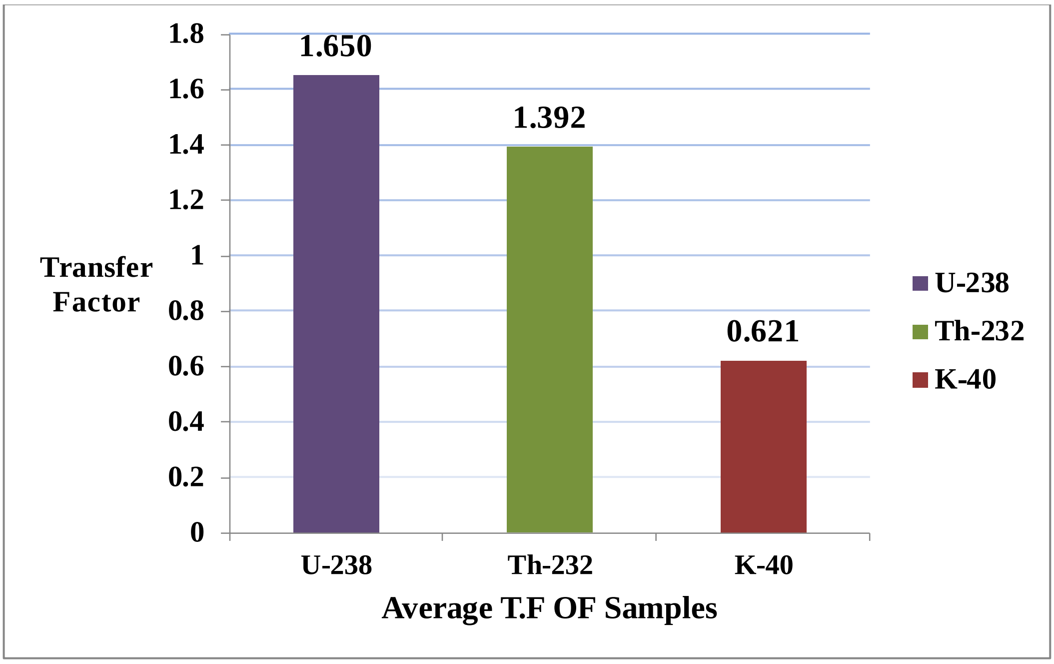

Figure 4.56: Comparison Average TF of ^{238}U, ^{232}Th and ^{40}K from Agricultural Soil to Plant which Irrigated with Surface Water.

4.1.4.4 The Transfer Factor from Agricultural Soil to Fruit which Irrigated with Surface Water

The results are summarized in Table (4.20). The table presents the ranges and average transfer factors (TF) for ^{238}U, ^{232}Th and ^{40}K. The TF ranges were from 0.054 to 1.742 with an average of 0.424±0.117 for ^{238}U, from 0.255 to 2.234 with an average of 0.750±0.111 for ^{232}Th, from 0.288 to 0.691 with an average of 0.435±0.109 for ^{40}K .

The resultes of this studyes indicates that the (TF) of ^{238}U and ^{232}Th , in most samples were less than 1. This suggests that the average specific activity concentrations of ^{238}U and ^{232}Th in plants are lower than those in the soil. Conversely, the transfer factors of ^{40}K in the agricultural soil recorded lower values compared to ^{238}U and ^{232}Th, as all the transfer factors in this area were greater than 1, as shown in Figure (4.57).

The findings of this study's research demonstrate that the transfer factors of ^{238}U , ^{40}K and ^{232}Th in most samples are less than (1). This indicatres that, the averge of spacific activityes concenttrations of ^{238}U , ^{40}K and ^{232}Th in plants are less than those in the soil. So all the transfer factors of ^{238}U , ^{40}K and ^{232}Th in this area were less than one Figure (4.57) .

This can be interpreted as ^{40}K is classified as a light element, whereas ^{238}U and ^{232}Th are considered heavy elements. As a result, ^{40}K exhibits greater mobility than ^{238}U and ^{232}Th, and ^{232}Th has greater mobility than ^{238}U. Furthermore, the water solubility of ^{40}K is greater than that of ^{238}U and ^{232}Th so that the specific activity of ^{40}K is higher[187-190].

Tabe 4.20: Transfer Factor of ^{238}U , ^{232}Th and ^{40}K from Agricultural Soil to Fruit which Irrigated with Surface Water.

No.	Sample code	Transition Factor		
		^{238}U	^{232}Th	^{40}K
1	SBFT1	0.112	1.034	0.498
2	SBFT2	0.241	0.937	0.455
3	SBFT3	0.576	0.78	0.427
4	SBFT4	0.147	0.165	0.415
5	SBFT5	1.021	1.014	0.376
6	SBFT6	1.742	0.95	0.432
7	SBFT7	0.125	0.113	0.288
8	SBFT8	0.495	0.974	0.549
9	SBFT9	0.912	1.143	0.429
10	SBFT10	0.203	0.311	0.311
11	SBFT11	0.432	1.095	0.328
12	SBFT12	0.76	0.562	0.545
13	SBFT13	0.054	0.399	0.401
14	SBFT14	0.309	0.8	0.464
15	SBFT15	0.787	2.234	0.691
16	SBFT16	1.19	1.262	0.53
17	SBFT17	0.21	0.255	0.361
18	SBFT18	1.496	0.526	0.386
19	SBFT19	0.133	0.508	0.353
20	SBFT20	1.27	0.948	0.47
Minimum		**0.054**	**0.255**	**0.288**
Maximum		**1.742**	**2.234**	**0.691**
Average ± S.D		**0.424±0.117**	**0.7503±0.111**	**0.435±0.109**

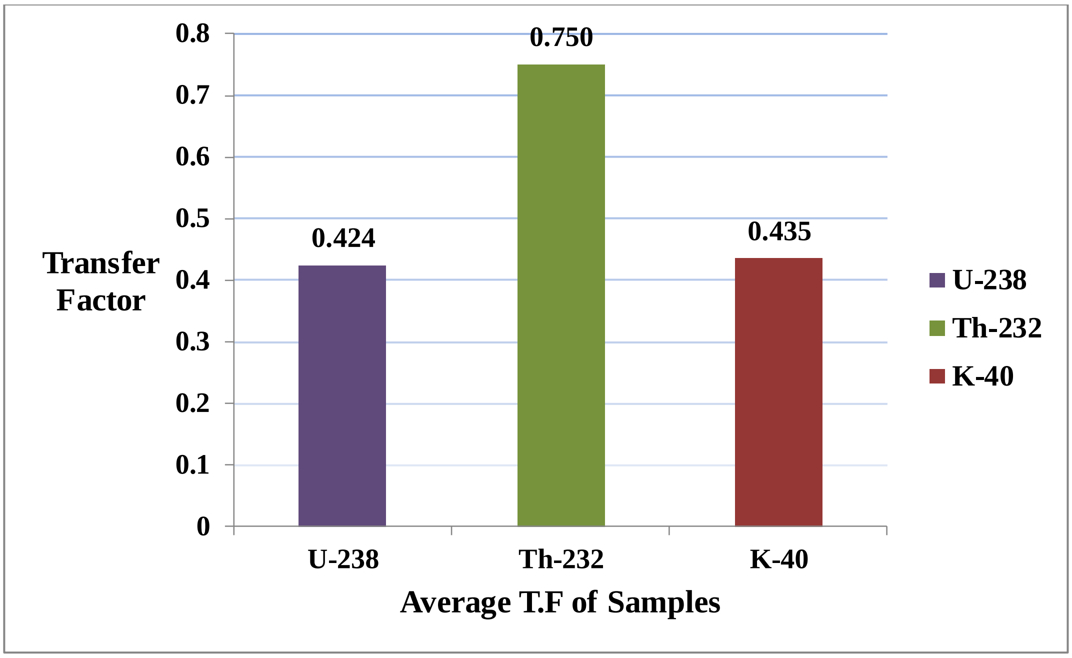

Figure 4.57: Comparison Average TF of ^{238}U, ^{232}Th and ^{40}K from Agricultural Soil to Fruit which Irrigated with Surface water.

4.1.4.5 Comparison Transfer Factors (TF)

Comparison Transfer Factors (TF) of ^{238}U, ^{232}Th, ^{40}K and ^{235}U different agricultural soil, plant and fruit which irrigtation with groundwater and surfacewater

4.1.4.5.1 Comparison TFs of agricultural soil to plant and fruit which irrigtation with groundwater

Figure (4.58), indicates that the values of transfer factors for the ^{238}U from agriculture soil to plant and fruit was relatively lowe in the study area as many the transfer factors in this area were smaller than one. It is followed by ^{232}Th, also was relatively lowe but is higher than ^{238}U, where were the transfer factors of plant high than fruit, however were smaller than one, as for ^{40}K most the values of the transfer factors in all plant and fruit samples were higher than one, noting that the transfer factor for fruit recorded the highest value than plant of the transfer factors for ^{40}K .

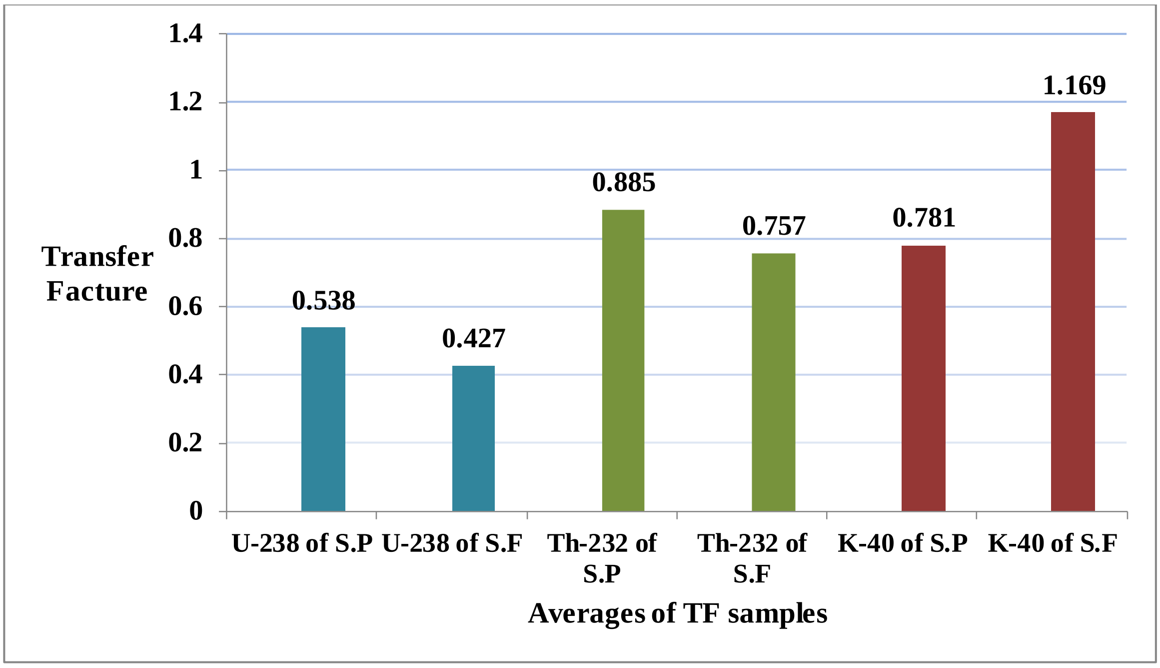

Figure 4.58: Comparison TF of ^{238}U, ^{232}Th, ^{40}K and ^{235}U in different Agricultural Soil, Plant and Fruit which Irrigtation with Groundwater.

4.1.4.5.2. Comparison TF of Agricultural Soil to Plant and Fruit which Irrigtation with SurfaceWater

Figure (4.77) illustrates the transfer factors (TF), for, ^{238}U, ^{235}U, ^{232}Th, and ^{40}K , in the study area. The (TF) values represent the transferes of these radioactivees elements from agricultural soils, to plants and fruits samples.

From the figure, it can be observed that the TF values for ^{238}U from soil to plant were higher than one, indicating a higher transfer of ^{238}U to the plants. Similarly, the TF values from soil to fruit samples for ^{238}U were lower than those to the plants, suggesting a lower uptake of ^{238}U by the fruits.

Regarding ^{232}Th, the TF values were relatively lower for fruit samples compared to plants, indicating a lower transfer of ^{232}Th to the fruits. The TF values from soil to plant were higher than those from soil to fruit samples, suggesting a higher uptake of ^{232}Th by the plants.

As for ^{40}K, the TF values from agricultural soil to both plant and fruit samples were higher than one. Notably, the TF values for fruit samples recorded the highest values among all elements, indicating a higher transfer of ^{40}K to the fruits compared to plants.

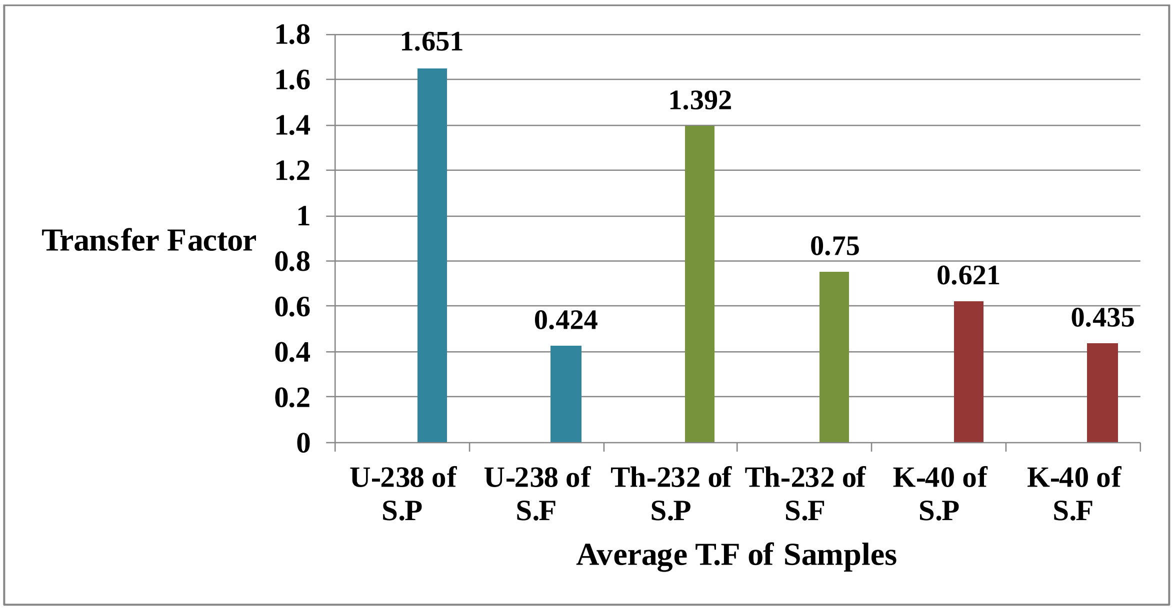

Figure 4.59: Comparison TF of ^{238}U, ^{232}Th and ^{40}K in different Agricultural Soil, Plant and Fruit which Irrigated with Surface water.

4.1.5 Result of Fertilizers

Three samples of chemical fertilizers were taken, whose use rate is about 95% by farmers in the study area (agricultural lands). The natural radioactivity of these samples was measured using a system NaI(TI) and the results were as follows :

The natural radioactivity of specific **f**ertilizers samples in the study area was measured and campared to the permissible limits for ^{238}U, ^{232}Th, ^{40}K and ^{235}U, as indicated in references [185], along with a Ra_{eq} limit of 370 [186]. The results, presented in Table (4.21), illustrate the specific of activity of (^{238}U), and (^{40}K). For sample ($S1$), the spaecific acttivity are (2.903±0.329, 2.419±0.139 and 42.59±1.418) Bq/kg, for sample ($S2$), the spaecific acttivity are (1.956±0.302, 1.676±0.17 and 62.252±1.774) Bq/kg, and for sample ($S3$), the spaecific acttivity are (1.376±0.251, 1.463±0.158 and 8087.64±20.06) Bq/kg.

Comparing these values to global averages, it can be observed that the spaecific activity of (^{238}U) , (^{232}Th) and (^{40}K) are lower of all samples except (^{40}K) of sample (S3) exhibits significantly higher specific activity compared to the worldwide average [185].

Table (4.22) provides the following values: Ra_{eq} (Radium equivalent activity) measured in Bq/Kg, D_r (absorbed dose rate) measured in nGy/h, H_{in} (Indoor hazard index), H_{ex} Indoor external dose, I_γ (Gamma index), and I_α (Alpha Index). The respective for sample (S1) are as follows: 13.832 Bq/Kg, 6.375 nGy/h0.047, 0.037, 0.051and 0.017, for sample (S2) on respective are, 9.1463 Bq/Kg, 4.512 nGy/h, 0.03, 0.025, 0.036, 0.01, and for sample (S3) on respective are, 626.22 Bq/Kg, 338.77 nGy/h, 1.695, 1.691, 2.708 and 0.007 are respective. All these values of all samles are comparable to the worldwide average [186,187], with all valuesof the samples (S1,S2) are being lower except for the (S3), which is higher for (^{40}K) .

Moving on to Table (4.23), it presents the values for Exposure, the AEDE (Annual Effective Dose Equivalent), AGED (Annual Gonadal Equivalent Dose), and ELCR (Excess Lifetime Cancer Risk). The respective of all samples are as follows: For samples (S1), 26.192 μR/h, 0.031 mSv/y, 44.846 mSv/y and 0.14, for samples (S2), 19.122 μR/h, 0.022 mSv/y, 32.597 mSv/y and 0.099, for samples (S3), 1598.9 μR/h, 1.662 mSv/y, 2549.88 mSv/y and 7.445.

Similar to the previous Table, the all of these values are comparable to the worldwide average [185-187] with all values of samples (S1,S2) are being lower except of samples (S3) which are all higher.

Table 4.21 : The Specific of Activity of Fertilizers.

No.	Sample code	Specific activity in (Bq/Kg)		
		^{238}U	^{232}Th	^{40}K
1	S1	2.903±0.329	2.419±0.139	42.59±1.418
2	S2	1.956±0.302	1.676±0.17	62.252±1.774
3	S3	1.376±0.251	1.463±0.158	8087.64±20.06
World Wide Average		35	45	412

Table 4.22: The Results Raeq , Dr , Hex , Hin and Iγ of Fertilizers.

No.	Sample code	Raeq (Bq/kg)	AD (nGy/h)	Hin	Hex	Iγ	Iα
1	**S1**	13.832	6.375	0.047	0.037	0.051	0.017
2	**S2**	9.1463	4.512	0.03	0.025	0.036	0.01
3	**S3**	626.22	338.77	1.695	1.691	2.708	0.007
World Wide average		**<370**	**<55**	**≤1**	**≤1**	**≤1**	**≤1**

Table 4.23: The Exposure, AEDE ,AGED and ELCR of Fertilizer.

No.	Sample code	Exposure (μR/h)	AEDE (mSv/y)	AGED (mSv/y)	ELCR× 10^{-3}
1	**S1**	26.192	0.031	44.8463	0.14
2	**S2**	19.122	0.022	32.5977	0.099
3	**S3**	1598.9	1.662	2549.88	7.445
World Wide average		....	≤ 1	**300**	**2.5**

The Figures (4.60, 4.61 and 4.62), it can be seen that the values of the average of the specific activity but of (^{40}K) for samples S3 was ahighlights a notable difference in potassium levels in sample S3 compared to the other samples, possibly due to the presence of three natural potassium isotopes, one of which is unstable, while the others remain stable. This isotopic variation could explain the higher potassium content in sample S3.

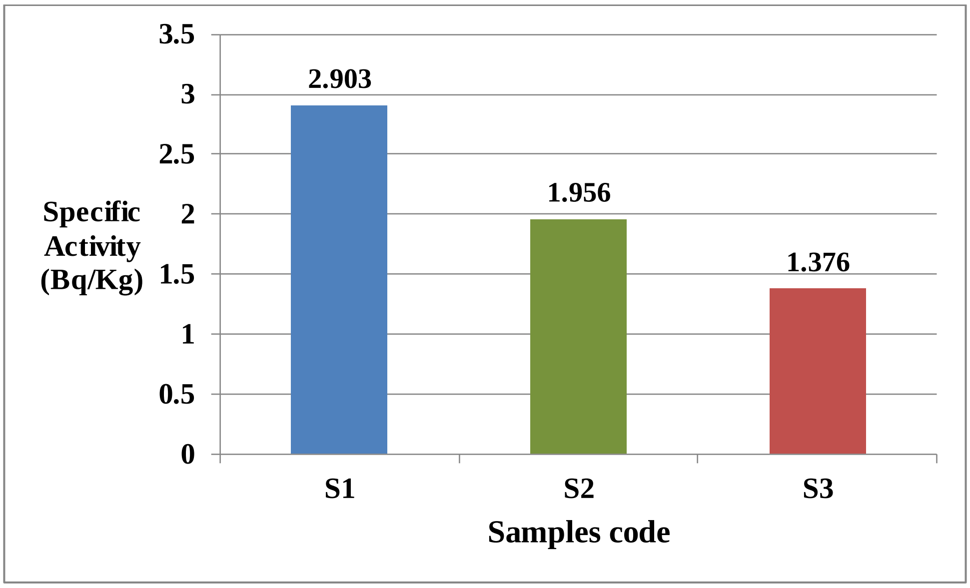

Figure 4.60: Specific Activity of ^{238}U(Bq/kg) for Fertilizer.

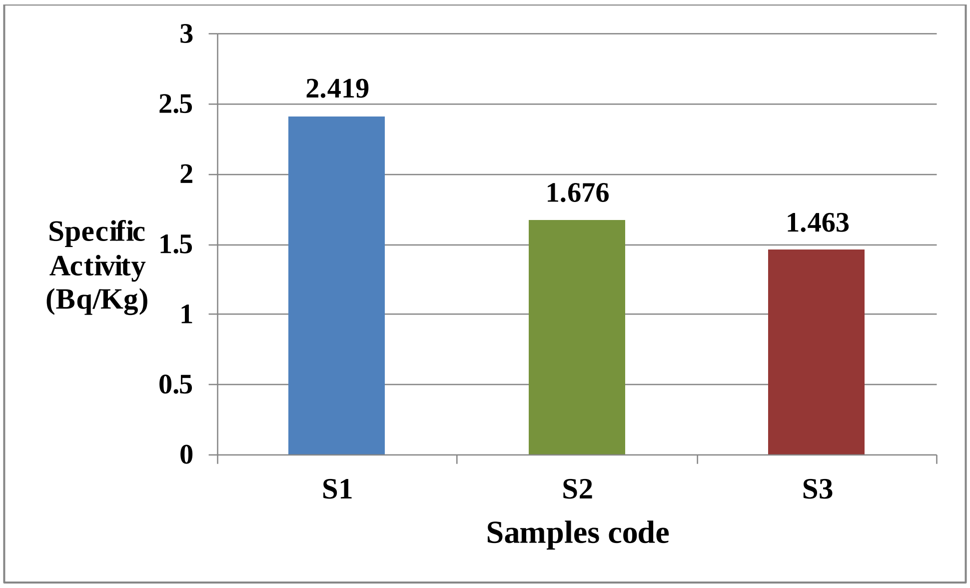

Figure 4.61: Specific Activity of ^{232}Th(Bq/kg) for Fertilizer.

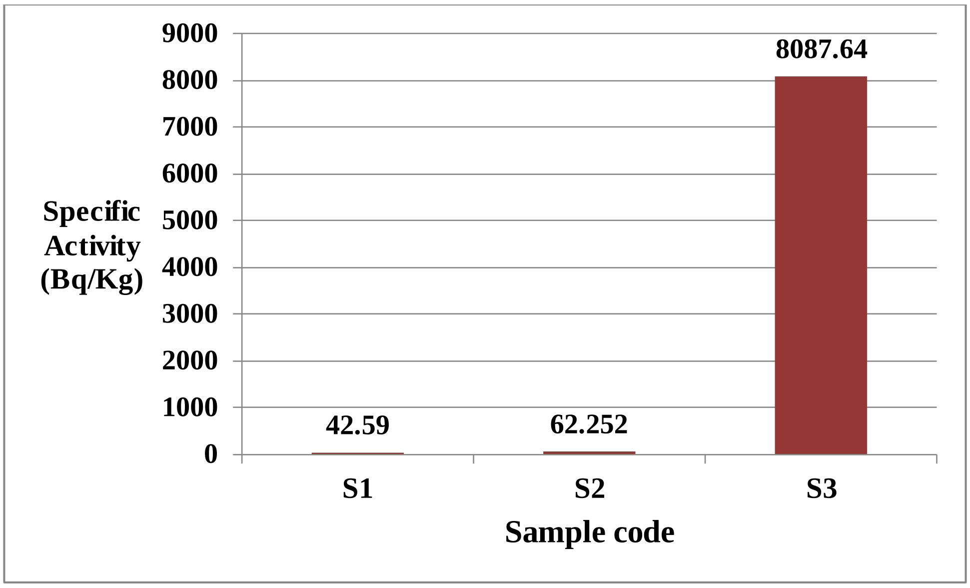

Figure 4.62: Specific Activity of ^{40}K (Bq/kg) for Fertilizer.

Chapter Five

Conclusion, Future Work and Recommendation

5.1 Introduction

This chapter shows the conclusions future works and recommendations.

5.2 Conclusions

The following conclusions have been reached by analyzing the groundwater, surface water, agricultural soil, plant and fruit in Al-Haydria Which was obtained through detection and measurement techniques such as Rad7, NaI(TI) and CR-39.

1. It was found that the majority of ^{222}Rn concentrations in groundwater and surface water samples from Agricultural Areas in Al Hayderiah in Al-Najaf Alashraf which was measured by Rad7 a system were below the levels considered harmful or effective by various organizations such as the of the US Environmental Protection Agency Water Office (US EPA). Therefore, it can be concluded that most samples are safe for household use and consumption. It was also observed that the annual effective doses (AED) for all age groups in every location studied were expected to be less than 0.1m Sv/y.

2. The acverage of specific activity of ^{238}U, ^{232}Th and ^{40}K was evaluated for samples of agricultural soil and tomato plants and fruits in the two regions using a NaI(TI) detector system. For ^{238}U and ^{232}Th, they were lower than the the global average for all samples, while for ^{40}K they were higher than the values of the global average and for all samples. However, the average values of all indicators were the radiation risks are less than the average global values for all samples, and from this can be concluded that there are no radiation risks to the health of the local population.

3. The transfer factor rate for the radionuclides ^{238}U, ^{232}Th and ^{40}K from the soil to the plant and fruit is less than one n in the first period, while the transfer factor rate for the radionuclides ^{238}U and ^{232}Th from soil to plant for the second region are greater than one and from soil to fruit less than one, while the values of the transfer coefficients for the nucleus ^{40}K were less than one Soil for plants and fruits.
4. The average concentrations of ^{222}Rn gas in the air and inside samples, as well as ^{226}Ra in samples of agricultural soil and tomato fruits from both regions, were evaluated. All values of gas concentrations were ^{222}Rn in The air and ^{226}Ra for the two regions are lower than the global averages, and the gas concentrations ^{222}Rn inside the samples were all values slightly higher than the global average.

5.3 Future Works

1. Further studies should be conducted to investigate the effect of radon gas concentration using RAD-7 detection and evaluating radioactive parameters in water, air, soil, and agricultural soil samples in additional governorates to obtain a more comprehensive understanding of the situation.

2. Additional research using various types of detectors (CN-85, CR-39, LR-115) is needed to determine radon and thorone concentrations in soil, air, surface water, and groundwater in other regions and to make comparisons.

3. Future studies should expand the statistical and experimental investigation to detect natural radioactive nuclei and radon gas in the

cancer cells of lung cancer patients in other regions in Iraq to determine the prevalence and potential causes of the disease.

4. Investigating the effect of soil types on the Transfer Factor for radionuclides to better understand how different soils impact the transfer of radionuclides to plants.

5. Conduct research to estimate the transfer factor for NORMs from soil to different types of trees to gain a more comprehensive understanding of the potential impact of radionuclides on the environment.

5.4 Recommendations

1. It is recommended that competent authorities, such as the Ministry of Health, the Ministry of the Environment, the local government, and the Geological Survey, take necessary measures to reduce the detrimental consequences of radiation dangers on the environment and general public health. Competent authorities should promote the use of organic fertilizers in agriculture and reduce reliance on chemical fertilizers. This can help lower the concentrations of radionuclides in the soil.
2. Modern cultivation methods and regular watering processes should be adopted to reduce the transportation of radionuclides to plants.
3. Consumption of tomatoes should be reduced from these areas due to their high transfer factor of radionuclides.
4. Radon gase and radioactivity, if their concentrations exceed the permissible levels, it could lead to cancer. Therefore, continuous measurement of these concentrations throughout the year, as is practiced in developed countries is necessary.
5. Furthermore, it is suggested that such studies be repeated for all governorates of Iraq and a radioactivity map for be created.

References

REFERENCES

[1] Ralph E. Lapp and Howard L. Andrews.(1972). *Nuclear Radiation Physics;* fourth edition, Prentice- Hall Inc., Englewood Cliffs, New Jersey.

[2] Knoll, G. F. (2010). Radiation detection and measurement. John Wiley & Sons.

[3] Asaduzzaman, K., Khandaker, M. U., Amin, Y. M., Bradley, D. A., Mahat, R. H., & Nor, R. M. (2014). Soil-to-root vegetable transfer factors for ^{226}Ra, ^{232}Th, ^{40}K, and 88Y in Malaysia. *Journal of environmental radioactivity*, *135*, 120-127.

[4] Bakım, M., & Görgün, A. U. (2015). Radioactivity in soils and some terrestrial foodstuffs from organic and conventional farming areas in Izmir, Turkey. *Journal of Radioanalytical and Nuclear Chemistry*, *306*, 237-242.

[5] Smičiklas, I., & Šljivić-Ivanović, M. (2016). Radioactive contamination of the soil: assessments of pollutants mobility with implication to remediation strategies. *Soil Contamination–Current Consequences and Further Solutions. Rijeka: InTech [Internet]*, 253-276.

[6] Senthilkumar, R. D., & Narayanaswamy, R. (2016). Assessment of radiological hazards in the industrial effluent disposed soil with statistical analyses. *Journal of Radiation Research and Applied Sciences*, *9*(4), 449-456.

[7] Al-Ghamdi, A. H. (2019). Health risk assessment of natural background radiation in the soil of Eastern province, Saudi Arabia. *Journal of Radiation Research and Applied Sciences*, *12*(1), 219-225.

[8] Syarbaini, S., Warsona, A., & Iskandar, D. (2014). Natural radioactivity in some food crops from Bangka-Belitung Islands, Indonesia. *Atom Indonesia*, *40*(1), 27-32.

[9] Olobatoke, R. Y., & Mathuthu, M. (2015). Radionuclide exposure in animals and the public health implications. *Turkish Journal of Veterinary & Animal Sciences*, *39*(4), 381-388.

[10] Isinkaye, O. M., Jibiri, N. N., & Olomide, A. A. (2015). Radiological health assessment of natural radioactivity in the vicinity of Obajana cement factory, North Central Nigeria. *Journal of Medical Physics/Association of Medical Physicists of India*, *40*(1), 52.

[11] Ghetti, F., Checcucci, G., & Bornman, J. F. (Eds.). (2006). *Environmental UV Radiation: Impact on Ecosystems and Human Health and Predictive Models: Proceedings of the NATO Advanced Study Institute on Environmental UV Radiation: Impact on Ecosystems and Human Health and Predictive Models Pisa, Italy June 2001*. Dordrecht: Springer Netherlands.

[12] Ahmed, N. K. (2004). Natural radioactivity of ground and drinking water in some areas of upper Egypt. *Turkish Journal of Engineering and Environmental Sciences*, *28*(6), 345-354.

[13] Bonotto, D. M., Bueno, T. O., Tessari, B. W., & Silva, A. (2009). The natural radioactivity in water by gross alpha and beta measurements. *Radiation Measurements*, *44*(1), 92-101.

[14] Povinec, P., Hirose, K., & Aoyama, M. (2013). *Fukushima accident: radioactivity impact on the environment*. Newnes.

[15] UNSCEAR, U. (2000). Sources and effects of ionizing radiation. *United Nations Scientific Committee on the Effects of Atomic Radiation*.

[16] United States Environmental Protection Agency. (1990). *National radon proficiency program handbook. Appendix A: Radon proficiency program measurement method definitions.* U.S. Environmental Protection Agency Office of Radiation and Indoor Air (6604J) 401 M Street, S.W. Washington, DC 20460, pp. 70–74.

[17] Giammanco, S., Immè, G., Mangano, G., Morelli, D., & Neri, M. (2009). Comparison between different methodologies for detecting radon in soil along an active fault: The case of the Pernicana fault system, Mt. Etna (Italy). *Applied Radiation and Isotopes*, *67*(1), 178-185..

[18] Asano, T., Sato, K., & Onodera, J. I. (2001). United nations scientific committee on the effects of atomic radiation 2000 report. *Japanese Journal of Health Physics*, *36*(2), 149-158.

[19] Durrance, E. M. (1986). Radioactivity in geology: principles and applications.

[20] Mireles, F., García, M. L., Quirino, L. L., Dávila, J. I., Pinedo, J. L., Ríos, C., ... & Villalba, L. (2007). Radon survey related to construction materials and soils in Zacatecas, México using LR-115. *Radiation Measurements*, *42*(8), 1397-1403.

[21] Fleischer, R. L., & Mogro‐Campero, A. (1978). Mapping of integrated radon emanation for detection of long‐distance migration of gases within the Earth: Techniques and principles. *Journal of Geophysical Research: Solid Earth*, *83*(B7), 3539-3549.

[22] Prasad, G., Prasad, Y., Gusain, G. S., & Ramola, R. C. (2008). Measurement of radon and thoron levels in soil, water and indoor atmosphere of Budhakedar in Garhwal Himalaya, India. *Radiation Measurements*, *43*, S375-S379.

[23] Annex, D., & United Nations Scientific Committee on the Effects of Atomic Radiation. (2000). Sources and effects of ionizing radiation. *Investigation of I*, *125*.

[24] Vaupotič, J., Barišić, D., Kobal, I., & Lulić, S. (2007). Radioactivity and radon potential of the terra rossa soil. *Radiation measurements*, *42*(2), 290-297.

[25] Lu, X., & Zhang, X. (2008). 226 Ra, 232 Th and 40 K activities in soils of Cuihua Mountain National Geological Park, China. *Environmental Geology*, *56*, 353-357.

[26] Alaamer, A. S. (2008). Assessment of human exposures to natural sources of radiation in soil of Riyadh, Saudi Arabia. *Turkish Journal of Engineering and Environmental Sciences*, *32*(4), 229-234.

[27] Al-Hamarneh, I. F., & Awadallah, M. I. (2009). Soil radioactivity levels and radiation hazard assessment in the highlands of northern Jordan. *Radiation measurements*, *44*(1), 102-110.

[28] Senthilkumar, B., Dhavamani, V., Ramkumar, S., & Philominathan, P. (2010). Measurement of gamma radiation levels in soil samples from Thanjavur using γ-ray spectrometry and estimation of population exposure. *Journal of Medical Physics/Association of Medical Physicists of India*, *35*(1), 48.

[29] Hasan, A. K., Subber, A. R., & Shaltakh, A. R. (2011). Measurement of radon concentration in soil gas using RAD7 in the environs of Al-Najaf Al-Ashraf City-Iraq. *Advances in Applied Science Research*, *2*(5), 273-278.

[30] Hussain, R. O., & Hussain, H. H. (2011). Investigation the natural radioactivity in local and imported chemical fertilizers. *Brazilian archives of biology and technology*, *54*, 777-782.

[31] Al-Hamidawi, A. A. (2012). Measurement of radon and thoron concentrations of soil-gas in Al-Kufa city using RAD-7 detector. *Iraqi Journal of Physics*, *10*(19), 110-116.

[32] Yousuf, R. M., & Abullah, K. O. (2013). Measurement ofnatural radioactivity in soil collected from the Eastern of Sulaimany Governorate in Kurdistan Region, Iraq. *ARPN Journal of Science and Technology*, *3*(7), 749-757.

[33] Ademola, A. K., Bello, A. K., & Adejumobi, A. C. (2014). Determination of natural radioactivity and hazard in soil samples in and around gold mining area in Itagunmodi, south-western, Nigeria. *Journal of Radiation research and applied sciences*, *7*(3), 249-255.

[34] Al-Gazaly, H. H., Al-Ulum, M. A. B., Al-Hamidawi, A. A., & Al-Abbasi, A. M. (2014). Natural radioactivity in soil at regions around the uranium mine in Abu-Skhair Najaf Province, Iraq. *Advances in Applied Science Research*, *5*(1), 13-17.

[35] Alsaffar, M. S., Jaafar, M. S., Kabir, N. A., & Ahmad, N. (2015). Distribution of ^{226}Ra, ^{232}Th, and ^{40}K in rice plant components and physico-chemical effects of soil on their transportation to grains. *Journal of Radiation Research and Applied Sciences*, *8*(3), 300-310.

[36] Isinkaye, M. O., & Emelue, H. U. (2015). Natural radioactivity measurements and evaluation of radiological hazards in sediment of Oguta Lake, South East Nigeria. *Journal of Radiation Research and Applied Sciences*, *8*(3), 459-469.

[37] Almayahi, B. (2015). NaI (Tl) spectrometry to natural radioactivity measurements of soil samples in Najaf City. *Iranica Journal of Energy Environment*, *6*(3), 207-211.

[38] Hatif, K. H. (2015). Natural Radioactivity level and the measurement of soil gas Radon, Thoron concentrations in Hilla city. *journal of kerbala university*, *13*(1).

[39] Hatif, K. H. (2016). Determination of natural radioactivity and radon, thoron concentrations of soil in Hilla City-Iraq. *Journal of University of Babylon*, *24*(5).

[40] Ajiboye, Y., Badmus, O. G., Ojo, O. D., & Isinkaye, M. O. (2016). Measurement of Radon Concentration and Radioactivity in Soil Samples of Aramoko, Ekiti State, Nigeria. *International Journal of Public Health Research*, *4*(5), 37-41.

[41] Karim, M. S., Daroysh, H. H., & Hameed, T. K. (2016). Measurement of natural radioactivity in selected soil samples from the archaeological of Babylon City, Iraq. *Journal of Radiation and Nuclear Applications*, *1*(1), 31-35.

[42] Kadhim, I. H., & Muttaleb, M. K. (2016). Measurement of radioactive nuclides present in soil samples of district Touirij of Karbala province for radiation safety purposes. *Int. J. Chem. Tech. Res*, *9*, 228-235.

[43] Rejah, B. K., & Ashoor, G. T. (2017). Radon gas concentration measurement in air of Al-Haswaa City in Province of Baghdad. *Iraqi Journal of Science*, *58*(2A), 663-668.

[44] Alusa, S. K., Odunaike, K., & Adeniji, I. A. (2017). Transfer factor of radionuclides from soil-to-palm oil produced from Elere palm tree plantation near Ibadan Oyo state, Nigeria. *Nigeria Journal of pure and applied Physics*, *7*(1), 7-12.

[45] Rajesh, S., Kerur, B. R., & Anilkumar, S. (2017). Radioactivity measurements of soil samples from Devadurga and Lingasugur of Raichur district of Karnataka, India. *Int J Pure Appl Phys*, *13*(1), 127-130.

[46] Opoku-Ntim, I., Gyampo, O., and Andam, A. B. (2019). Risk assessment of radon in some bottled water on the Ghanaian market. *Environmental Research Communications*, *1*(10), 105001.

[47] El-Araby, E. H., Soliman, H. A., and Abo-Elmagd, M. (2019). Measurement of radon levels in water and the associated health hazards in Jazan, Saudi Arabia. *Journal of Radiation Research and Applied Sciences*, *12*(1), 31-36.

[48] Rejah, B. K., Aljanabi, A. T., Fzaa, W. T., Hussein, A. A., & Ali, A. H. (2019, February). Calculation of Concentrations and Transfer Factors of Uranium from Soil to Plants Using Nuclear Track Detector CR-39. In *Journal of Physics: Conference Series* (Vol. 1178, p. 012012). IOP Publishing.

[49] Al-Alawy, I. T., & Hasan, A. A. (2018). Measurement of radon gas concentrations and hazard effects in underground water samples in Karbala Governorate of Iraq. *Engineering and Technology Journal*, *36*(2), 118-122.

[50] Ridha, A. A., Jameel, A. N., & Kadhim, N. F. (2020, March). Transfer factor of natural radionuclides from soil to silhouette plants using gamma spectroscopy. In *AIP Conference Proceedings* (Vol. 2213, No. 1, p. 020124). AIP Publishing LLC.

[51] Elsaman, R., Ali, G. A. M., Uosif, M. A. M., El-Taher, A., & Chong, K. F. (2020). Transfer factor of natural radionuclides from clay loam soil to sesame and Cowpea: radiological hazards. *International Journal of Radiation Research*, *18*(1), 157-166

[52] Okeme, I. C., Scott, T. B., Martin, P. G., Satou, Y., Ojonimi, T. I., & Olaluwoye, M. O. (2020). Assessment of the Mode of Occurrence and Radiological Impact of Radionuclides in Nigerian Coal and Resultant Post-Combustion Coal Ash Using Scanning Electron Microscopy and Gamma-Ray Spectroscopy. *Minerals*, *10*(3), 241.

[53] El-Taher, A., Abojassim, A., Najam, L., & Mraity, H. (2020). Assessment of annual effective dose for different age groups based on radon concentrations in the groundwater of Qassim, Saudi Arabia. Iranian Journal of Medical Physics, 17(1), 15-20.

[54] Abojassim, A. A. Evaluation of Natural Radionuclides in Groundwater Samples of Some Villages of Mashhad-Iran.

[55] Silva, L. B., Lopes, J. M., Pereira, W. S., Garcêz, R. W., Silva, A. X., & Talhofer, J. L. (2021). Committed effective dose and lifetime cancer risk due to ingestion of natural radionuclides in grains grown in an area of high background radiation. *Applied Radiation and Isotopes*, *172*, 109656.

[56] Ahmed, R. S. (2022). The concentration of radioactive materials in Iraqi soils, water and plants: A review. *Journal of Radiation Research and Applied Sciences*, *15*(1), 245-256.

[57] Hady, H. N., & Baqer, Z. S. (2023). Calculation of natural radiation transfer factors in some agricultural crops in Al-Hussainiya-Karbala-Iraq. *International Journal of Scientific Trends*, *2*(1), 23-33.

[58] Amoatey, E. A., Glover, E. T., Kpeglo, D. O., Otoo, F., & Adotey, D. K. (2023). Radiological Baseline Assessment of a Naturally Occurring Radioactive Material (NORM) Waste Disposal Facility in Ghana. *Journal of Mining and Environment*.

[59] Ng, K. H. (2003, October). Non-ionizing radiations–sources, biological effects, emissions and exposures. In Proceedings of the international conference on non-ionizing radiation at UNITEN (pp. 1-16). sn.

[60] Abdul Hamid Helmi Al-Jazar and Mohammed Abdul-Moneim Saqr. (2011). Atomic Radiation and its Peaceful Uses. Knowledge World, Kuwait. Arabic.

[61] Murakami, Y., Danno, A., & Kobayashi, M. (1982). Radiation data book.

[62] UNSCEAR, S. (2000). Effects of Ionizing Radiation, United Nations Scientific Committee on the Effect of Atomic Radiation Report Vol. 1 to the General Assembly, with Scientific Annexes. *United Nations Sales Publication, United Nations, New York*.

[63] Knoll, G. F. (2000). Radiation Detection and Measurement3rd edition John Wiley and Sons. *New York*.

[64] Zaboon, A. H. (2004). *Public Exposure to Ambient Gamma Radiation* (Doctoral dissertation, M. Sc. Thesis, Al-Rasheed College for Engineering and Science, Iraq).

[65] Silberberg, R., & Tsao, C. H. (1990). Spallation processes and nuclear interaction products of cosmic rays. *Physics Reports*, *191*(6), 351-408.

[66] Flores, O. B., Estrada, A. M., Suarez, R. R., Zerquera, J. T., & Pérez, A. H. (2008). Natural radionuclide content in building materials and gamma dose rate in dwellings in Cuba. *Journal of environmental radioactivity*, *99*(12), 1834-1837.

[67] Friedberg, W., Copeland, K., Duke, F. E., O'Brien III, K., & Darden Jr, E. B. (1999). Guidelines and technical information provided by the US Federal Aviation Administration to promote radiation safety for air carrier crew members. *Radiation Protection Dosimetry*, *86*(4), 323-327.

[68] Abojassim, A. A. (2020). Comparative study between active and passive techniques for measuring radon concentrations in groundwater of Al-Najaf city, Iraq. *Groundwater for Sustainable Development*, *11*, 100476.

[69] National Academy of Sciences Report. (1999). Risk assessment of radon in drinking water. *National Academy Press, Washington, DC*.

[70] Ojovan, M. I., Lee, W. E., & Kalmykov, S. N. (2019). *An introduction to nuclear waste immobilisation*. Elsevier.

[71] Hore-Lacy, I. (1999). *Nuclear electricity*. Uranium Information Centre, Ltd., GPO Box 1649N, Melbourne 3001, Australia.

[72] Van Schmus, W. R. (1995). Natural radioactivity of the crust and mantle. In Global earth physics: A handbook of physical constants (Vol. 1, pp. 283-291). Washington, DC: American Geophysical Union.

[73] Sutton, G. A., Napier, S. T., John, M., & Taylor, A. (1993). Uranium-238 decay chain data. Science of the total environment, 130, 393-401.

[74] Eisenbud, M., & Gesell, T. F. (1997). Environmental radioactivity from natural, industrial and military sources: from natural, industrial and military sources. Elsevier.

[75] Henriksen, T., Hole, E. O., Sagstuen, E., Pettersen, E., Malinen, E., & Edin, N. J. (2009). Biophysics group at UiO. *Radiation and Health*.

[76] Krane, K. S., & Halliday, D. (1988). Introductory Nuclear Physics, John Wiley&Sons. *Inc., Kanada*.

[77] Podgorsak, E. B. (2005). Radiation Oncology Physics: A Handbook for Teachers and Students, International Atomic Energy Agency, Technical Editor, Vienna. *Thirth Edition.(179-191)*.

[78] Cottingham, W. N., Greenwood, D. A., & Greenwood, D. A. (2001). *An introduction to nuclear physics*. Cambridge University Press.

[79] World Health Organization. (1996). The basic safety standards on diskette. International basic safety standards for protection against ionizing radiation and for the safety of radiation sources.

[80] Serway, R. A., Moses, C. J., & Moyer, C. A. (2004). *Modern physics*. Cengage Learning.

[81] Meyerhof, W. E., & Meyerhof, W. E. (1967). *Elements of nuclear physics* (Vol. 174). New York: McGraw-Hill.

[82] Beyzadeoglu, M., Ozyigit, G., & Ebruli, C. (2010). *Basic radiation oncology* (Vol. 71). Berlin: Springer.

[83] Al-Ubaidi K. H. M., (2006). Identification and Measurements of Natural and Industrial Radioactive Pollutants in Environment of Baghdad City using Gamma Spectrometry and Solid State Nuclear Track Detector CR-39. Ph.D. Thesis, Ibn Al-Haitham College, Baghdad University, Iraq.

[84] Attallah, M. F., Abdelbary, H. M., Elsofany, E. A., Mohamed, Y. T., & Abo-Aly, M. M. (2020). Radiation safety and environmental impact assessment of sludge TENORM waste produced from petroleum industry in Egypt. Process Safety and Environmental Protection, 142, 308-316.

[85] Shagalova, E. D. (1986). U-238 content in soils of Byelorussia. Pochvovedenie, 140-145.

[86] Choppin, G. R., & Wong, P. J. (1998). The chemistry of actinide behavior in marine systems. Aquatic Geochemistry, 4(1), 77-101.

[87] Hodgson, P. E., Gadioli, E., & Gadioli-Erba, E. (1997). Introductory nuclear physics. Oxford Univ. Press.

[88] Turner, J. E. (2007). Atoms, radiation and radiation protection. 3. comp. rev. and enl.

[89] Lee, S., Tewolde, G., & Kwon, J. (2014, March). Design and implementation of vehicle tracking system using GPS/GSM/GPRS technology and smartphone application. In 2014 IEEE world forum on internet of things (WF-IoT) (pp. 353-358). IEEE.

[90] United Nations Scientific Committee on the Effects of Atomic Radiation. (2009). Effects of Ionizing Radiation, UNSCEAR Report Volume II, Scientific Annex E, Sources-to-effects Assessment for Radon in Homes and Workplaces. United Nations, New York.

[91] Ali, M. A. (2021). Determination of radon gas concentrations Rn-222 in water samples of Rivers and ground wells in Basrah Governorate, Iraq. *Mesopotamian Journal of Marine Science*, *36*(1).

[92] Leovic, K. W., & Craig, A. B. (1994). Radon Prevention in the Design and Construction of Schools and Other Large Buildings.

[93] United States. Environmental Protection Agency. Indoor Environmental Division. (2002). *A Citizen's Guide to Radon: The Guide to Protecting Yourself and Your Family from Radon*. US Environmental Protection Agency, Indoor Environments Division.

[94] NCRP (1988). Measurement of Radon and Daughters in Air, NCRPT, Bethesda, (M.D.) U.S.A.,15(97).

[95] Buttafuoco, G., Tallarico, A., & Falcone, G. (2007). Mapping soil gas radon concentration: a comparative study of geostatistical methods. *Environmental Monitoring and Assessment*, *131*, 135-151.

[96] Wilde, F. D., & Radtke, D. B. (Eds.). (1998). *Handbooks for Water-resources Investigations: National field manual for the collection of water-quality data. Field measurements* (Vol. 9). US Department of the Interior, US Geological Survey.

[97] Norris, L. A., Montgomery, M. L., & Warren, L. E. (1987). Triclopyr persistence in western Oregon hill pastures. *Bull. Environ. Contam. Toxicol*, *39*, 134-141.

[98] Virk, H. S., & Singh, B. (1993). Radon anomalies in soil-gas and groundwater as earthquake precursor phenomena. *Tectonophysics*, *227*(1-4), 215-224.

[99] Otton, J. K. (1992). *Radon in soil gas and soil radioactivity in Prince George's County, Maryland*. US Geological Survey.

[100] Kang, J. K., Seo, S., and Jin, Y. W. (2019). Health effects of radon exposure. *Yonsei medical journal*, *60*(7), 597-603.

[101] Abumurad, K. M., and Al-Omari, R. A. (2008). Indoor radon levels in irbid and health risk from internal doses. *Radiation Measurements*, *43*, S389-S391.

[102] Sekudewicz, I., & Gąsiorowski, M. (2019). Determination of the activity and the average annual dose of absorbed uranium and polonium in drinking water from Warsaw. *Journal of Radioanalytical and Nuclear Chemistry*, *319*, 1351-1358.

[103] John Wiley & Sons Ltd. (2008), G. R. G. P. Gamma-ray Spectrometry 2nd Edition, Nuclear Training Services Ltd, Warrington, UK.

[104] Kligerman, S., & White, C. (2011). Epidemiology of lung cancer in women: risk factors, survival, and screening. *American journal of roentgenology*, *196*(2), 287-295.

[105] MG, D. S. G., & Setayandeh, S. (2013). A review on natural background radiation. Adv. *Biomed. Res, 2*, 65.

[106] Espinosa, G., Golzarri, J. I., & Navarrete, J. M. (2016). Determination of the natural and artificial radioactivity of a selection of traditional Mexican medicinal herbs by gamma spectrometry. *Journal of Radioanalytical and Nuclear Chemistry*, *307*, 1717-1721.

[107] Dragović, S., Janković, L., Onjia, A., & Bačić, G. (2006). Distribution of primordial radionuclides in surface soils from Serbia and Montenegro. *Radiation measurements*, *41*(5), 611-616.

[108] Inigo Valan I, Mathiyarasu R, Sridhar SGD, Narayanan V, Stephen A (2015) Investigation of terrestrial radioactivity in Krusadai–Rameswaram Islands, Northern Coast of Chennai And Tamiraparani River–India. J Radioanal Nucl Chem. https:// doi. org/ 10. 1007/ s10967- 014- 3864-9.

[109] Chandrasekaran, A., Ravisankar, R., Senthilkumar, G., Thillaivelavan, K., Dhinakaran, B., Vijayagopal, P., & Venkatraman, B. (2014). Spatial distribution and lifetime cancer risk due to gamma radioactivity in Yelagiri Hills, Tamilnadu, India. *Egyptian Journal of basic and applied sciences*, *1*(1), 38-48.

[110] Atwood, D. A. (Ed.). (2013). *Radionuclides in the Environment*. John Wiley & Sons.

[111] Hamideen, M. S., Bdair, O. M., Chandrasekaran, A., Saleh, H., & Elimat, Z. M. (2020). Multivariate statistical investigations of natural radioactivity and radiological hazards in building materials mainly used in Amman Province, Jordan. *International Journal of Environmental Analytical Chemistry*, *100*(2), 189-203.

[112] Ravisankar, R., Vanasundari, K., Suganya, M., Raghu, Y., Rajalakshmi, A., Chandrasekaran, A., & Venkatraman, B. (2014). Multivariate statistical analysis of radiological data of building materials used in Tiruvannamalai, Tamilnadu, India. *Applied Radiation and Isotopes*, *85*, 114-127.

[113] Aly Abdo, A. A., Hassan, M. H., & Huwait, M. R. A. (1999, November). Radioactivity assessment of fabricated phosphogypsum mixtures. In *Fourth Radiation Physics Conference* (pp. 15-19).

[114] Tzortzis, M., Tsertos, H., Christofides, S., & Christodoulides, G. (2003). Gamma-ray measurements of naturally occurring radioactive samples from Cyprus characteristic geological rocks. *Radiation measurements*, *37*(3), 221-229.

[115] Vaiserman, A. M. (2010). Radiation hormesis: historical perspective and implications for low-dose cancer risk assessment. *Dose-Response*, *8*(2), dose-response.

[116] Cothern, C. R., Lappenbusch, W. L., & Michel, J. (1986). Drinking-water contribution to natural background radiation. *Health Physics*, *50*(1), 33-47.

[117] Fisenne, I. M., Perry, P. M., Decker, K. M., & Keller, H. W. (1987). The daily intake of U-234,U-235,U-238 , Th-228,Th-230,Th-232 and Ra-226, Ra-228 by New York City residents. *Health Physics*, *53*(4), 357-363.

[118] Ramachandran, T. V., & Mishra, U. C. (1989). Measurement of natural radioactivity levels in Indian foodstuffs by gamma spectrometry. *International Journal of Radiation Applications and Instrumentation. Part A. Applied Radiation and Isotopes*, *40*(8), 723-726.

[119] Shiraishi, K., Tagami, K., Muramastu, Y., & Yamamoto, M. (2000). Contributions of 18 food categories to intakes of Th-232 and U- 238 in Japan. *Health physics*, *78*(1), 28-36.

[120] World Health Organization. (2013). INFOSAN activity report 2011-2012.

[121] Annex, D., & United Nations Scientific Committee on the Effects of Atomic Radiation. (2000). Sources and effects of ionizing radiation. *Investigation of I*, *125*.

[122] United Nations. Scientific Committee on the Effects of Atomic Radiation. (2011). *Sources and Effects of Ionizing Radiation: United Nations Scientific Committee on the Effects of Atomic Radiation: UNSCEAR 2008 Report to the General Assembly, with Scientific Annexes* (Vol. 2). United Nations Publications.

[123] International Atomic Energy Agency. Technologically Enhanced Natural Radiation (TENR II) (Vienna, Austria: IAEA) (2002).

[124] Paschoa, A. S., & Steinhausler, F. (2009). *TENR-Technologically Enhanced Natural Radiation*. Elsevier.

[125] Maslyakov, G. (2004). *Research and development of measures to be taken for long term stabilization and isolation of uranium mill tailings* (No. IAEA-TECDOC--1403).

[126] Shanthi, G., Thanka Kumaran, J. T., Gnana Raj, G. A., & Maniyan, C. G. (2012). Transfer factor of the radionuclides in food crops from high-background radiation area of south west India. *Radiation protection dosimetry*, *149*(3), 327-332.

[127] Guidebook, A. (1989). Measurement of Radionuclides in Food and the Environment. *Vienna: International Atomic Energy Agency*.

[128] Alam, M. N., Chowdhury, M. I., Kamal, M., Ghose, S., Islam, M. N., & Anwaruddin, M. (1999). Radiological assessment of drinking water of the Chittagong region of Bangladesh. *Radiation protection dosimetry*, *82*(3), 207-214.

[129] United Nations Scientific Committee on the Effects of Atomic Radiation. (2000). *Sources and Effects of Ionizing Radiation, United Nations Scientific Committee on the Effects of Atomic Radiation (UNSCEAR) Report, Volume I: Report to the General Assembly, with Scientific Annexes-Sources*. United Nations..

[130] World Health Organization. (2010). *Hardness in drinking-water: background document for development of WHO guidelines for drinking-water quality* (No. WHO/HSE/WSH/10.01/10). World Health Organization.

[131] Jayasheelan, A., Manjunatha, S., Yashodhara, I., & Karunakara, N. (2014). Study of natural radioactivity and estimation of radiation dose in the environment of Tumkur, Karnataka, India. *Radiation protection dosimetry*, *158*(1), 73-78.

[132] Hussein, E. M. (1994). Radioactivity of phosphate ore, superphosphate, and phosphogypsum in Abu-Zaabal phosphate plant, Egypt. *Health Physics*, *67*(3), 280-282.

[133] United Nations Scientific Committee on the Effects of Atomic Radiation. (1988). Report of the United Nations Scientific Committee on the effects of atomic radiation.

[134] Reddy, K. U., Ningappa, C., & Sannappa, J. (2017). Natural radioactivity level in soils around Kolar gold fields, Kolar district, Karnataka, India. *Journal of Radioanalytical and Nuclear Chemistry*, *314*, 2037-2045.

[135] Tufail, M. (2012). Enhancement of natural radioactivity in fertilized soil of Faisalabad, Pakistan. Environmental Science and Pollution Research, 19, 3327-3338.

[136] Beretka, J., & Mathew, P. J. (1985). Natural radioactivity of Australian building materials, industrial wastes and by-products. *Health physics*, *48*(1), 87-95.

[137] United Nations Scientific Committee on the Effects of Atomic Radiation. (1996). Sources and effects of ionizing radiation. UNSCEAR 1996 report to the General Assembly, with scientific annex.

[138] Nordic (2000) Naturally occurring radiation in the Nordic countries-recommendations. The Flag-Book Series, the Radiation Protection Authorities in Denmark, Finland, Iceland, Norway and Sweden.

[139] EC (European Commission). (1999). Radiological protection principles concerning the natural radioactivity of building materials. Radiation Protection 112, Directorate General Environment.

[140] Almayahi, B.A.(2014) Gamma Spectroscopic of Soil Samples from Kufa in Najaf Governorate, Iraq. World Applied Sciences Journal 31 (9): 1582-1588.

[141] Erees, F. S., Dayanıklı, S. A., & Çam, S. (2006). Natural radionuclides in the building materials used in Manisa city, Turkey. *Indoor and Built Environment*, *15*(5), 495-498.

[142] Adewoyin, O. O., Omeje, M., Joel, E. S., Akinwumi, S. A., Ehi-Eromoseled, C. O., & Embong, Z. (2018). Radionuclides proportion and radiological risk assessment of soil samples collected in Covenant University, Ota, Ogun State Nigeria. *MethodsX*, *5*, 1419-1426.

[143] CENGİZ, G. B.(2017). Natural radioactivity analysis in soil samples of Ardahan province, Turkey for the assessment of the average effective dose. journal of Sakarya Üniversitesi Fen Bilimleri Enstitüsü Dergisi, 21 (6), 1583~1590

[144] Maphoto, K. P. (2004). Determination of natural radioactivity concentrations in soil: a comparative study of Windows and Full Spectrum Analysis (Doctoral dissertation, University of the Western Cape).

[145] Tufail, M., Akhtar, N., & Waqas, M. (2006). Radioactive rock phosphate: the feed stock of phosphate fertilizers used in Pakistan. Health physics, 90(4), 361-370.

[146] Arthur, R. J., Miley, H. S., & Todd, L. C. (2008). BE-7 Cross-talk in RASA Continuous Air Samplers. In 24th Seismic Research Review–Nuclear Explosion Monitoring: Innovation and Integration (pp. 689-693).

[147] Tahir, S. N. A., Jamil, K., Zaidi, J. H., Arif, M., Ahmed, N., & Ahmad, S. A. (2005). Measurements of activity concentrations of naturally occurring radionuclides in soil samples from Punjab province of Pakistan and assessment of radiological hazards. Radiation Protection Dosimetry, 113(4), 421-427.

[148] Alaamer, A. S. (2008). Assessment of human exposures to natural sources of radiation in soil of Riyadh, Saudi Arabia. Turkish Journal of Engineering and Environmental Sciences, 32(4), 229-234.

[149] Tufail, M., Akhtar, N., & Waqas, M. (2006). Measurement of terrestrial radiation forassessment of gamma dose from cultivated and barren saline soils of Faisalabad in Pakistan. Radiation Measurements, 41(4), 443-451.

[150] Tzortzis, M., Tsertos, H., Christofides, S., & Christodoulides, G. (2003). Gamma-ray measurements of naturally occurring radioactive samples from Cyprus characteristic geological rocks. Radiation Measurements, 37(3), 221-229.

[151] Ziqiang, P., Yin, Y., & Mingqiang, G. (1988). Natural radiation and radioactivity in China. Radiation Protection Dosimetry, 24(1-4), 29-38.

[152] Carnelo, L. G. L., de Miguez, S. R., & Marbán, L. (1997). Heavy metals input with phosphate fertilizers used in Argentina. Science of the Total Environment, 204(3), 245-250.

[153] Da Conceicao, F. T., & Bonotto, D. M. (2006). Radionuclides, heavy metals and fluorine incidence at Tapira phosphate rocks, Brazil, and their industrial (by) products. Environmental Pollution, 139(2), 232-243.

[154] Abojassim, A. (2017). Alpha particles concentrations from soil samples of Al-Najaf/Iraq. *Polish Journal of Soil Science, 50*(2).

[155] Ali, & Abojassim.(2021) *A THESIS SUBMITTED TO* (Assessment of Natural Radioactivity and Its Environmental Impacts in Some Decorative Materials in Iraq).

[156] Mohammed, E. J. (2016). Radon concentrations in some soil and air samples of dwellings in Karbala City and influencing factors on lung cancer risks using CR-39. *Ms.c thesis, University of Kerbala.*

[157] Subber, A. R., Al-Hashmi, N. H., Nader, A. F., Jebur, J. H., and Khodier, M. K. (2015). Constructasa simple radon chamber for measurement of radon detectors calibration factors. *Pelagia research library, Advances in applied Science research*, *6*(2), 128-131.

[158] Elzain, A. E. A. (2014). Measurement of Radon-222 concentration levels in water samples in Sudan. *Advances in Applied Science Research*, *5*(2), 229-234.

[159] Abojassim, A. A., and Lawi, D. J. (2018). Alpha particles emissions in some samples of medical drugs (capsule) derived from medical plants in Iraq. *Plant arches*, *18*(1), 1137-7.

[160] Rosén, K., Öborn, I., & Lönsjö, H. (1999). Migration of radiocaesium in Swedish soil profiles after the Chernobyl accident, 1987–1995. *Journal of Environmental Radioactivity*, *46*(1), 45-66.

[161] Ebtihal, T. A. K., & Mohsin, F. A. R. (2020). Spatiotemporal Monitoring of Urban Expansion Utilizing Remote Sensing Data: The Case Study of An Najaf Governorate.

[162] Kadhim, A. P. K. N., & Al-Baaj, G. A. J. (2016). The geotechnical maps for gypsum by using GIS for Najaf City (Najaf-Iraq). *International Journal of Civil Engineering and Technology*, *7*(4), 329-338.

[163] Al-Khafaji, M. K. J. (2012). Cartography Representation of The Geographical Characteristics of AL-Najaf Governorate. *Submitted to Council Collage of Arts Athesis University of Kufa*.

[164] Abojassima, A. A., Shltake, A. R., Najam, L. A., and Merzaa, I. R. (2017). Radiological parameters due to radon-222 in soil samples at Baghdad Governorate (Karakh), Iraq. *Pak. j. sci. ind. res. Ser. A: phys. sci*, *60*(2), 72-8.

[165] Zbalh, M. A., Ali Bakir, H. A., Abojassim, A. A., and Hassan, A. B. (2019). Monte Carlo Simulation to Estimate the Male and Female Effective Dose due to Radon Exposure in Al-Najaf. *Indian Journal of Public Health Research & Development*, *10*(7).

[166] Qasim, A. M. S., Hussain, H. H., and Abojassim, A. A. (2018). Radon concentrations and annual effective dose in cigarette samples (domestic and importer) at the Iraqi markets. *Journal of Radiation and Nuclear Applications*, *3*(2), 83.

[167] Attiyah, M. M. (2013). Determination of uranium concentration and annual effective dose in drinking water of Baghdad and Nineveh Governorates using kinetic phosphorescence analyzer (KPA) and CR-39 nuclear track detector. *Ms.c thesis*, *Baghdad University*.

[168] Durridge Company Inc. (2017). Reference Manual . RAD-7 Electronic Radon Detector.

[169] Durridge Company Inc. (2010), Reference Manual version 6.0.1, RAD-7 Electronic Radon Detector.

[170] Al-Hamidawi, A. (2014). Assessment of radiation hazard indices and excess life time cancer risk due to dust storm for Al-Najaf, Iraq. *WSEAS Trans. Environ. Dev*, *10*, 312.

[171] Tsoulfanidis, N. (2010). Measurement and detection of radiation 2nd edition.

[172] Lipkowitz, K. B., Cundari, T. R., and Boyd, D. B. (Eds.). (2008). *Reviews in computational chemistry* (Vol. 51). John Wiley & Sons.

[173] Rajamannan, B., Viruthagiri, G., & Suresh Jawahar, K. (2013). Natural radionuclides in ceramic building materials available in Cuddalore district, Tamil Nadu, India. Radiation protection dosimetry, 156(4), 531-534.

[174] Gröning, M., & Rozanski, K. (2003). Uncertainty assessment of environmental tritium measurements in water. Accreditation and quality assurance, 8(7), 359-366.

[175] Almayahi, B. A., Tajuddin, A. A., & Jaafar, M. S. (2012). Radiation hazard indices of soil and water samples in Northern Malaysian Peninsula. Applied radiation and isotopes, 70(11), 2652-2660.

[176] Majeed, F. A., Kadhim, I. H., Muhsen, A. O., & Abass, K. H. (2015). Determination of Alpha Particles Concentration in Toothpaste Using CR-39 Track Detector. Detection, 3(02), 9.

[177] Colijn A.P and Van Vulpen I. B., (2013), "The performance of NaI(Tl) scintillation detectors", M.Sc. in Physics, University of Amsterdam Nikhef

[178] Kobeissi, M. A., El Samad, O., Zahraman, K., Milky, S., Bahsoun, F., & Abumurad, K. M. (2008). Natural radioactivity measurements in building materials in Southern Lebanon. Journal of Environmental Radioactivity, 99(8), 1279-1288.

[179] Eappen. K.P and Mayya. Y.S, (2009),"Factors affecting the registration and counting of alpha tracks in solid state nuclear track detector", Indian Journal Physics,83(6),751-757.

[180] Al-Jubbori, M., and Al-Shumaisy, S. (2015). Computer Algorithm for Counting and Measuring Alpha Particles Track Diameters in CR-39 Detectors. *Jordan Journal of Physics*, *8*(1), 57-65.

[181] World Health Organization, & WHO. (2004). *Guidelines for drinking-water quality* (Vol. 1). World Health Organization.

[182] United Nations Scientific Committee on the Effects of Atomic Radiation. (1996). Sources and effects of ionizing radiation. UNSCEAR 1996 report to the General Assembly, with scientific annex.

[183] US Environmental Protection Agency. (1999). National Primary Drinking Water Regulations; Radon-222: Proposed Rule.

[184] Ting, D. S. K. (2010). WHO handbook on indoor radon: a public health perspective.

[185] UNSCEAR (2010) United Nations Scientific Committee on the Effects of Atomic Radiation.Sources and effects of ionizing radiation Report to the general assembly, with scientific Annexes United Nations, New York.

[186] United Nations Scientific Committee on the Effects of Atomic Radiation, & Annex, B. (2000). Exposures from natural radiation sources. *Cosmic rays*, *9*(11).

[187] ICRP-65. (1993). International commission on radiological protection, ICRP publication 65.

[188] Hafsi, C., Debez, A., & Abdelly, C. (2014). Potassium deficiency in plants: effects and signaling cascades. *Acta Physiologiae Plantarum*, *36*(5), 1055-1070.

[189] Carvalho, F., Chambers, D., Fernandes, S., Fesenko, S., Goulet, R., Howard, B., ... & Yankovich, T. (2014). *The environmental behaviour of radium: revised edition*. International Atomic Energy Agency.

[190] Kumar, A., Singhal, R. K., Preetha, J., Rupali, K., Narayanan, U., Suresh, S., ... & Ranade, A. K. (2008). Impact of tropical ecosystem on the migrational behavior of K-40, Cs-137, Th-232 U-238 in perennial plants. *Water, air, and soil pollution*, *192*, 293-302.

[191] World Health Organization. (2009). WHO handbook on indoor radon: a public health perspective. World Health Organization.

[192] ICRP, P. A. (1993). Radou-222 at Home and at Work, ICRP Report 65.

[193] United Nations. Scientific Committee on the Effects of Atomic Radiation. (2000). UNSCEAR... Report to the General Assembly, with Scientific Annexes. United Nations

[194] Aswood, M. S., Jaafar, M. S., & Bauk, S. (2013). Assessment of radionuclide transfer from soil to vegetables in farms from Cameron Highlands and Penang,(Malaysia) using neutron activation analysis. *Applied Physics Research*, *5*(5), 85.

[195] Guillén, J., Baeza, A., Salas, A., Muñoz-Muñoz, J. G., & Muñoz-Serrano, A. (2017). Factors influencing the soil to plant transfer of radiocaesium. *Impact of Cesium on Plants and the Environment*, 19-33.

جمهورية العراق
وزارة التعليم العالي والبحث العلمي
جامعة بابل / كلية العلوم
قسم الفيزياء

قياس تركيز غاز الرادون في التربة والماء ونقل النويدات المشعة الطبيعية الى النباتات في المناطق الزراعية في الحيدرية

أطروحة مقدمة إلى
مجلس كلية العلوم - جامعة بابل
وهي جزء من متطلبات نيل درجة دكتوراه الفلسفة في علوم الفيزياء.

من قبل

ليث يوسف جبر طاهر

بكالوريوس علوم في الفيزياء/ 2001
ماجستير علوم في الفيزياء/ 2017

بإشراف

أ. د. محسن كاظم مطلب الجنابي

1445 هـ　　　　2023 م

الخلاصة

تبحث هذه الدراسة في المنطقة الزراعية في الحيدرية في محافظة النجف الاشرف حيث تم تقسيم منطقة الدراسة الى منطقتين ، الاولى تعتمد بالري على المياه الجوفية والاخرى على المياه السطحية وهذه المناطق هي مصادر مهمة للمنتجات الزراعية الموسمية للاسواق المحلية.

تهدف الدراسة في حساب تراكيز غاز الرادون و النشاط النوعي وعامل النقل الخاصة بالنويدات المشعة الطبيعية في الممنطقتين المذكورة أعلاه ولعينات مختلفة من المياه الجوفية والسطحية والتربة الزراعية والنبات والثمر(محصول الطماطم) في تلك المناطق. حيث تم جمع عينات المياه الجوفية والسطحية و التربة الزراعية وعينات محصول الطماطم (النباتات والثمر) وتم استخدام ثلاث تقنيات للقياس وهي مقياس كاشف الراد سفن لعينات المياه الجوفية والسطحية و طيف أشعة جاما NaI(Tl) للتربة والنبات والثمر وكاشف الاثر النووي للحالة الصلبة CR-39 للتربة والثمر.

أشارت النتائج إلى أن متوسط تركيز الغاز (^{222}Rn) في المياه الجوفية كان أعلى منه في المياه السطحية وكانت قيمته 0.23 بيكريل / لتر ولكنها أقل من المتوسط العالمي مثل وكالة حماية البيئة الامريكية مكتب المياه. كان متوسط قيمة النشاط النوعي (^{238}U) و (^{232}Th) في جميع عينات التربة والنبات والثمر (الطماطم) وللمنطقتين اقل من قيم المتوسط العالمي ، باستثناء (^{40}K) ولجميع العينات كانت اعلى من قيم المتوسط العالمية، مع هذه كانت قيم مؤشرات الخطورة ولجميع العينات اقل من قيم المعدلات العالمية.

كما وجدت الدراسة أن معدل عامل النقل للنويدات المشعة (^{238}U) و (^{232}Th) و (^{40}K) من التربة الى النبات والثمر اقل ن واحد في المنطفقة الاولى بينما معدل عامل النقل للنويدات المشعة (^{238}U) و ^{232}Th) من التربة الى النبات للمنطقة الثانية أكبر من واحد ومن التربة الى الثمر اقل من واحد بينما كانت قيم معاملات الانتقال لنواة (^{40}K) اقل من واحد من التربة للنبات والثمر.

تم قياس تراكيز غاز (^{222}Rn) في الهواء وداخل العينات وكذلك (^{226}Ra) في عينات مختارة من التربة الزراعية وثمار الطماطم لكلا المنطقتين، وكانت جميع قيم تراكيز غاز (^{222}Rn) في الهواء و(^{226}Ra) وللمنطقتين اقل من المعدلات العالمية و تراكيز غاز (^{222}Rn) في داخل العينات كانت جميع القيم أعلى من المتوسط العالمية.